國立臺灣大學生命科學院生命科學系

博士論文

Department of Life Science

College of Life Science

National Taiwan University

Doctoral Dissertation

類鐸受體訊息傳遞路徑參與調控瓢體蟲前端再生之研究

Study of toll-like receptor (TLR) signaling pathway in the regulation of anterior regeneration process in *Aeolosoma viride*

陳巧坪

Chiao-Ping Chen

指導教授：陳俊宏 博士

Advisor: Jiun-Hong Chen, Ph.D.

中華民國 109 年 1 月

January 2020

doi:10.6342/NTU202000204

國立臺灣大學博士學位論文
口試委員會審定書

類鐸受體訊息傳遞路徑參與調控瓢體蟲前端再生之研究

Study of toll-like receptor (TLR) signaling pathway in the regulation of anterior regeneration process in *Aeolosoma viride*

本論文係陳巧坪君(D01B41005)在國立臺灣大學生命科學學系、所完成之博士學位論文，於民國109年01月08日承下列考試委員審查通過及口試及格，特此證明

口試委員：陳俊亨（簽名）

（指導教授）

李心予　楊忠達

郭典勳

生命科學系 系主任 黃偉邦（簽名）

doi:10.6342/NTU202000204

致謝

那年夏天，從屏東回到家鄉臺北，帶著緊張的心情開始了每天通勤來回兩小時的博士班生涯，能夠進入地龍實驗室在恩師陳俊宏老師的指導之下發揮所學，對我來說是一件很幸運的事，畢竟這是一條許多人不會選擇的道路，而選擇之後走到今天終於準備要邁向下一步，真的需要向一路上的所有人表達感謝。

第一位當然要感謝指導教授陳俊宏老師多年來待我如同自己的孩子般，在不順利的時候鼓勵我，在順利的時候找我喝酒精飲料，使我多年來可以專心於研究上，當然他也鼓勵大家除了研究外也要注重教學，因此在教學方面我也有所斬獲抱了傑出教學獎座回家，真的非常感謝也佩服當初老師有勇氣收留我這個屏東回來的小屁孩；除了我的指導教授之外，也要特別感謝郭典翰老師這段時間慷慨給予實驗上的所有幫助，不管是方向、材料以及寫作的指導，都讓我了解科學研究應該如何更上一層樓，以及如何對自己的研究更有信心；還有要感謝在最後一個大魔王關卡審視我多年來成果的李心予老師，一針見血的給予我方向，賴時磊老師對於未來發表的建議及肯定，以及同樣身為恩師的楊忠達老師，給予我的關心和高度評價讓我感覺到自己的成果是有價值的，瞬間讓人信心大增啊！

除了老師們，當然也要感謝給予我許多幫助的前輩們，首先是現在去到屏東的賴亦德學長，因為有你讓我在這條路上有了不一樣的思考方向，感謝你教會我人生很重要的道理，就是要學會把自己看的更重要；此外同樣身為地龍實驗室的畢業生，張智涵學長雖然是去年才回到臺灣，卻在我最後的博士生生涯中給予極大的幫

doi:10.6342/NTU202000204

助，讓我少了許多人生的煩惱；而阿倖學姐也是從作為帶領我進入實驗教學的助教開始，就一直給予我相當多的關心，希望以後我還能跟你們夫妻倆一起吃烏龍麵幫你們拍閃光照！接下來要感謝地龍實驗室多年來陪伴我又離我而去的助理及學弟妹們，首先是一直還沒離開又喜歡假裝霸凌我的學弟其嶸，感謝你示範有邏輯又有信心的人生，一起努力做實驗拚發表的日子裡要不是有你的督促現在也許我還沒有機會寫下對你的感謝；還有教會我不要相信任何人的學弟際帆，因為你對於研究的認真和邏輯思考，讓我學著更仔細地審視自己的實驗；此外還有比我晚進來卻一年半就開心畢業的堯翔，你的認真讓我感受到自己的不足，怎麼會有人可以養老蟲養到快要住實驗室的地步？接著謝謝最初帶我進入瓢體蟲實驗漩渦的翡曼、教學及實驗示範謝郁、努力踏實每一步的岳老、雖然碎嘴其實很替我想的易揚、實驗室後勤擔當小八、老是督促我畢業和小孩的東東、地縛靈子倫、每天都很開心叫人不要吵架的明衡、一起瘋貓且給我糧食的虹彣、認真且會找我說心事的紘瑜、教會我顯微鏡和繪圖軟體使用的思卉、一起在東京看你看妹子的俊儒、照顧我常常給我零食的秀晶，還有雖然是學弟但是待的比我久人稱生科系台柱而且真的是台柱的貫浤，讓大家在講最久最老的時候不會先想到我？！

最後當然要感謝多年來帶著徬徨心情等待的我的家人，感謝你們容忍我的任性讓我選擇這條路，感謝男朋友昱瑋及貓女兒 Jessie 的支持和耐心，在我最脆弱的時候陪伴在身邊鼓勵我，讓我知道不孤單要堅強；最後的最後就是 *Aeolosoma viride*，謝謝你們的犧牲讓再生領域的研究又前進了一小步！！

doi:10.6342/NTU202000204

摘要

受傷時為了避免嚴重感染，免疫系統及發炎反應扮演相當重要的角色，現今的研究者主張免疫系統的發展和再生能力的減弱是互為權衡下的結果，然而，關於受傷所引發的發炎反應是否真的與再生能力有相互調控之關係的研究至今依然相當有限，本研究旨在闡明並釐清類鐸受體訊息傳遞路徑(TLRs signailing pathway)如何參與並調控具有全身再生能力之淡水生環節動物瓢體蟲 *Aeolosoma viride* 前端再生，首先我詳細描述瓢體蟲前端及尾端再生的形態學變化，如芽體(blastema)、嘴以及尾板(pygidium)的形成，接著亦證實此過程是透過變形再生(epimorphosis)包含大規模的細胞增生以及極少數的細胞遷移所完成。另一方面為了使用瓢體蟲為模式研究類鐸受體訊息傳遞路徑參與再生的過程，此路徑中古老且保守的 TLR、MyD88 以及 TNF 同源基因亦從瓢體蟲中被鑑定及分析，並分別命名為 *Avi*-TLR-a、*Avi*-TLR-b、*Avi*-MyD88-a、*Avi*-MyD88-i、*Avi*-TNF-1 及 *Avi*-TNF-2，這些基因於瓢體蟲切除頭部後大多先降低其表現量而後才又回升至未受損傷時的水平，其中只有缺少標準 MyD88 蛋白質序列中的 TIR domain，*Avi*-MyD88-i，於傷口形成後立即大量提升其基因表現量並維持直至再生完成。此外使用抗生素及病原相關分子模式(PAMP)中的聚肌胞苷酸(poly I:C)進行再生實驗，亦證實可透過促進或抑制細胞增生達到調控再生成功與否的結果，使用聚肌胞苷酸可於再生過程中進行前發炎細胞激素的雙向調控，其一為透過 *Avi-TLR-a*、*Avi-MyD88-a* 及 *Avi-TNF-1* 的增加，其二為 *Avi-TLR-b*、*Avi-MyD88-i* 及 *Avi-TNF-2* 的基因表現量減少進而抑制了瓢

doi:10.6342/NTU202000204

體蟲的再生能力，再者，此雙向調控可被類鐸受體訊息傳遞路徑之抑制劑 C34 所恢復，利用 RNA 干擾減少 *Avi-MyD88-i* 表現後亦導致瓢體蟲減緩其再生速度，這些結果指出透過類鐸受體訊息傳遞路徑引發的發炎反應於再生過程中需要被正確且確實的調控，而本研究也支持了互為權衡下的免疫系統及再生能力之理論。

關鍵字：環節動物、再生、割處再生、類鐸受體訊號傳遞路徑、發炎

doi:10.6342/NTU202000204

Abstract

The immune system and inflammatory responses associated with injury to prevent deadly infection have been implicated as critical roles during wound healing and regeneration. Nowadays, some scientists have proposed that immune system has been trade-off with the capacity of regeneration in animals. However, the involvement and regulation of injury-induced inflammatory responses with regeneration remains poorly understood in invertebrates. The aim of this study is to unravel the involvement of toll-like receptors (TLRs) signaling pathway in the regeneration of *Aeolosoma viride*, a 3 mm long freshwater annelid with an exceptional whole body regenerative ability. I detailedly described the sequential morphological events during the process of regeneration, such as wound healing and the formation of blastema, mouth, and pygidium after amputation. Massive proliferation and the absence of cell migration indicated that the animal regenerates primarily through epimorphosis. On the other hand, the homologous genes with TLR, myeloid differentiation primary response 88 (MyD88) and tumor necrosis factor (TNF) of the ancient and conserved TLRs signaling pathway were characterized in *A. viride*, namely *Avi*-TLR-a, *Avi*-TLR-b, *Avi*-MyD88-a, *Avi*-MyD88-i, *Avi*-TNF-1 and *Avi*-TNF-2. The expression level of most these genes were reduced after head amputation then back to normal, but that of *Avi-MyD88-I*, that deficiency of toll/interleukin-1 receptor (TIR) domain, induced immediately and kept in higher level. Moreover, the inverse

doi:10.6342/NTU202000204

regulation of regeneration using either antibiotic cocktail or poly I:C, the one of PAMPs were demonstrated through increasing or suppression of cell proliferation. The opposite modulation of poly I:C affected on inflammatory responses of pro-inflammatory cytokine production have been confirmed by two directions of TLR signaling pathway in this worm. One way is to increase transcript levels of *Avi-TLR-a*, *Avi-MyD88-a* and *Avi-TNF-1*, the other way is to decrease gene expression of *Avi-TLR-b*, *Avi-MyD88-i* and *Avi-TNF-2* during wound healing at regenerative tissues. Furthermore, this two regulations of TLR signaling pathway can be rescued by the inhibitor of TLR, C34. Also, the inhibitory effect of regeneration was showed by knockdown of *Avi-MyD88-i.* These results indicated the necessary management of inflammatory responses from TLR signaling pathway during *A. viride* regeneration. Summary, the modulation of TLR signaling pathway in this study supported the trade-off theory between immunity and regeneration.

Key words: annelids, regeneration, epimorphosis, TLR signaling pathway, inflammation

doi:10.6342/NTU202000204

Contents

doi:10.6342/NTU202000204

doi:10.6342/NTU202000204

doi:10.6342/NTU202000204

doi:10.6342/NTU202000204

Figures

doi:10.6342/NTU202000204

doi:10.6342/NTU202000204

doi:10.6342/NTU202000204

doi:10.6342/NTU202000204

Chapter 1

Introduction of immune responses involving in regeneration

doi:10.6342/NTU202000204

1.1 Introduction of regeneration

Regeneration has long been attractive as a scientific interest for its potential to restore the lost, damaged, or aged body structures. This ability is widely distributed and varied among animals. The restoration following injury, amputation, or autotomy can be triggered at various levels of biological organization, such as cell, tissue, organ, structure and even though whole body (Bely & Nyberg, 2010; Brockes et al., 2001; Sanchez Alvarado & Tsonis, 2006). For epimorphic regeneration, some well-known models are studied since the 1700s (Dinsmore, 1991). *Hydra* can regenerate their whole body parts from the re-aggregation of the separated cells (Gierer et al., 1972). Although the cnidarian has a simple body plan, their regenerative mechanism is still not fully understood. The complexity of regeneration can explain why regenerative medicine has been one of the major focuses on medical and biological science in the past 200 years (Chen & Poss, 2017). Planarians are free-living flatworms (Phylum Platyhelminthes) and are well-known for their powerful capacity of regeneration (Reddien & Sánchez Alvarado, 2004; Scimone et al., 2014). They can regenerate new heads, tails, or entire body from small fragments in several days to weeks (Reddien, 2018). In phylum Annelida, the regenerative capacity of anterior, posterior, or both are widespread. However, the multiple independent losses of regeneration were demonstrated, and therefore, the evolutionary history of regeneration is highly complicated in this phylum (Bely & Nyberg, 2010). Another

doi:10.6342/NTU202000204

exemplary model of regeneration is the sea star, all groups of echinoderms can regenerate larval structures and adult arms after bisection (Heyland et al., 2018). Regenerative processes revealed the relationship between larval regeneration and asexual reproduction in which larval arms can regenerate into complete larvae after they were cast off from the ophiopluteus larva (*Ophiopluteus opulentus*) (Vickery et al., 2001).

On the other hand, there are also powerful vertebrate models of regenerative research. Amphibians, including axolotl, newt and clawed frog, can regenerate brain heart, lens, limbs, or spinal cord by cellular transdifferentiation at the wound site (Mitashov et al., 2004; Nye et al., 2003). Zebrafish (*Danio rerio*) has a potential to regenerate the lost tissues such as caudal fin and heart. The availability of genetic approaches and transgenic lines, and ease to control in laboratory and short reproductive cycle make this model very useful for studying molecular mechanisms of organ regeneration (Beffagna, 2019). Unlike amphibian and fish, mammals regeneration occur in restricted developmental stage or organ such as fetal digit-tip, heart and liver in adult. That raise the question of why some organisms can regenerate perfectly and others cannot, but this problem remains unsolved (Maden, 2018). Epimorphic regeneration are categorized into two types, morphallaxis and epimorphosis, by Morgan, T. H (Morgan, 1901). Epimorphic regeneration normally involves the formation of a proliferative blastema that composes from stem or progenitor cells which will eventually differentiate into mature tissues or

doi:10.6342/NTU202000204

organs. The examples of epimorphosis are the regenerating planarian, annelid and amphibian limb (Gaete et al., 2012; Goss, 1969; Özpolat & Bely, 2016; Wenemoser & Reddien, 2010). Indeed, cell proliferation served as a key event in epimorphic regeneration; its quantity and onset differentiate the form of regeneration (Paulus & Müller, 2006; Reddien & Sánchez Alvarado, 2004). Morphallaxis is involving the transformation of existing body parts by cell reorganization with limited new cell growth, and *Hydra* is the prominent model for morphallaxis in which the re-organized body parts become smaller in size without blastema formation (Bosch, 2007).

Stem or progenitor cells are the popular candidates for studying the renewal and homeostasis of tissue in the field of regenerative medicine. These cell populations are well-known to actively proliferate and/or differentiate to maintain homeostasis in the vertebrates. However, direct transplantation of stem cells have been observed to be not fully effective, depending on species, type of tissue or organ, or the host. Therefore, a successful model in regeneration research is necessary for further application in medical therapy (Murry et al., 2004; Sánchez Alvarado & Tsonis, 2006).

1.2 Inflammation participate in hemostasis after injury

The inflammatory responses resulting from the injury-induced activation of the innate immune system have been implicated as critical regulators of wound repair and

doi:10.6342/NTU202000204

regeneration during the processes of inflammation, new tissue formation, and tissue remodeling (Godwin et al., 2013; Peiris et al., 2014). The process of inflammatory responses triggered by pathogens, harmful cells, toxic components, or irradiation is the first-line defense against deadly infection. After damage, the acute inflammation consists of a series of rapid complex reactions that interact and coordinate the events between cellular and molecular factors to maintain tissue homeostasis. A classic inflammatory response contains four steps: initiation from inflammatory inducers, the sensors that detect inducers, the inflammatory mediators produced by the sensors, and the damage tissues that are affected by the inflammatory mediators (Chen et al., 2018b; Medzhitov, 2010). The type of inflammatory trigger dictates the response of immune system. Microbial or pathogenic structures known as pathogen-associated molecular patterns (PAMPs) as inducers can activate the acute inflammation after injury through binding of the highly conserved pattern-recognition receptors (PRRs) as sensors expressed in both immune and nonimmune cells. Moreover, some PRRs also recognize endogenous signals such as high-mobility group box 1 (HMGB1), ATP, interleukin-1β (IL-1β), and DNA from damaged cells and are known as danger-associated molecular patterns (DAMPS) (Brusselle & Bracke, 2014; Venegas & Heneka, 2017). As a result, the inflammatory inducers are detected by PRRs, such as Toll-like receptors (TLRs), which are expressed on tissue-resident immune cells and induce the production of pro-inflammatory cytokines

doi:10.6342/NTU202000204

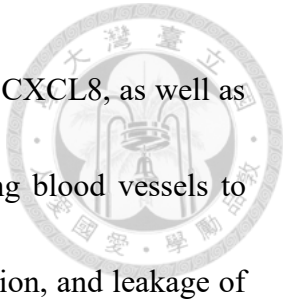

such as IL-1, IL-6 and TNF and chemokines, for instance CCL2 and CXCL8, as well as prostaglandins. These mediators then act on target tissues, including blood vessels to induce vasodilation, neutrophils recruited to sites of acute inflammation, and leakage of plasma into the infected or injury tissue. Then, tissue-resident macrophages, and mast cells seek and perform phagocytosis to eliminate debris from invading pathogens and apoptotic cells (Medzhitov, 2010; Pecchi et al., 2009).

After inflammation, and remodeling, growth factors and cytokines such as transforming growth factor- α (TGF-α), IL-10, and suppressors of cytokine signaling (SOCS), also released from macrophages to activate subsequent events such as tissue formation and remodeling. In vertebrate cutaneous wounds, the epithelial barrier is re-established by the migration of keratinocytes to the injure site. Then, fibroblasts move into the wound area to replace the temporary matrix with granulation of scar tissue composed of extracellular matrix (ECM) including fibronectin and collagen. Follow this replacement, damaged area is re-vascularized by endothelial cells, and fibroblasts differentiate into myofibroblasts that carry out wound closure. Finally, the collagen-rich scar tissue in the injury site then undergoes slow remodeling in the subsequent weeks to months (Mescher, 2017; Midwood et al., 2004). Besides, immune cells such as macrophage and monocyte have been shown to have essential roles in both of immunity and regeneration, for example, skin repair of mice and scar-free tail regeneration in

doi:10.6342/NTU202000204

amphibians (Mescher et al., 2017). That highlights the important correlation and regulation between the immune system and regeneration that I will discuss in next section.

The ability of regeneration is a widely diversity among different organisms in vertebrates and invertebrates. Mammals such as adult human and mice respond to tissue damage through activating resident progenitor cell proliferation, or by the scar formation (Aurora & Olson, 2014; Erickson & Echeverri, 2018). However, amphibians including salamander and frog display varying potential for scar-free regeneration. In mammals, fetal scar-free regeneration is connected with an immature immune system in a quiet inflammatory microenvironment. And a progressive loss of scar-free repair is observed in the frog after metamorphosis, which is associated with the maturation of immune system (Bertolotti et al., 2013; Godwin & Rosenthal, 2014). Therefore, the relationship between the loss of regenerative capacity and maturation of immune system has been established that through comparative study of deficiency immune responses. In the PU.1-null mice, whose macrophage and neutrophil are depleted, more mature epithelial layer at wound site was formed (Martin et al., 2003). In addition, *Xenopus laevis* tadpole failed to regenerate tail in a specific time of refractory period (stage 45–47). The ability of regeneration during this refractory period was significantly enhanced by knockdown of *PU.1* gene that cause immune suppression from leukocytes depletion (Fukazawa et al., 2009). The speed of the fin regeneration is also faster in the neutrophil-deficient *runx1*^{w84x}

doi:10.6342/NTU202000204

zebrafish, suggesting that neutrophil could play an inhibitory role in zebrafish regeneration (Li et al., 2012). These studies support the hypothesis of antagonizing interactions between the immune system and regeneration. Nevertheless, there is limited publication that related study reports in invertebrate model of scar-free regeneration. Although the well-known regenerative model of hydra and planarian have been studied about regenerative mechanism for hundred years, but the detail of the roles of immune system involving in regeneration is still unclear. Therefore, a new regenerative model of *Aeolosoma viride* is introduced to study the ancient and conserved TLR of PRRs during regeneration.

1.3 Inflammatory responses initiated by pattern recognition receptors (PRRs)

Innate immunity is understood as nonspecific defenses against pathogen infection in both of vertebrates and invertebrates. However, studies about immunological recognition of adaptive immune system between antigen and major histocompatibility complex (MHC) molecules on the surface of T cells have been published in 1990s (Fleischer & Schrezenmeier, 1988). After scientists identified antigen receptor molecules from T cells (T cell receptors, TCR) that related to the immunoglobulin family but separate from phylogeny, the family of PRRs was discussed in 1989 (Janeway, 1989). Moreover, the first Toll receptor was identified from *Drosophila* in 1985 (Anderson et al., 1985), the

doi:10.6342/NTU202000204

discovery of TLRs family presented the specificity in binding conserved PAMPs. And therefore, the innate immune system is also actually specific, relying on this family of receptor molecules to detect components of foreign pathogens. TLRs family became the first identified class of PRRs. Therefore, specific innate immune responses such as activation of complement cascades, phagocytosis, pro-inflammatory cytokine production, and apoptosis can be activate by PRRs after non-self antigens invasion (Akira et al., 2001; Janeway & Medzhitov, 2002; Kawai & Akira, 2010).

The families of PRRs include the C-type lectin receptors (CLRs), nucleotide oligomerization domain (NOD)-like receptors (NLRs), retinoic acid-inducible gene (RIG)-I-like receptors (RLRs) and TLRs (Kumagai & Akira, 2010). CLRs expressed on the surface of dendritic cells interact with pathogens that recognize carbohydrate structures. They can be divided into mannose receptor family and asialoglycoprotein receptor family, and activity of these receptors is mediated by conserved carbohydrate-recognition domains (CRDs) (Geijtenbeek & Gringhuis, 2009). In addition to innate immunity, CLRs such as Dectin-1 also work with other PRRs to activate T cells mutation in adaptive immunity (LeibundGut-Landmann et al., 2007; Palm & Medzhitov, 2009). NLRs and RLRs are intracellular cytosolic sensors that are primarily involved in virus and bacteria recognition. Nucleotide-binding oligomerization domain (NODs) is the specific domain of NLRs, which binding to nucleoside triphosphate

doi:10.6342/NTU202000204

activate inflammatory caspases (Franchi et al., 2009; Martinon & Tschopp, 2007). The family of RLRs detects RNA virus in cytoplasm and activates the innate immune system through the production of pro-inflammatory cytokines and type I interferons (IFNs) (Yoneyama & Fujita, 2009). This family also crosstalk with TLRs to trigger innate immunity and to control programming of cell-mediated immunity in the adaptive immune responses (Loo & Gale, 2011). Finally, TLRs has been shown to play an ancient and crucial role in host defense of pathogen in vertebrates and invertebrates (Akira et al., 2006; Buchmann, 2014).

The first member of TLRs family, Toll, was identified in fruit fly *D. melanogaster*, and Toll is required for dorso-ventral axis formation in embryos (Anderson et al., 1985; Hashimoto et al., 1988). Toll (Toll-1) was identified as an activator of immune response linking to induction of the cecropin gene promoter in a *Drosophila* hemocyte cell line in 1995 (Rosetto et al., 1995). Since the relationships between Toll and immunity has been demonstrated, more related studies focused on the characterization of homologous genes in mammals. First identified human Toll is a type I transmembrane receptor consisting of a leucine-rich repeat (LRR) domain in extracellular domain, and a homologous domain of the human interleukin (IL)-1 receptor domain on the cytoplasmic side (Medzhitov et al., 1997; Valanne et al., 2011). Both of *Drosophila* and human Tolls activate NF-κB through the conserved adaptor myeloid differentiation primary response 88 (MyD88) and

doi:10.6342/NTU202000204

transduce the signal through homologous protein kinases—Pelle and interleukin-1 receptor-associated kinase (IRAK) to initiate the production of antimicrobial peptides (AMPs) or cytokines (Janeway & Medzhitov, 2002). This pathway also associates with the cellular immune response, which includes phagocytosis and encapsulation of parasites by macrophages (Doyle et al., 2004; Holmblad & Söderhäll, 1999). Nowadays, nine and ten functional TLRs have been identified in fly and human (Kadowaki et al., 2001; Valanne et al., 2011). Only one in *Drosophila* has been confirmed to responsed to bacterial, fungal, and viral infection through the endogenous ligand Spätzle in innate immunity (De Gregorio et al., 2001; Jang et al., 2006). On the other hand, human TLRs can respectively recognize of various PAMPs, such as TLR1, 2, 6 and 10 by bacterial lipopeptide, TLR3 by virus dsRNA, TLR4 by lipopolysaccharide (LPS) from Gram-negative bacteria , TLR5 by bacterial flagellin, and TLR7, 8 and 9 by nucleic acid and heme motifs (Kawai & Akira, 2010; Roach et al., 2005). Therefore, the TLRs signaling pathway can be activated from specific ligand binding to their receptor, and further processes the signal cascade lead to the upregulation or suppression of downstream genes including cytokines and chemokines of inflammatory responses (Kawai & Akira, 2005).

1.4 TLR signaling pathway in invertebrates

doi:10.6342/NTU202000204

In addition to fly and human, TLRs have been identified in many animals ranging from cnidarians to mammals, and detected in immune cells including macrophages, lymphocytes, dendritic cells , T cells, and B cells and non-immune cells such as epithelial cells, endothelial cells and fibroblasts (Delneste et al., 2007). Because innate immunity is the major defense mechanism against infection from pathogens (Zheng et al., 2005), undoubtedly, pattern recognition features of TLRs display a dominate role in the innate immunity in invertebrates. Therefore, numerous TLRs or TLR-like genes have been documented in invertebrates (Coscia et al., 2011), for example, horseshoe crab *Tachypleus* and lobster *Homarus americanus* from phylum Arthropoda, squid *Sepiella japonica*, oyster *Crassostrea gigas* and mussel *Mytilus coruscus* from phylum Mollusca, sea urchin *Strongylocentrotus intermedius* from phylum Echinodermata, earthworm *Eisenia andrei* and leech *Hirudo medicinalis* from Annelida and nematode *C. elegams* (Clark et al., 2013; Cuvillier-Hot et al., 2011; Inamori et al., 2000; Pujol et al., 2001; Skanta et al., 2013; Wang et al., 2018; Xu et al., 2018; Zhang et al., 2011). Although one TLR has been found from *C. elegams*, functional assay showed that this TLR gene (*CeTol-1*) appears no function in immunity. Wide distribution of TLRs in animals suggests the evolutionary importance across invertebrates and vertebrates in innate immunity (Ausubel, 2005; Kimbrell & Beutler, 2001).

In human TLR signaling pathway, five adaptor proteins including Toll/interleukin-1

doi:10.6342/NTU202000204

(IL-1) receptor (TIR) domain including MyD88, MyD88-adaptor-like protein (MAL), TIR-domain-containing adaptor protein inducing interferon-β (IFNβ) (TRIF) and TRIF-related adaptor molecule (TRAM) can be recruited to TIR domains on the C' terminal of TLR to initiate the signaling. Conversely, the sterile α- and armadillo-motif-containing protein (SARM) serves as a negative regulator to inhibit TRIF-dependent signaling (Carty et al., 2006; O'Neill & Bowie, 2007). The sequence and structure of MyD88 are conserved across evolution and its key role in immunity has been verified in both vertebrates and invertebrates (Rodet et al., 2015). This adapter protein has been shown to respond the signaling receptors such as TLR2, TLR4, TLR5, TLR7 and TLR9 in MyD88-mutant mice (Kawai et al., 1999). To overexpress the homolog of mammalian Myd88 from *Drosophila* named *Dm*MyD88, can induce the expression of the antifungal peptide Drosomycin, but the induction of Drosomycin were reduced in *Dm*MyD88-deficient flies (Tauszig-Delamasure et al., 2002). Besides, MyD88 is strongly up-regulated the expression of mRNA or protein levels after LPS challenge in sponge *Suberites domuncula*, Zhikong scallop *Chlamys farreri*, white shrimp *Litopenaeus vannamei*, mussel *Mytilus coruscus*, disk abalone *Haliotis discus discus*, oyster *Crassostrea gigas*, leech *Hirudo medicinalis* and sea cucumber *Apostichopus japonicus* (Guo et al., 2018; Lu et al., 2013; Priyathilaka et al., 2018; Qiu et al., 2007; Rodet et al., 2015; Wiens et al., 2005; Xin et al., 2016; Zhang et al., 2012). All of those evidences show that the conserved functions of MyD88 involves

doi:10.6342/NTU202000204

in innate immunity to respond pathogen invasion (Ren et al., 2017).

Furthermore, the downstream of TLR signaling pathway can induce expression of several cytokines including type I interferon (IFN), pro-inflammatory cytokines and other inflammatory cytokines (Takeda & Akira, 2004). Tumor necrosis factor (TNF) belongs to TNF superfamily that is a large family of structurally related proteins among pro-inflammatory cytokines (MacEwan, 2002). TNF is a multifunctional cytokine that plays many important roles in cellular events such as cell survival, cell proliferation, cell differentiation, and cell death (Wang & Lin, 2008). In comparison with vertebrates, the research of TNF superfamily in invertebrates is still required. In 2002, the first protein of TNF superfamily in *Drosophila* named Eiger was discovered which can induce cell death indirectly by triggering JNK signaling (Moreno et al., 2002). Then, four genes of TNF superfamily were identified as potential members with LIGHT and TL1A from sea urchin *Strongylocentrotus purpuratus* genome database (Hibino et al., 2006). Following the discovery of TNF superfamily members from sea urchin, more TNF superfamily members were identified from invertebrates such as shrimp *Marsupenaeus japonicas*, abalone *H. discus discus*, oyster *C. gigas* and ascidian *Ciona savignyi* (De Zoysa et al., 2009; Mekata et al., 2010; Sun et al., 2014; Zhang et al., 2008). Similar as TLR and MyD88, TNF superfamily is also involved in responses to pathogen infection. CsTL from *C. savignyi* was upregulated in the hemocytes after LPS challenge (Zhang et al., 2008).

doi:10.6342/NTU202000204

In addition, recombinant CgTNF-1 incubated with oyster haemocytes was determinated the crucial modulation roles of apoptosis and phagocytosis to be involved in the oyster innate immunity (Sun et al., 2014).

1.5 Roles of TLR signaling pathway in the processes of regeneration

TLRs played essential roles in innate and adaptive immunity (Caamaño & Hunter, 2002; Olson & Miller, 2004; Pasare & Medzhitov, 2005). Additionally, significance roles of TLRs signaling pathway in tissue repairing were documented and can be a potential therapeutic strategy in regenerative medicine. In the leech *H. medicinalis*, intracellular receptors of *Hm*TLR1 and *Hm*NLR responsed to microbial challenges and are involved in neuroimmune response. These two receptors are accumulated in the injury site of the nerve cord and are involved in neural defense and regeneration (Cuvillier-Hot et al., 2011). Further characterization of MyD88 and sterile alpha and amardillo-motif-containing protein (SARM), *Hm*-MyD88 and *Hm*-SARM, was also published by the same team. Down-regulation of *Hm*-MyD88 and up-regulation of *Hm*-SARM in both RNA and protein levels take place during the early stage of the axon repair (Rodet et al., 2015). Besides, defects in epithelial wound healing in $Toll^{-/-}$ and *Dif dl* (NF-κB in *Drosophila*) were observed in the mutant embryos following injury. Therefore, Toll/NF-κB pathway not only plays essential roles in dorsal-ventral polarity but also essential for epidermal

doi:10.6342/NTU202000204

wound closure in *Drosophila* embryos (Carvalho et al., 2014). To summarize, there are limited studies about the involvement of TLRs signaling pathway in invertebrate regeneration. The freshwater annelid *A. viride*, which possesses with the whole body regenerative ability may be a suitable for studying the relationship between innate immunity and regeneration.

1.6 The regenerative model of *A. viride*

In this study, regenerative capacity and TLR signaling pathway involving in regenerative processes of *Aeolosoma viride* STEPHENSON 1911 was described. This worm belongs to the family Aeolosomatidae (Annelida, Aphanoneura), a group of cosmopolitan minute annelids residing mostly in freshwater habitats around the world (Glasby & Timm, 2008; Glasby et al., 2009). Approximately 30 species have been identified in this family, and they predominantly reproduce by agametic reproduction; sexual reproduction had only been reported in one species, *A. singulare* (Falconi et al., 2015; Marotta et al., 2003). Agametic reproduction is associated with strong regenerative abilities because of the extensive similarities occurring in both processes (Bely, 1999; Berrill, 1952; Galloway, 1899). Paratomy is a form of agametic reproduction in which linear chain of zooids can simultaneously form by fission in the posterior segment. In *A. viride*, paratomic fission appears to be the prevalent form of asexual reproduction. This

doi:10.6342/NTU202000204

reproductive strategy has been reported only in a few families of Annelida such as Aeolosomatidae, Naididae, Spionidae and Spionidae (Herlant-Meewis, 1951; Radashevsky, 1996; Smith, 1985; Zattara & Bely, 2016). Although the ability to regenerate the anterior and posterior segments after injury has been demonstrated in certain species of Aeolosomatidae (Brace, 1901; Herlant-Meewis, 1953; Herlant-Meewis, 1964), a detailed description of this process is still unavailable. Therefore, the detailed description of the regeneration process in *A. viride* was first documented in the present study, and follow this capacity that the essential mechanisms from immune responses were also revealed.

The body of individuals of *A. viride* was typically ~2–3 mm in length and contained 10–12 segments; on each segment, there were two bilateral pairs of chaetal bundles. The mouth was a simple circular opening on the ventral surface of the peristomium. Anterior to the peristomium was the prostomium, which bore no chaetae. The prostomium took the form of an enlarged lobe and was morphologically distinguished from the narrower peristomium. Posterior to the peristomium were the chaetae-bearing body segments. The alimentary canal was located at the center of the segmented body, which included the esophagus, midgut, and hindgut. The pharynx chamber with muscular wall was connected to the esophagus, and the midgut was located at the segmented middle body region (segments 4–8). In the more posterior segments (segment 9 and beyond) of alimentary

doi:10.6342/NTU202000204

canal forms the hindgut. The pygidium, which was also free of chaetae, was at the posterior terminus of the body, and the intestine opened to the exterior through the anus, which was located at the posterior tip of the pygidium. The regionalized alimentary canal could be clearly observed under a dissecting microscope and was used as a morphological landmark to distinguish body regions (Fig. 1-1A). After amputation at the anterior position, the worm was divided into a regenerating head and tail fragments (Fig. 1-1B).

In *A. viride*, individuals underwent nutrition-dependent growth by adding new body segments at the posterior growth zone (pgz), which is similar to the growth pattern seen in many other annelid species such as *Nais communis* and *Pristina leidyi* (Kharin et al., 2006; Zattara & Bely, 2013). In worms >3 mm in length, an unusually long posterior region which contained the narrow hindgut could be easily observed (Fig. 1-1C). In these worms, a new head (prostomium and peristomium) developed in the posterior middle body region while remaining connected to the anterior body segments (parental chain; Fig. 1-1D). The area where the zooid (filial chain) developed was morphologically characterized by two ring-shaped thickenings of body wall, which was referred to as the fission zone (fz). Once the head structure had fully formed, the zooid detached and became an independent individual (Fig. 1-1E). Among these species, life history and population dynamics have been previously characterized in *A. viride* (Falconi et al., 2015; Falconi et al., 2006; Herlant-Meewis, 1951). TLR signaling pathway is conserved from

doi:10.6342/NTU202000204

invertebrate to vertebrate, and some PRRs have been documented in phylum Annelid such as earthworm *E. andrei* and leech *H medicinalis* (Cuvillier-Hot et al., 2011; Skanta et al., 2013). The objective of this study was to evaluate the regenerative ability and demonstrated the roles of the TLR signaling pathway from innate immunity during *A. viride* regeneration.

doi:10.6342/NTU202000204

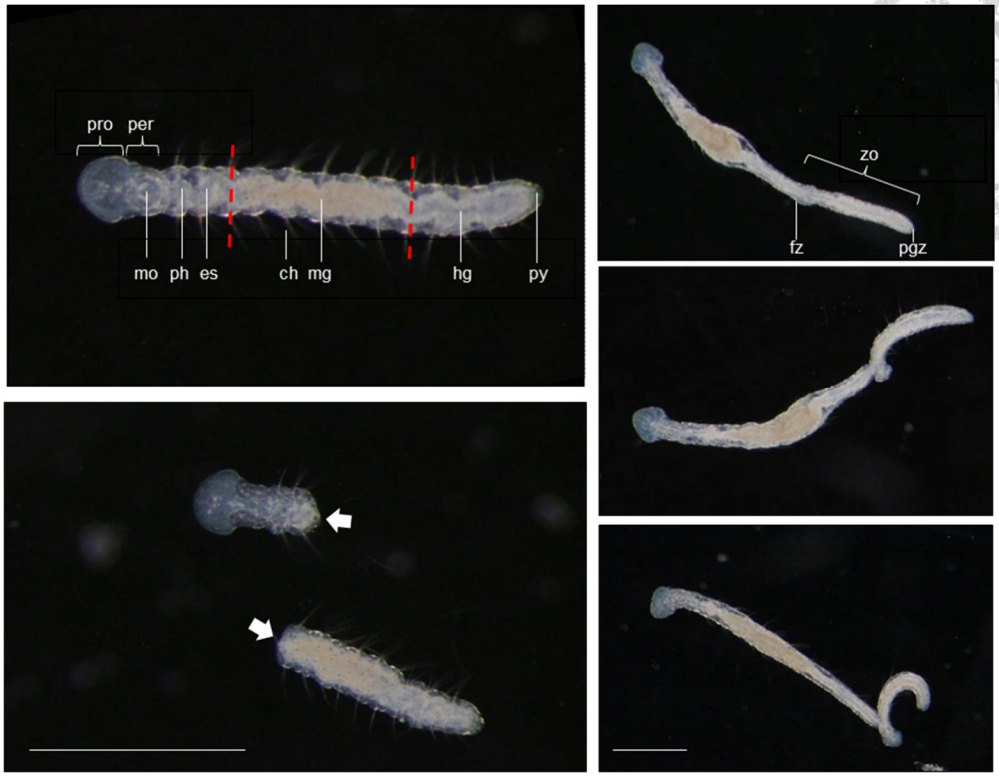

Figure 1-1. Morphology and paratomic fission in *A. viride*. (A) The first segment of an intact individual of *A. viride* has a prostomium and a peristomium with a mouth. The transparent body has an enlarged midgut located at the center of its alimentary canal. The pygidium is located on the last segment of the posterior end. The red dashed lines indicate the amputation sites anterior and posterior to the enlarged midgut. (B) After the worm was amputated at the anterior site indicated in A, the two fragments individually proceeded to undergo anterior or posterior regeneration (indicated by white arrows). (C–E). The process of paratomic fission separated an intact worm into a parental chain and a zooid. Scale bars: 1 mm. ch, chaetae; es, esophagus; fz, fission zone; hg, hindgut; mg, midgut; mo, mouth; per, peristomium; pgz, posterior growth zone; ph, pharynx; pro, prostomium; py, pygidium; zo, zooid

doi:10.6342/NTU202000204

Chapter 2

General characterization of regeneration in *Aeolosoma viride*

(Annelida, Aeolosomatidae)

doi:10.6342/NTU202000204

2.1 Introduction

Annelids are known for their ability to regenerate lost body segments, but how annelids regenerate is not as well studied as other popular invertebrate models for regeneration research, such as hydra and planarian (Bode, 2003; Reddien & Sánchez Alvarado, 2004; Sánchez Alvarado & Tsonis, 2006). In this study, I described the regenerative process of *Aeolosoma viride* STEPHENSON 1911. *A. viride* belongs to family Aeolosomatidae (Annelida, Aphanoneura), a group of cosmopolitan minute annelids residing mostly in freshwater habitats around the world (Glasby & Timm, 2008; Glasby et al., 2009). Approximately 30 species have been identified in this family, and they predominantly reproduce by agametic reproduction; sexual reproduction had only been reported in one species, *A. singulare* (Falconi et al., 2015; Marotta et al., 2003).

Agametic reproduction is highly associated with strong regenerative abilities because of the extensive similarities occurring in both processes (Bely, 1999; Berrill, 1952; Galloway, 1899). Paratomy is a form of agametic reproduction in which linear chain of zooids can simultaneously form by fission in posterior segment. This reproductive strategy has been reported only in a few families of Annelida such as Aeolosomatidae, Naididae, Spionidae and Spionidae (Herlant-Meewis, 1951; Radashevsky, 1996; Smith, 1985; Zattara & Bely, 2016). Species from these families are different in their regenerative capacities to regenerate anterior and posterior segments

doi:10.6342/NTU202000204

(Bely & Sikes, 2010). The Naididae, *Pristina leidyi* is best known to reproduce by paratomic fission and is capable to complete both anterior and posterior regeneration via epimorphosis (Zattara & Bely, 2013). Epimorphic regeneration normally involves the formation of a proliferative blastema, which will eventually differentiate into mature tissues or organs (Morgan, 1901). Indeed, cell proliferation served as a key event in epimorphic regeneration; its quantity and onset differentiate the form of regeneration (Paulus & Müller, 2006; Reddien & Sánchez Alvarado, 2004).

Although an ability to regenerate the anterior and posterior segments after injury has been demonstrated in certain species of Aeolosomatidae (Brace, 1901; Herlant-Meewis, 1953; Herlant-Meewis, 1964), a detailed description of the process is still unavailable. Among these species, life history and population dynamic have been previously characterized in *A. viride* (Falconi et al., 2015; Falconi et al., 2006; Herlant-Meewis, 1951). The objective of this study is to evaluate the regenerative ability of *A. viride* by documenting specific morphological events during the regenerative process, determining the minimum number of segments required for the worm to regenerate, and identifying the location of proliferating cell population during the process of regeneration. My study also aims to distinguish whether *A. viride* regenerates primarily by morphallaxis or epimorphosis in this chapter.

This study provided a detailed description of the regeneration process in *A. viride*,

doi:10.6342/NTU202000204

and reported that this worm can restore its lost body parts, both anteriorly and posteriorly. Furthermore, a high level of cell proliferation was demonstrated that occurred at the wound site is critical for the completion of regeneration. Finally, this research demonstrated the potential of *A. viride* to be a feasible model for regenerative studies.

2.2 Materials and Methods

2.2.1 Animal cultures and regeneration procedure

Cultures of *Aeolosoma viride* was raised in artificial spring water (ASW, 48 mg/L $NaHCO_3$, 24 mg/L $CaSO_4 \cdot 2H_2O$, 30 mg/L $MgSO_4 \cdot 7H_2O$, and 2 mg/L KCl in distilled water, pH = 7.4) at 25°C under 12 hours of day-night cycles. Grounded oat meal was provided to the worms as primary food source. 20 mg of oat meal was fed to 500 ± 200 worms 3 to 5 times per week. In all regeneration experiments described here, worms with zooids were not selected for further experiment in this chapter. Animal preparation and basic experimental procedures were as described in previous study (Chen et al., 2018a). Briefly, the experimental procedures began with starvation in ASW overnight prior to amputation. Anterior regeneration was initiated by amputating four anterior segments including prostomium, perstomium and three segments with chaetae. Posterior regeneration was initiated by amputating segment posterior to the midgut, which is the enlarged portion located posterior to the ninth segment bearing chaetae (Fig. 1A). After

doi:10.6342/NTU202000204

amputation, ten worms for each group were transferred into fresh ASW or ASW containing 2.5 μM taxol (Sigma-Aldrich) for subsequent regenerative experiments. Regenerating worms were collected for the following 0 to 7 days after amputation. Specimens were examined live (in ASW) or fixed in 4% paraformaldehyde by use of a dissecting microscope (WILD M8, Leica) for detailed morphological observation. For fixations, worms were anesthetized for 20 s in cold (4℃) 50% menthol in ASW, then fixed for 35 s in 2% paraformaldehyde in 25% menthol, and transferred to 4% paraformaldehyde (PFA) in ASW overnight at 4℃. At least 10 individuals were examined for all observations and experiments and at different time points.

2.2.2 Labeling with 5-ethynyl-2′-deoxyuridine for cell proliferation and migration

Cell proliferation was monitored by *in vivo* labeling with EdU (Salic & Mitchison, 2008). Each group of five worms were exposed to 0.1 mM of EdU (Invitrogen) in ASW for 12 or 24 hours. Two labeling protocols were separately applied for different experimental purposes regarding cell proliferation and migration. For the cell proliferation experiment, worms were amputated, and incubated in EdU solution for 12 hours prior to collection. For the pulse-chase experiment, worms were incubated in EdU solution for 24 hours prior to amputation, and specimens were then fixed in 4% PFA at 24, 72 and 120 hours post-amputation (hpa). EdU incorporated during S-phase of mitosis

doi:10.6342/NTU202000204

was detected by immunohistochemistry (IHC) using the Click-it EdU Alexa Fluor 488 Imaging Kit (Invitrogen) according to the manufacturer's instructions. Specimens were mounted in Fluoromount-G^{TM} (eBioscience) and images were taken on an Olympus DP80 microscope.

2.2.3 Plasmid DNA constructs for RNA interference (RNAi)

A partial sequence of *Avi-beta tubulin isoform 1* was identified from unpublished transcriptome of *A. viride*. To extend the partial sequence of *Avi-beta tubulin isoform 1*, rapid amplification of cDNA ends (RACE) was performed to obtain a full sequence; this sequence was published in National Center for Biotechnology Information (NCBI; GenBank accession no. KY079093.1). The RNAi protocol was modified from methods described previously (Kamath et al., 2001). A partial sequence of 300 base pairs (bp) of yellow fluorescent protein (*YFP*, as MOCK group) or *Avi-beta tubulin isoform 1* were constructed with L4440 vector (provided by Dr. Wu's lab, Institute of Molecular and Cellular Biology, National Taiwan University, Taiwan) and transformed into a ribonuclease (RNase) III-deficient competent cell strain HT115 (DE3). Worms were fed with 1×10^8 competent cells containing double-stranded (dsRNA) for three consecutive days. The microinjection method used to deliver dsRNA was modified from the method described previously (Newmark et al., 2003). Both the *YFP* and *Avi-beta tubulin isoform*

doi:10.6342/NTU202000204

1 dsRNA were transcribed in vitro with T7 polymerase (Ambion). I used a Nanoliter 2000 injector (World Precision Instruments) to inject each individual animal with 50 ng of dsRNA on each of two consecutive days. Each injection was set at slow mode. The injection was made into the body cavity of the fourth anterior segment. Worms were then collected for RNA extraction or regeneration study

2.2.4 RNA exaction for quantitative real-time RT-PCR (qRT-PCR)

The total RNAs were extracted from five intact worms using TRIzol and reverse-transcribed to cDNA using SuperScript III Kit (Invitrogen). Transcriptional levels were determined by Bio-Rad iCycler™ using SYBR green system (Bio-Rad). The primers used to amplify *Avi-beta tubulin isoform 1* were 5'- CTGTACTGCCAGGCCGATATAC-3' and 5'-GACAAGAGTCTGTCTGACAATGACA-3'. *Avi-actin* was used as internal control with specific primers: 5'-ATGGAGAAGATCTGGCATCA-3' and 5'-GGAGTACTTGCGCTCAGGTG-3' designed from *Avi-actin* (NCBI # KY079092.1). Relative quantification of gene expression was calculated by the $\Delta\Delta C_T$ method. Three technical replicates were performed in each real-time PCR reaction, and a no-template blank was served as negative control.

2.2.5 Statistics

doi:10.6342/NTU202000204

Data were tested for significance using two-tailed unpaired student's t-test. Probability values of $p < 0.05$ were regarded as statistically significant.

2.3 Results

2.3.1 Anterior and posterior regeneration in *A. viride*

The body of *A. viride* is about 2-3 mm in length and contains 10 to 12 segments. After amputation at anterior or posterior position, the worm will be divided into a regenerating head and tail fragments. The fragments disengaged with the alimentary canal, and coelomic fluids gushed from the inner cavity. After amputation, the regenerating head *A. viride* adhered to the bottom of culture chamber, and its wounded area remained rough and uneven from 0 to 3 hpa. The epithelium formed an outer layer that covered and smoothened the rough wounded area within 6 hpa. At 12 hpa, a small amount of hyaline cell masses started to develop at the regenerating area, and formed the regenerative blastema. The protruding blastema expanded from the center of the wounded area and became apparent from 24 to 48 hpa. Vertical contraction could be observed from 72 hpa, but the regenerating worms were still unable to move freely. The anterior segment took the form of a narrower lobe and circular structure reappeared at the ventral side that characterized mouth formation in peristomium at 96 hpa. At this point, a tubular structure (esophagus) extended to connect with the enlarged alimentary canal. After 96 hours of

doi:10.6342/NTU202000204

regeneration, the regenerating prostomium gradually bulged and became wider than posterior segments. During 96 to 120 hpa, newly formed mouth in peristomium is clearly connect to alimentary canal (Fig. 2-1). During the entire process of anterior regeneration, the regenerating *A. viride* remained adhered to the bottom of culture chamber. Most of them could swim freely around 120 hpa, which was considered as an indicator for successful anterior regeneration in *A. viride*.

In the intact worm, a double ring-shaped fission zone could be clearly observed in hindgut. Physiological response similar to anterior amputation was observed, the worm instantly and severely twisted after posterior amputation. Similar to anterior regeneration, posterior amputation had created a rough and uneven wounded area at 0 and 3 hpa. The wound area was covered by epithelium around 6 hpa, posterior of midgut narrowed and the blastema started to develop at the same time during 12 to 24 hpa. The size of the regenerative blastema remained relatively stable during the next 48 hours, no significant sign of enlargement was observed. The regenerating posterior end extended and narrowed during at 72 hpa. After 72 hpa, fission zone formed in hindgut at 96 hpa. Finally, the posterior end indented and the pygidium with anus re-formed, indicated the completion of the regenerative process at 120 hpa (Fig. 2-2).

To characterize the regenerative capacity, the *A. viride* was anteriorly or posteriorly amputated to 3, 6 or 9 body segments. Amputated worms with three posterior segments

doi:10.6342/NTU202000204

could still complete anterior regeneration, but the percentage of successful regenerates was decreased to around 40%. Over 60% of worms with 6 or 9 posterior segments completed their anterior regeneration within 5 dpa. Posterior regeneration shared a similar pattern. On average 60% of worms with three anterior segments completed their posterior regeneration. The percentage of successful regenerates in posterior regenerating worms with 6 or 9 anterior segments increased to over 80% at 5 dpa (Fig. 2-3).

2.3.2 Cell proliferation in the regenerative process of *A. viride*

Incorporation of EdU followed by fluorescent staining was used to identify proliferating cells in *A. viride*. In this study, EdU incorporation was used to detect the amount of proliferating cells in *A. viride.* To reach optimal condition, worms were incubated with EdU 12 hours prior to amputation (Fig. 2-4). The proliferating cells was confirmed by co-staining with a nuclear dye Hoechst 33342 (Fig. 2-5A). EdU signals were present on both the internal and superficial surface of the regenerating worm (Fig. 2-5B). Most of the proliferation took place in the anterior mouth, fission zone, and posterior growth zone where EdU signal formed a circle and two rings respectively (Fig. 2-6 and 7). Minor EdU signals randomly distributed in intact and anterior regenerating worms from 0 to 12 hpa. During anterior regeneration, the EdU signal became concentrated at the blastema; the strongest signal was observed from 24 to 48 hpa, and

doi:10.6342/NTU202000204

then gently decreased from 72 to 120 hpa. At 96 and 120 hpa, EdU^+ cell formed a circular structure at the center of peristomium, which indicated the development of mouth (Fig. 2-6). On the other hand, posterior regeneration showed a similar pattern of cell proliferation. During the first 12 hours of posterior regeneration, few proliferative signals were observed near the wounded area. At 24 hpa, minor EdU signal remained randomly dispersed, but the majority of proliferating cells were distributed along the hindgut near the posterior end. EdU signal significantly increased and became most concentrated at the posterior regenerating site during the next 48 hours. At 72 hpa, EdU^+ cell formed a ring-shaped posterior growth zone at the wounded site and reached its maximum intensity. Although the general EdU signal intensity decreased, anterior ring area surrounding the segment which indicated the fission zone re-appeared at 96 hpa. (Fig. 2-7).

2.3.3 Cell proliferation is required for anterior regeneration

Worms were treated with taxol, an inhibitor of cell proliferation that works by interfering with the normal function of microtubules. The EdU signals in the blastema were apparently reduced by treatment with 2.5 μM taxol at 48 hpa, and the proper formation of proliferating blastema at both anterior and posterior regenerating segments was inhibited (Fig. 2-8A and B). The bulged prostomium of the regenerating *A. viride* was absent after taxol treatment, and only a tiny blastema was observed at 7 dpa. The

doi:10.6342/NTU202000204

indented pygidium which characterized the anus was also absent in the posterior regenerating segment (Fig. 2-9C). Statistically, the percentage of successful regenerates in *A. viride* treated with taxol decreased by 33% at 5 dpa and 31% at 7 dpa in anterior regenerating worms (Fig. 2-9A). Although there was no significant difference in posterior regeneration at 7 dpa, the percentage of successful regenerate in *A. viride* treated with taxol was significantly reduced from 3 to 6 dpa (Fig. 2-9B).

To further investigate the importance of cell proliferation on regeneration in *A. viride*, I also used gene-specific dsRNA to perform RNA interference. Both feeding and microinjecting *Avi-beta tubulin isoform 1* dsRNA successfully reduced the mRNA expression of *Avi-beta tubulin isoform 1* mRNA by 30 and 50% compared to *YFP* dsRNA (MOCK) treated group (Fig. 2-10A and B). Morphologically, worms treated with *YFP* dsRNA regenerated normally. By contrast, the regeneration of *Avi-beta tubulin isoform 1* RNAi treated animals by feeding and microinjecting were both significantly inhibited at 7 dpa. Interestingly, posterior regeneration appeared to be more notably affected by RNAi treatment (Fig. 2-11A and B). This inhibitory effect was confirmed by bright field microscopy. Only a tiny blastema was observed after feeding with bacteria containing dsRNA during anterior regeneration at 7 dpa (Fig. 2-11C). Furthermore, worms injected with *Avi-beta tubulin isoform 1* dsRNA showed significantly smaller head with no bulged prostomium at 7 dpa (Fig. 2-11D). Smaller or missing anus at the end of pygidium were

doi:10.6342/NTU202000204

observed in posterior regenerating worms at 7 dpa (Fig. 2-11C and D).

2.3.4 Regenerative cells are non-proliferative prior to amputation in *A. viride*

To examine the sources of proliferative cell in the regenerative blastema, pulse-chase experiment with EdU labeling was performed. Worms were incubated in EdU solution for 24 hours prior to amputation. After amputation, the worms were transferred into pure ASW. Randomly dispersed EdU signals could be observed at 24 hpa, but only a few EdU^+ cells were detected at the outermost layer of regenerating area at 72 and 120 hpa. However, the distribution of EdU^+ cells around non-regenerated area was evident from 72 to 120 hpa (Fig. 2-12A and B).

2.4 Discussion

Although the ability of regeneration is universally distributed among annelid, their capacity varies significantly even among closely related species (Bely, 2006). For example, many species from Dorvilleidae, Naididae, and Spionidae are capable of anterior and posterior regeneration (Foulkes, 1953; Gibson & Paterson, 2003; Muller & Henning, 2004). However, not all the species in these families have the ability to perform both types of regeneration. Most annelids that have been documented for regenerative ability are capable to regenerate posterior segments rather than anterior segments, such

doi:10.6342/NTU202000204

as *Ophryotocha notoglandulata*, *Amphichaeta raptisae* and *Streblospio benedicti* (Bely, 2006; Bely & Sikes, 2010; Pfannenstiel, 1974). This study have confirmed that *A. viride* can completely restore lost body parts within 5 days in response to either anterior or posterior amputation, which demonstrated a similar regenerative capacity to *Dorvillea bermudensis*, *Allonais paraguayensis*, and *Marenzelleria viridis* in phylum Annelida (Essink & Kleef, 1993; Hyman, 1938; Muller & Henning, 2004). Similar to the oligochaete *Enchytraeus japonensis* and the polychaete *Dorvillea bermudensis* that can completely regenerate from two segments, most *A. viride* could survive and regenerate with three segments, with its percentage of successful regenerates increased with the number of regenerating segments (Paulus & Müller, 2006; Takeo et al., 2010). Comparative study in the regeneration of annelid might contribute to explain the long-lasting question on the loss or gain of regenerative abilities.

Anterior regeneration showed lower percentage of successful regenerates than posterior regeneration in the experiment of regenerative capacity. Presumably, the lower successful regenerate percentage in anterior regeneration can be attributed to the restoration of a more complex structures including brain and mouth (Bely, 2006; Zattara & Bely, 2013). However, posterior regeneration which is considered to be a simpler process did not demonstrate a quicker regenerative response.

Cell proliferation assay indicated very differently during these two process. In this

doi:10.6342/NTU202000204

study, EdU incorporation was used to detect the amount of proliferating cells in *A. viride*. In anterior regeneration, the signal of cell proliferation could be detected around 12 hpa and peaked at 24 to 48 hpa. This proliferation pattern is comparable to *P. leidyi*, in which proliferation onset between 12 to 24 hpa, and peaked around 48 to 72 hpa (Bely & Sikes, 2010). Surprisingly, cell proliferation in posterior regeneration initiated later at around 24 hpa, and reached its maximum at 72 hpa. This delay pattern was also observed in *D. bermudensis* and resulted in the difference of blastema size at 300 hpa (Paulus & Müller, 2006). Similar phenomenon can also be observed in *P. leidyi,* in which maximum amount of proliferative cells could be observed at 72 hpa in posterior but not anterior regeneration (Zattara & Bely, 2013). We hypothesized that the delay in cell proliferation might be attributed to the process of de-differentiation evidenced by the reappearance of EdU^+ cells at fission zone after 72 hpa. In anterior regeneration, somatic cell only need to de-differentiate into stem cell which is responsible for regeneration, but cells in the posterior end must de-differentiate into stem cells that are responsible for regeneration and reproduction.

The spatial and temporal proliferation pattern showed many similarities during regeneration and fission in *A. viride*. During anterior regeneration, EdU signals became concentrated at the blastema at 24 hpa, then gradually depleted as the regeneration was completed at 5 dpa. Similarly, when zooid was detached from the parental worm, EdU

doi:10.6342/NTU202000204

signals was observed at the prostomium region, but gradually depleted after the prostomium mature (data not shown). This observation showed that proliferating cells are only present when needed. As regeneration or reproduction complete, the proliferation signals disappear. Posterior regeneration also shares many common features to fission in *A. viride*. At first, the majority of proliferating cells were concentrated near the pygidium, after the regeneration or reproduction process is almost completed, the second ring of EdU signal (fission zone) appears. Both processes are initiated on the posterior growth zone first, then proliferate at the fission zone. These findings are largely similar to the study on *P. leidyi* (Zattara & Bely, 2011). The unpublished data from our laboratory will aim to classify the identities of cells involved in these two processes. It is widely accepted that blastema should be highly proliferative and displayed stem cell markers such as PIWI and SOX2 before differentiation (Gaete et al., 2012; Rossi et al., 2006). It will be great insight into see what roles these stem cell play during regeneration and reproduction.

Cell proliferation is generally considered to be the key event that occurs during regeneration (Nechiporuk & Keating, 2002; Schnapp et al., 2005). The contribution of cell proliferation to regeneration differs across metazoan models (Passamaneck & Martindale, 2012). In this study, large amount of EdU^+ cells present at blastema during regeneration. Combined with the changes in morphology, results showed that anterior amputation in *A. viride* is followed by the formation of blastema with great quantity of

doi:10.6342/NTU202000204

cell proliferation during regeneration. Also, significant decrease of proliferating cells was observed at the blastema after treated with a mitotic inhibitor, taxol. Together, these data demonstrated the importance of cell proliferation in the regenerative process of *A. viride*. Cell proliferation and the formation of blastema characterized epimorphic regeneration in many annelid models (Fernando et al., 2011; McCusker et al., 2015). Although some studies indicated that regeneration could not be solely classified as epimorphic or morphollatic (Brockes & Kumar, 2008; Reddien & Sánchez Alvarado, 2004), this study supported the hypothesis that *A. viride* carried out regeneration primarily by epimorphosis, which is consistent with most other annelids (Kalidas et al., 2015; Kozin & Kostyuchenko, 2015; Martinez et al., 2006; Özpolat & Bely, 2015).

In addition, according to the pulse-chase experiment, EdU^+ cells were limited in the anterior regenerating site, which inferred that only a small amount of proliferating cells was active prior to amputation. Most of the proliferating cells in the regenerating area were dormant or inactive prior to injuries. This finding support the hypothesis that de-differentiation might be involved in the regenerative process of *A. viride*. The somatic cells might be “non-regenerative” or “non-proliferative” prior to injuries, it will de-differentiate into stem cells after amputation. However, further studies using stem cell markers is needed to confirm the presence of de-differentiation.

This study have confirmed that *A. viride* can complete both anterior and posterior

doi:10.6342/NTU202000204

regeneration within five days after amputation. Cell proliferation is indeed required for the formation of blastema and the regenerative process of this worm. I hope the detailed description on epimorphic regeneration of *A. viride* could contribute to develop a clearer picture on the evolutionarily origin of regeneration in annelid.

doi:10.6342/NTU202000204

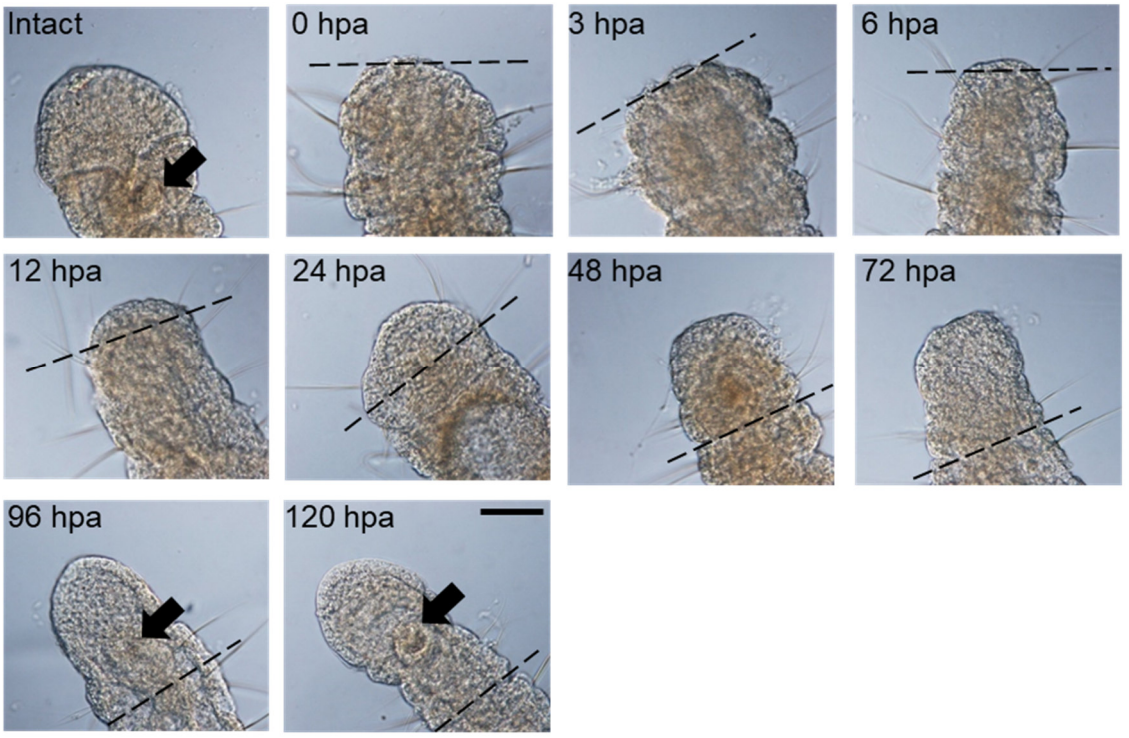

Figure 2-1. Anterior regeneration in *A. viride.* The external morphology was observed in intact and regenerating worm. The protruding regenerative blastema became apparent from 24 to 48 hpa in most regenerating *A. viride*. Mouth formation could be observed around 96 hpa. The amputation site was labeled by black dotted line. The black arrow indicated the mouth. Scale bar: 50 μm.

doi:10.6342/NTU202000204

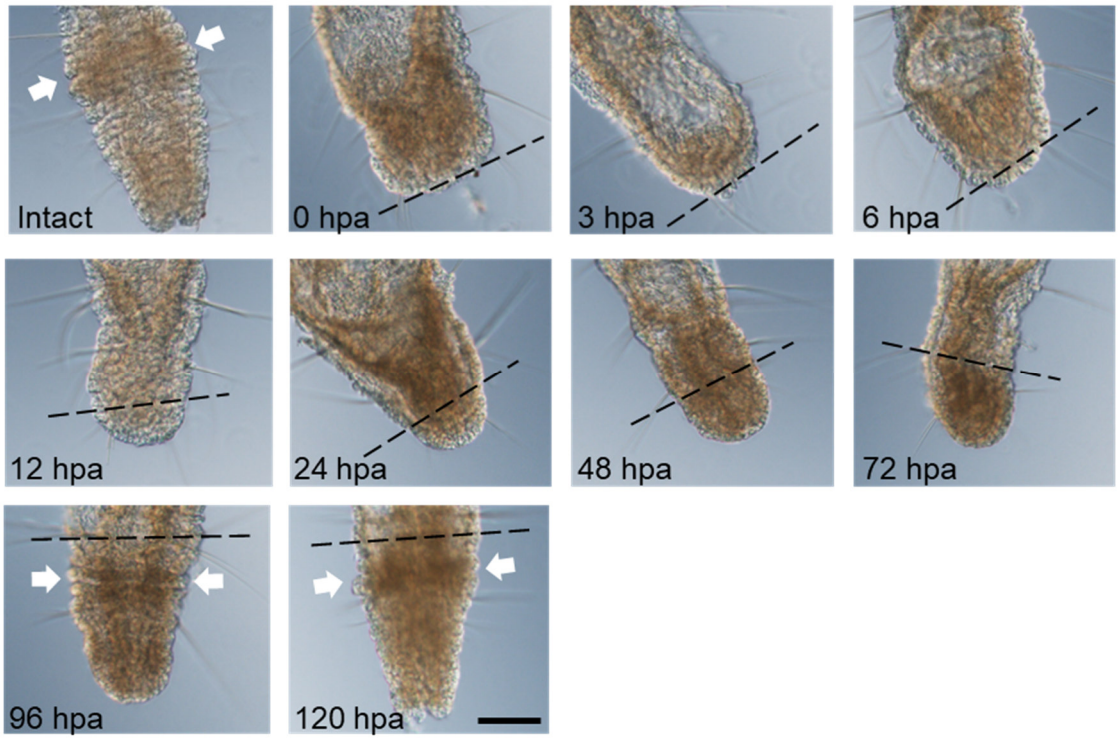

Figure 2-2. Posterior regeneration in *A. viride*. The external morphology was observed in intact and regenerating worm. In posterior regeneration, the regenerative blastema became apparent from 12 to 24 hpa in most regenerating *A. viride*. Fission zone could be observed around 96 hpa. The indented pygidium re-appeared at the posterior end in most regenerating *A. viride* at 120 hpa. The amputation site was labeled by black dotted line. The white arrow indicated fission zone. Scale bar: 50 μm.

doi:10.6342/NTU202000204

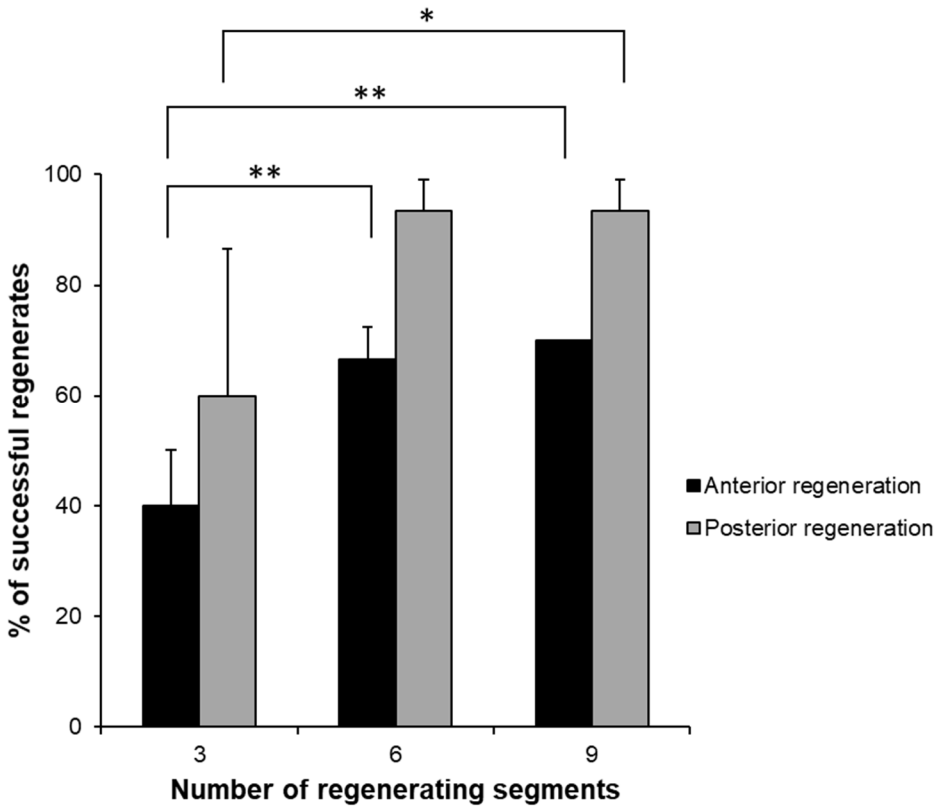

Figure 2-3. Minimum segments required for successful regeneration in *A. viride*. The percentage of successful regenerates in either anteriorly or posteriorly amputated worms regenerating from different segments were recorded at 5 dpa. The minimum segments required for successful regeneration in *A. viride* was three segments. Data represented the mean ± s.d. from three independent duplicate experiments (n = 3 biological replicates). Significant differences relative to three of regenerating segments were denoted by *. *: p <0.05; **: $p < 0.01$; ***: $p < 0.001$ using two-tailed unpaired student's t-test.

doi:10.6342/NTU202000204

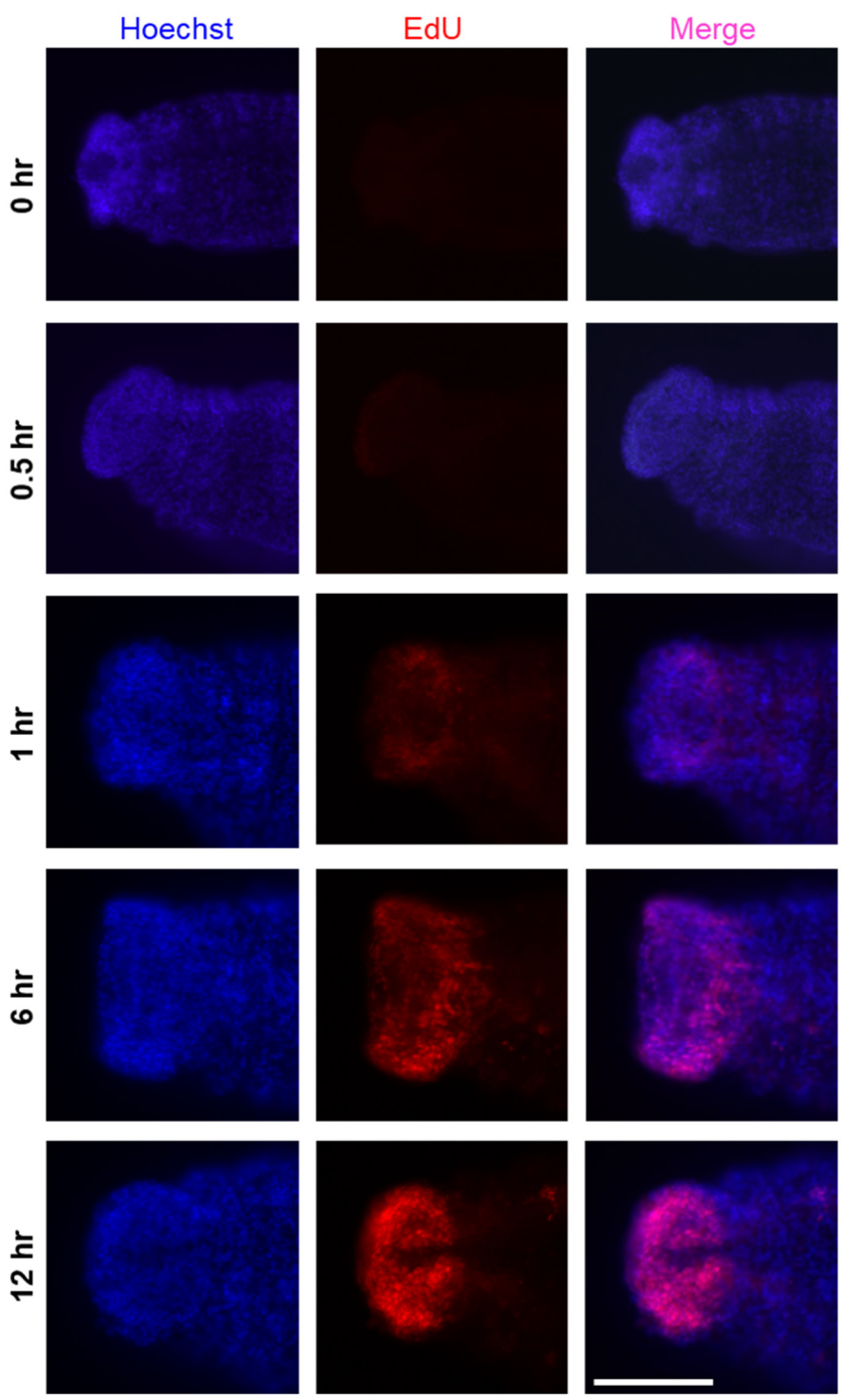

Figure 2-4. EdU treatment with different incorporation time. EdU signal (red) co-stained with Hoechst 33342 (blue). EdU was incorporated for 0, 0.5, 1, 6, 12 hours prior to fixation at 48 hpa. Scale bar: 100 μm.

doi:10.6342/NTU202000204

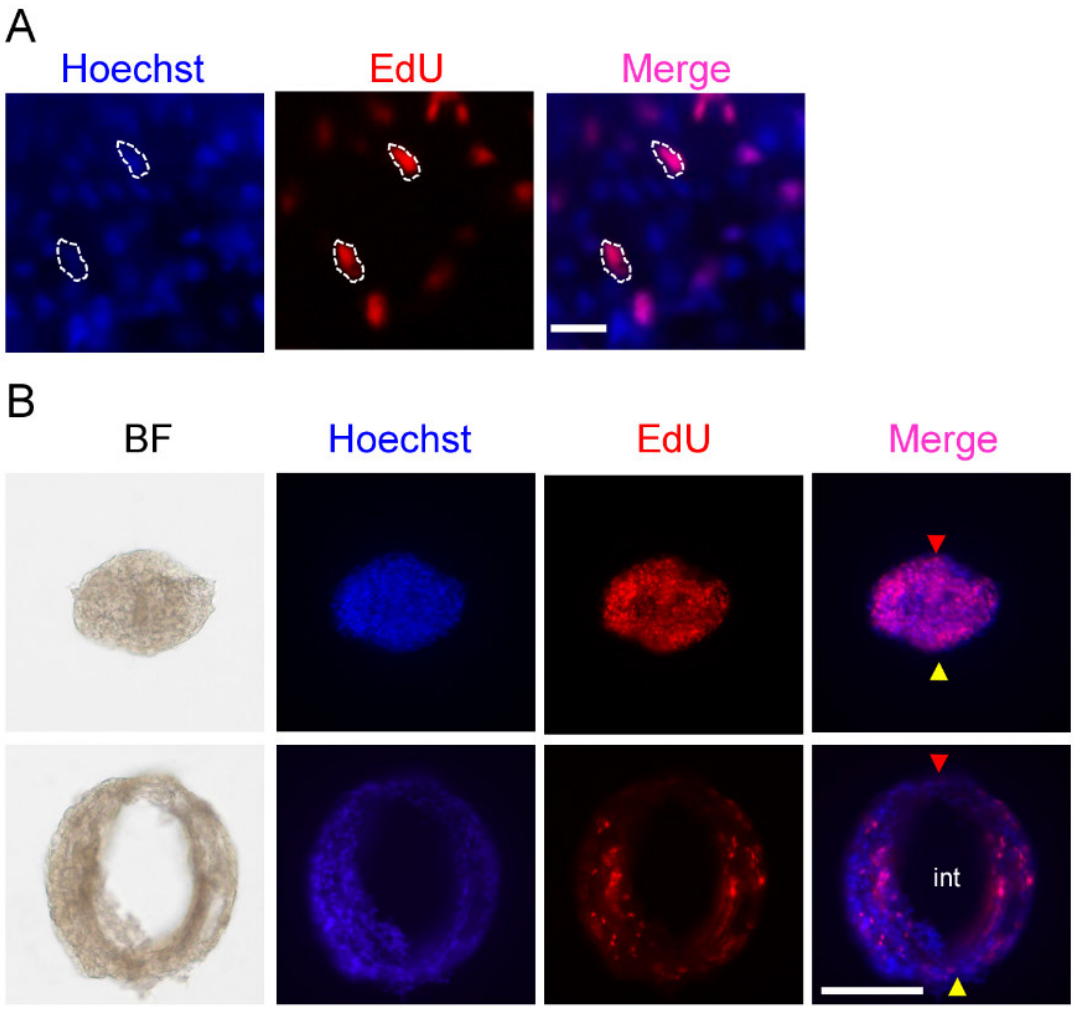

Figure 2-5. Cell proliferation detection in *A. viride*. (A) EdU signal (red) reveals cell proliferation and is confirmed by nuclei stained with Hoechst 33342 (blue). The white dotted line indicated the co-localization cells in three channels. Scale bar: 10 μm. (B) Cross section of blastema (upper panel) and midgut (lower panel) during anterior regeneration. The red arrow indicated dorsal side of the worm, and the yellow arrow indicated the ventral side of the worm. *int*, intestine. Scale bar: 100 μm.

doi:10.6342/NTU202000204

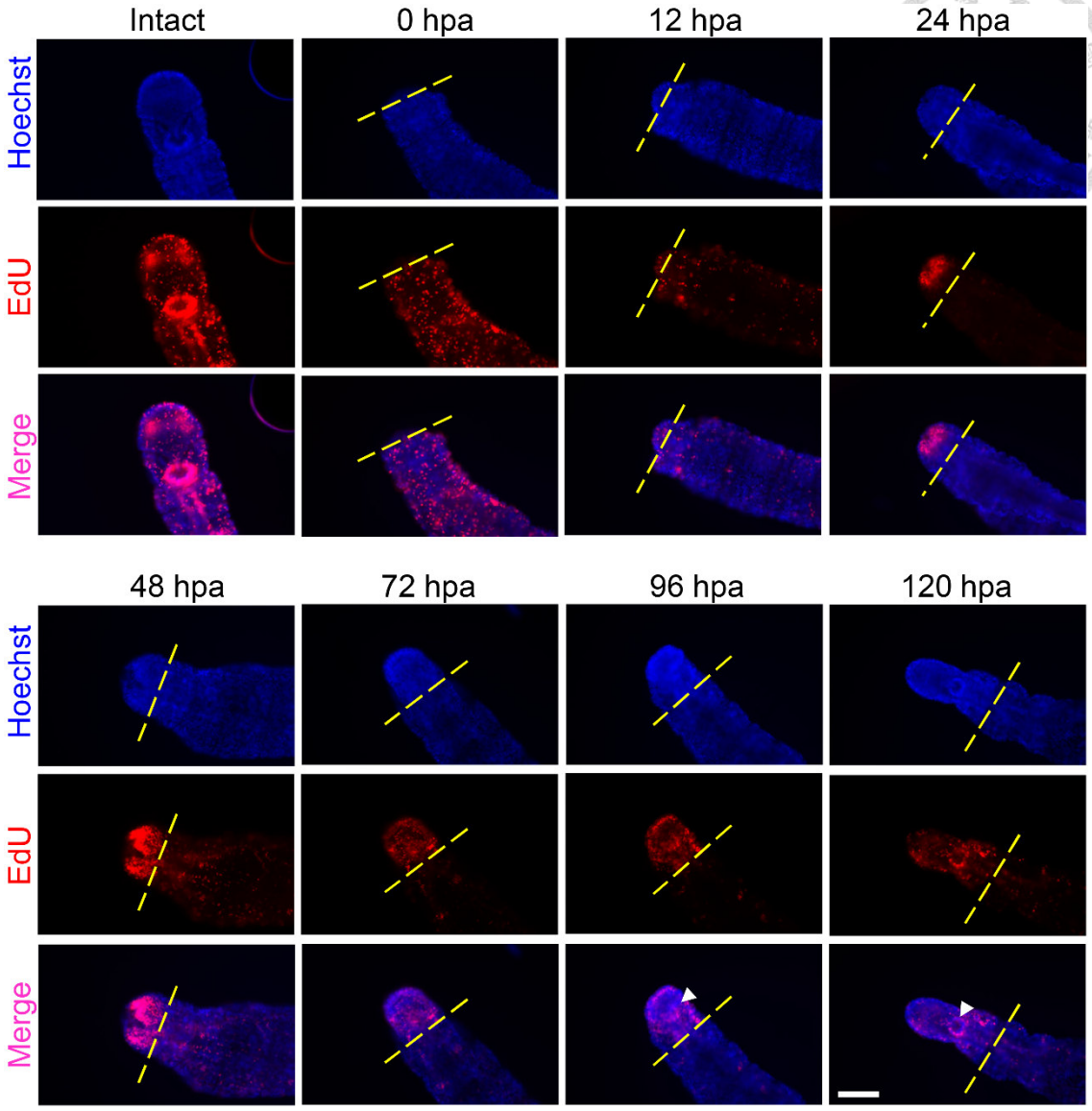

Figure 2-6. Cell proliferation was detected by EdU labeling during anterior regeneration in *A. viride*. Cell proliferation was detected on intact or anterior regenerating worms at different time points. The EdU signal peaked at 24 and 48 hpa. The amputation site is labeled by yellow dotted line. White triangle indicated the mouth. Scale bar: 100 μm.

doi:10.6342/NTU202000204

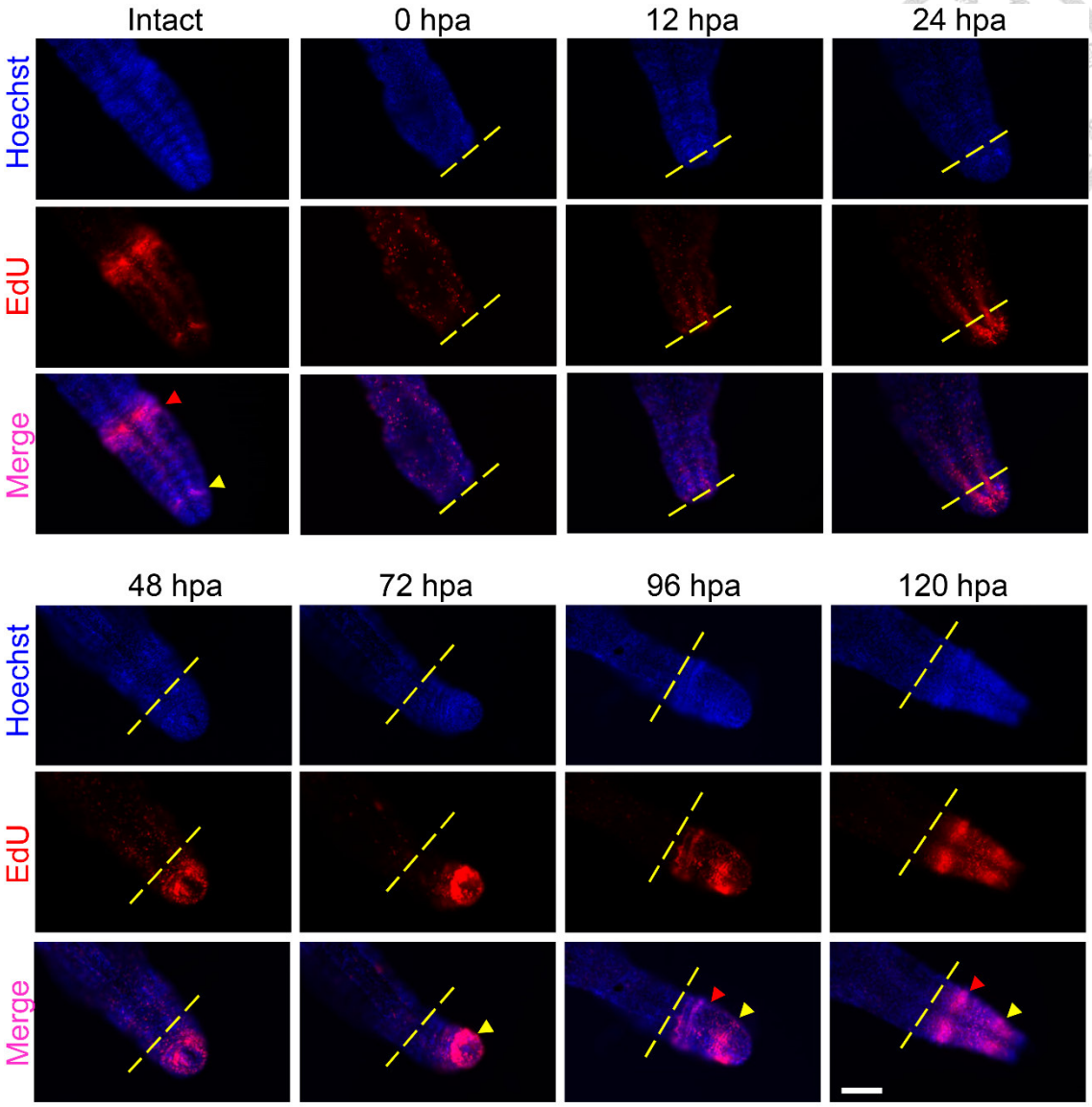

Figure 2-7. Cell proliferation was detected by EdU labeling during posterior regeneration in *A. viride*. Cell proliferation was detected on posterior regenerating site at different time points. EdU peaked at 48 and 72 hpa. At 96 and 120 hpa, EdU signal formed two rings indicated the fission and posterior growth zone at the posterior end. The amputation site is labeled by yellow dotted line. Red and yellow triangle indicated re-appearance of fission or posterior growth zone respectively. Scale bar: 100 μm.

doi:10.6342/NTU202000204

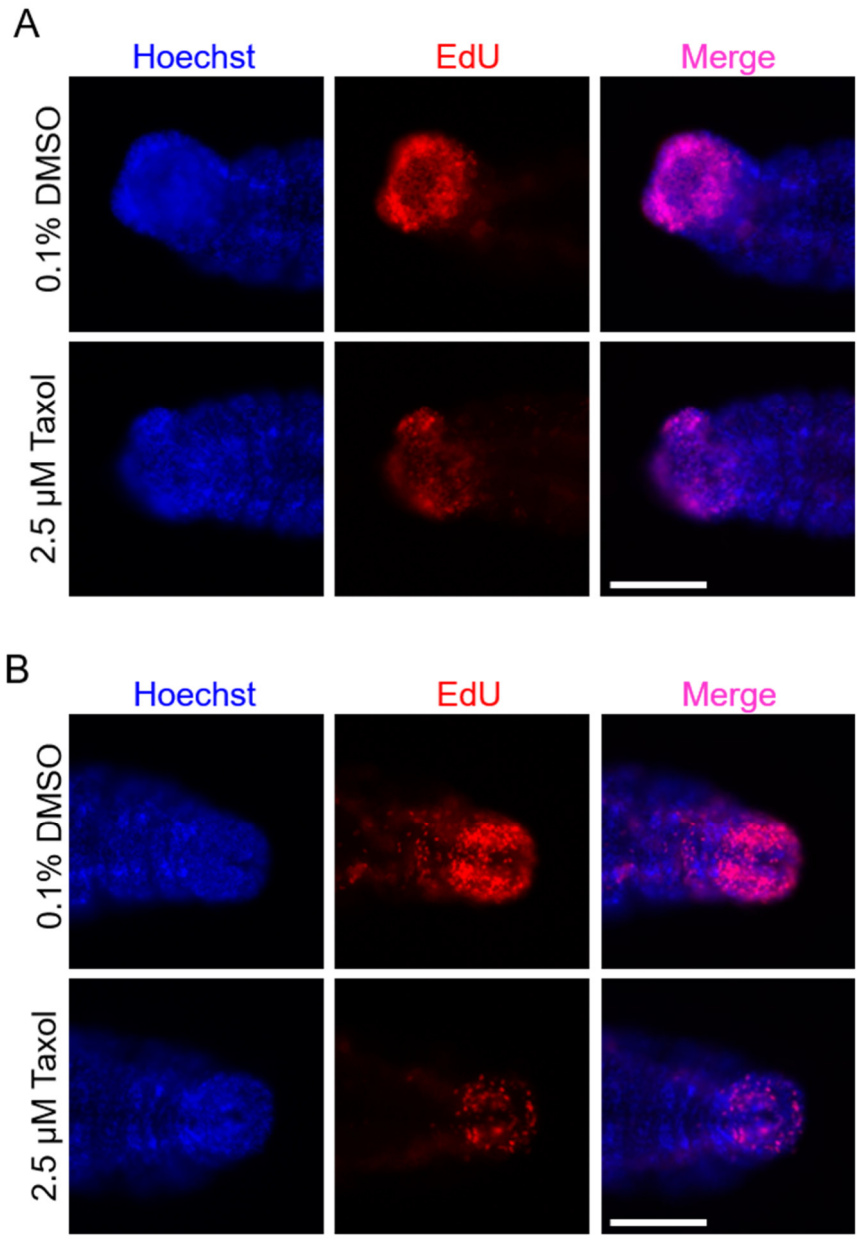

Figure 2-8. The inhibitory effect of taxol on cell proliferation during regeneration in *A. viride*. The amount of proliferating cells at the blastema was decreased after taxol treatment at 48 hpa in anterior (A) and posterior (B) regenerating segment. Scale bar: 100 μm.

doi:10.6342/NTU202000204

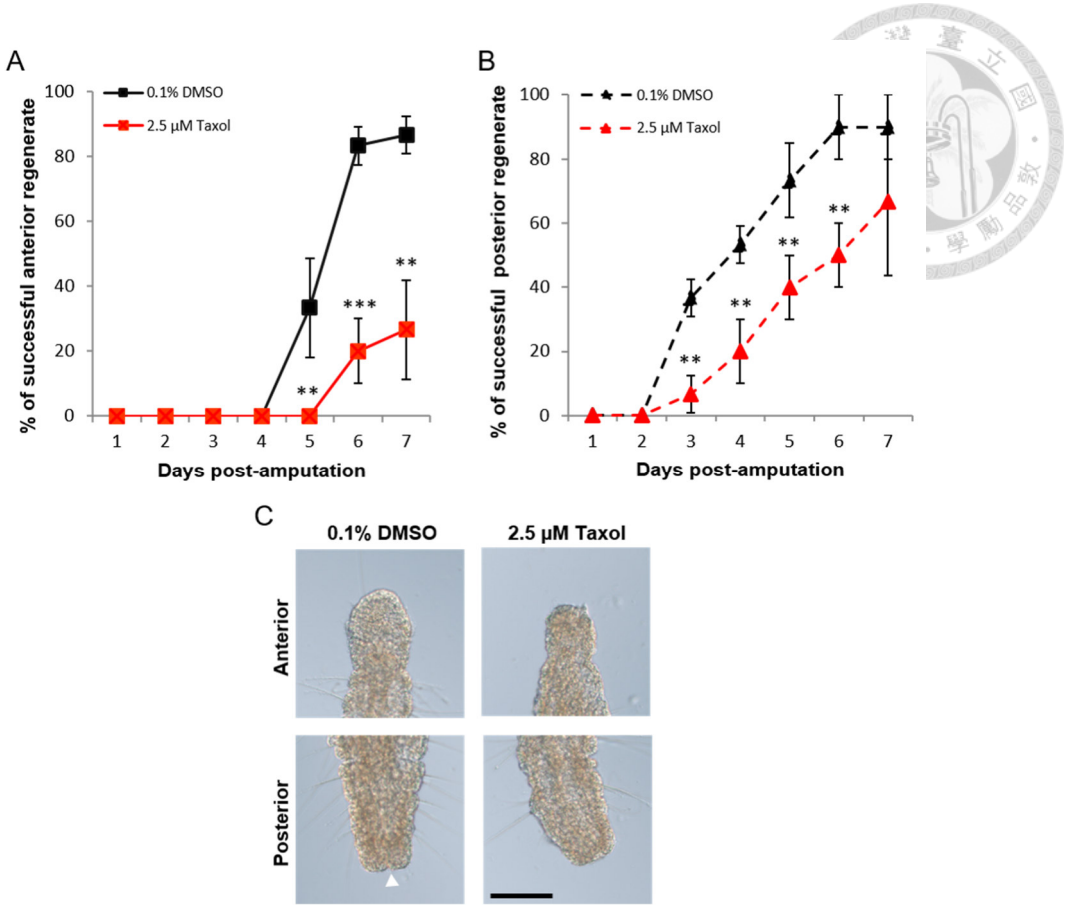

Figure 2-9. The inhibitory effect of taxol on the percentage of successful regenerate during regeneration in *A. viride*. After taxol treatment, the percentage of successful regenerate was examined from 1 to 7 dpa. (A) Anterior regenerating worms showed delayed regeneration compare to the control group from 5 to 7 dpa. (B) Posterior regenerating worms also showed delayed regeneration after taxol treatment. (C) The head and tail morphology of regenerating worms was obviously affected by taxol treatment. White triangle indicated the anus. Data represented the mean ± s.d. in figure A and B from three independent duplicate experiments (n = 3). Significant differences relative to 0.1% DMSO group at each day were denoted by *. **: p <0.01; ***: p < 0.001 using two-tailed unpaired student's t-test. Scale bar: 100 μm.

doi:10.6342/NTU202000204

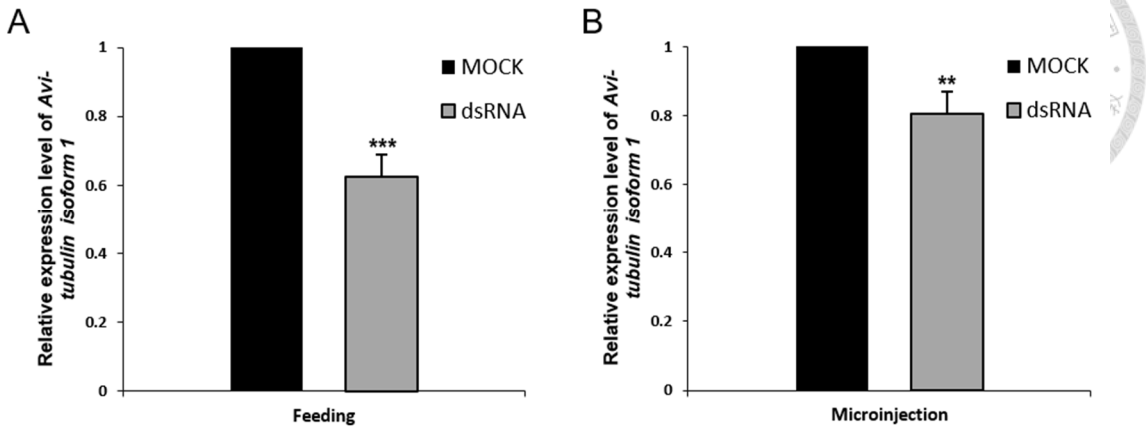

Figure 2-10. Knockdown experiment of *Avi-beta tubulin isoform 1* by dsRNA. The expression level of *Avi-tubulin isoform 1* mRNA were detected to assay the knock-down efficiency. The inhibitory effect on the gene expression by dsRNA feeding (A) or microinjection (B) was observed at intact worm. All data represented the mean ± s.d. from three independent duplicate experiments (n = 3 biological replicates). Significant differences relative to control group (MOCK) were denoted by *. **: p <0.01; ***: p < 0.001 using two-tailed unpaired student's t-test.

doi:10.6342/NTU202000204

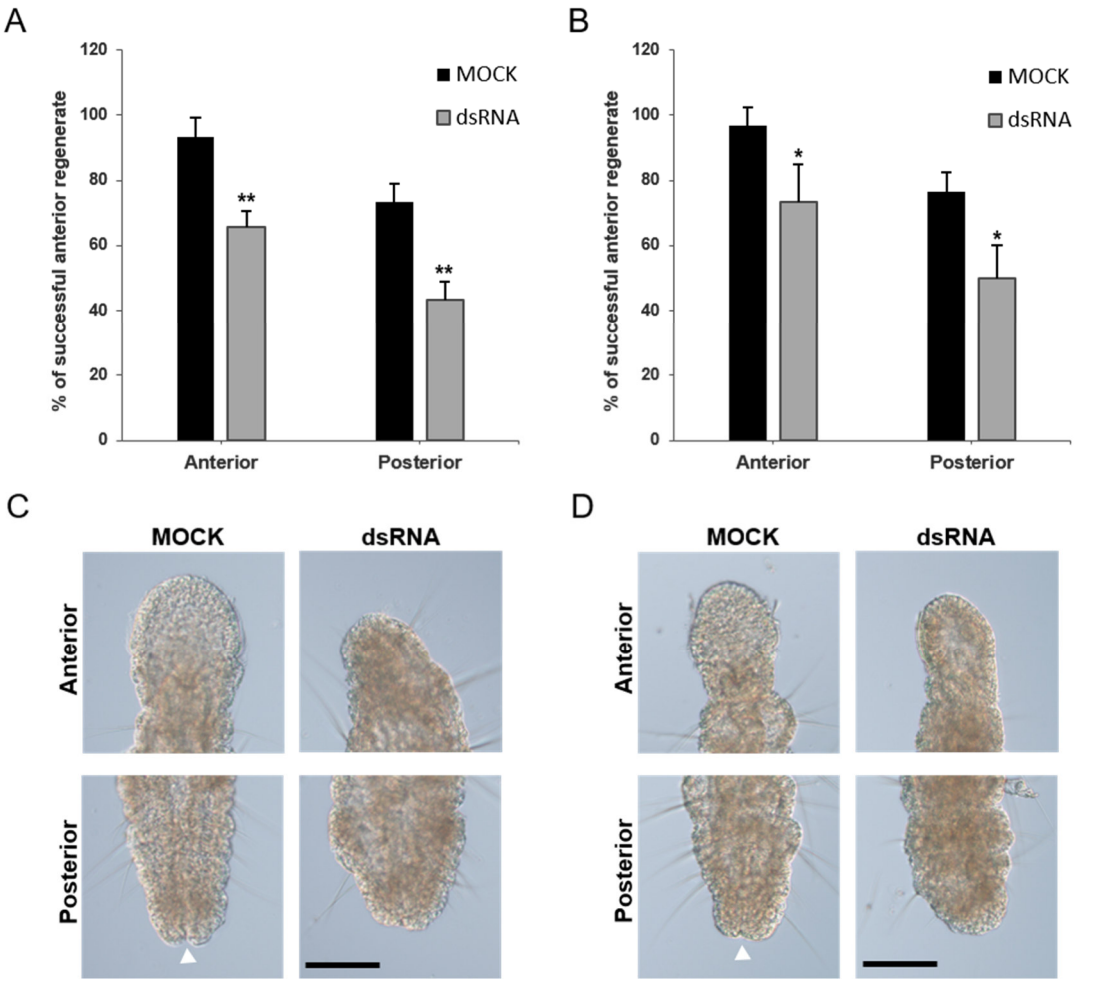

Figure 2-11. *Avi-beta tubulin isoform 1* RNAi inhibited regeneration in *A. viride*. The inhibitory effect on the percentage of successful regenerates by *Avi-beta tubulin isoform 1* RNAi feeding (A) or microinjection (B) was observed at 7dpa. The head and tail morphology of regenerating worms was obviously affected by feeding (C) or dsRNA microinjection (D) method. White triangle indicated the anus. Data represented the mean ± s.d. in figure A and B from three independent duplicate experiments (n = 3 biological replicates). Significant differences relative to control group (MOCK) were denoted by *. *: $p < 0.05$; **: $p < 0.01$ using two-tailed unpaired student's t-test. Scale bar: 100 μm.

doi:10.6342/NTU202000204

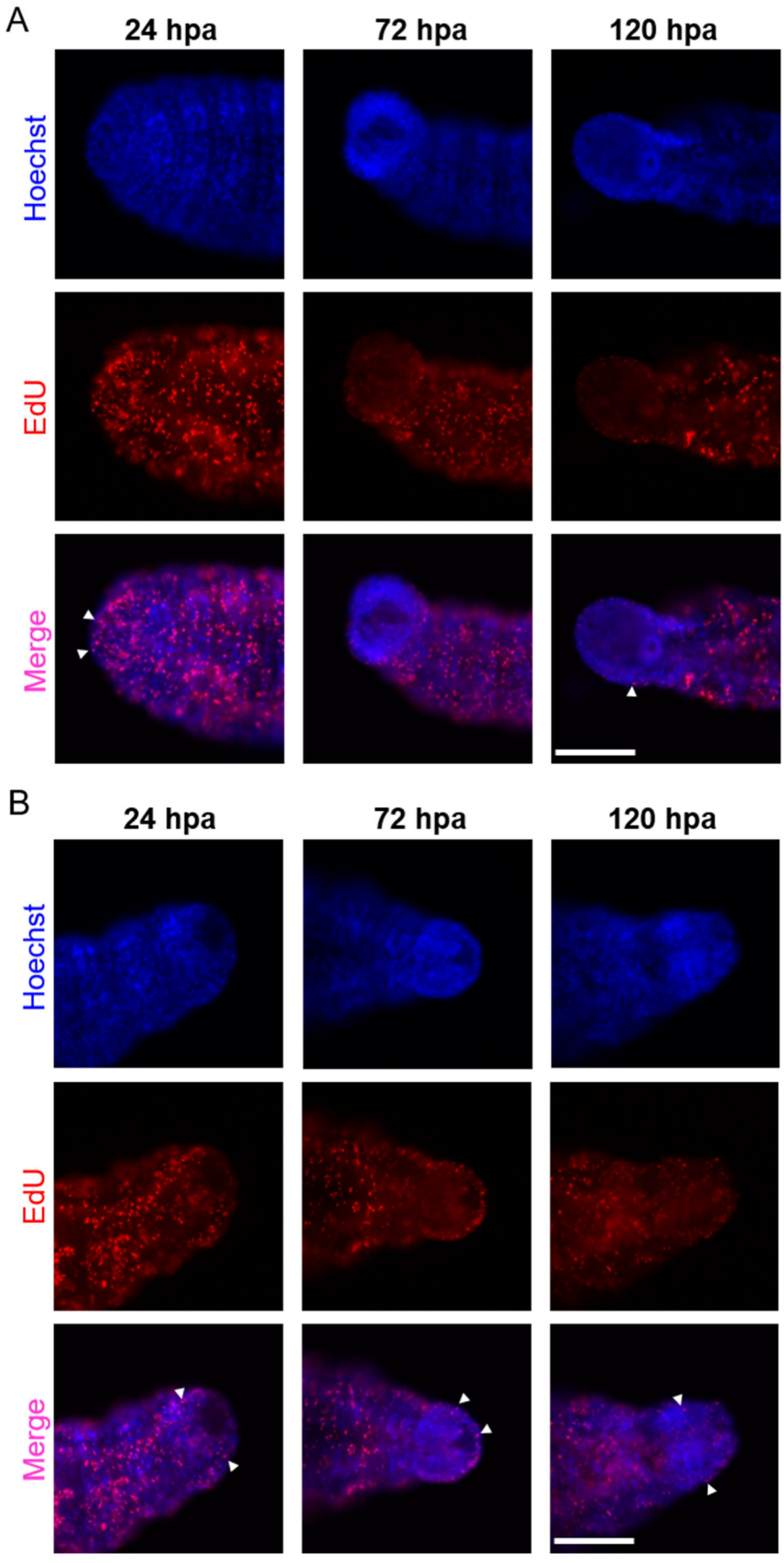

Figure 2-12. Regenerative cells are non-proliferative prior to injuries. Pulse-chase

doi:10.6342/NTU202000204

experiment with EdU labeling was performed during anterior (A) and posterior (B) regeneration at 24, 72 and 120 hpa. At 72, 120 hpa, minor EdU^+ cell were detected at anterior and posterior regenerating area. White arrow indicated the co-localized signal. Scale bar: 100 μm.

doi:10.6342/NTU202000204

Chapter 3

Characterization of toll-like receptor (TLR) signaling pathway in the annelid, *Aeolosoma viride*

doi:10.6342/NTU202000204

3.1 Introduction

Innate immunity is the first line to defensed pathogenic microorganisms in animals. Phylogenetically, ancient pattern recognition receptors (PRR) encoded in the host genome are able to recognize pathogen-associated molecular patterns (PAMPs) (Aderem & Ulevitch, 2000). Understanding the evolution of PRR mediated innate immunity is an essential topic in immunology. Due to their vital roles in host defense in various organisms, signal transduction by toll-like receptors (TLRs) have been extensively studied and the TLRs recruit their canonical adaptor Myd88 or others, leading to the activation of transcription factor NF-κB-mediated inflammation and/or immune response in mammalian and other vertebrate models (Hallman et al., 2001; O'Neill et al., 2013). Since the first Toll receptor was identified from *Drosophila* in 1985, linking between embryonic development and mammals' innate immunity is according to recognition of the conserved signaling pathway and motif between *Drosophila* and mammals after 10 years (Aderem & Ulevitch, 2000; Anderson et al., 1985; Lemaitre et al., 1996). Nowadays, these conserved receptors still have not been well-investigated on some invertebrate models, including annelids (Prochazkova et al., 2020). Due to innate immunity is the most important defense mechanism in invertebrates, to identify of TLR signaling pathway in *A. virid* will raise our understanding of the immune system.

The TLR family is one of subgroups of pattern recognition receptors expressed on

doi:10.6342/NTU202000204

the cell surface of immune cells. TLR pathway is activated by recognizing conserved microbial structures or products of microbial metabolism to trigger immune responses to counter the invaded pathogens (Aderem & Ulevitch, 2000). TLR recognizes PAMPs such as lipopolysaccharide (LPS) from gram-negative bacteria outer membrane, peptidoglycan (PGN) from gram-positive bacteria outer membrane or dsRNA of nucleic acid variants normally associated with viruses by leucine rich repeat (LRR) domain. Then myeloid differentiation primary response 88 (MyD88) is recruited to interact with the cytosolic part of TLR through a homophilic interaction of the Toll/IL-1R domain (TIR) domains. Its death domain (DD), in turn, homophilically binding with the DD of interleukin-1 receptor associated kinase (IRAK) to trigger signaling cascades that cause activation of NF-κB. Then, activated NF-κB translocates in to the nucleus to serve as a transcription factor to promote specific cytokine production, like tumor necrosis factor (TNF) and interleukin (IL). After the cytokine produced, the costimulatory molecules released on macrophages, several kinds of naïve immune cells can be activated to perform phagocytosis or recruiting more other immune cells such as lymphocytes (Hallman et al., 2001; Yamamoto et al., 2003).

The aim of this study was (i) to identify and clone TLR-related genes from *A. viride*, (ii) to verify their phylogenic relationships with that of other animals, (iii) to examine their participations and expressions in the innate immunity during *A. viride* anterior

doi:10.6342/NTU202000204

regeneration.

3.2 Materials and Methods

3.2.1 Gene cloning and sequence analysis

The partial sequence of *Avi-TLR*, *Avi-MyD88* and *Avi-TNF* were annotated from the *A. viride* transcriptome. Gene-specific primers were used to amplify the partial cDNA fragment using Supertherm Tag DNA polymerase (Bersing). The PCR product was purified and cloned by using T&A^{TM} Cloning Kit (Yeastern Biotech) for sequencing. All partial sequences were extend by 5′ and 3′ rapid amplification of cDNA ends (5′ and 3′RACE). For 5′RACE, two adaptor primers including 5′ AP (5′-GGCCACGCGTCGACTAGTACGGGGGGGGGGGGGGG-3′) and AP (5′-GGCCACGCGTCGACTAGTAC-3′) were used. For 3′RACE, two gene-specific forward primers from 3′ end of partial cDNA fragment were used to amplify 3’ end of target gene. The cDNA synthesized with oligo (dT) primers as templates for the first-round PCR with gene-specific forward primer and 3′ adaptor primer (3′ AP: 5′-GGCCACGCGTCGACTAGTACTTTTTTTTTTTTTTTTT-3′). The second-round PCR carried out with anther gene-specific forward primer and AP. The final PCR products from 5′ and 3′RACE were cloned and sequenced to obtain full-length sequence. The protein sequence of open reading frame (ORF) was annotated by SMART program

doi:10.6342/NTU202000204

(http://smart.embl-heidelberg.de/).

3.2.2 Phylogenetic analysis

Multiple sequence alignment was performed by using the MUSCLE program with default parameters in MEGA X. TLR sequences used were from *Homo sapiens* TLR 1 (AAC34137.1), *H. sapiens* TLR 2 (NP_001305716.1), *H. sapiens* TLR 3 (NP_003256.1), *H. sapiens* TLR 4 (NP_612564.1), *H. sapiens* TLR 5 (ACM69033.1), *H. sapiens* TLR 6 (AAY88762.1), *H. sapiens* TLR 7 (NP_057646.1), *H. sapiens* TLR 8 (NP_619542.1), *H. sapiens* TLR 9 (AAF78037.1), *H. sapiens* TLR 10 (AAK26744.1) *Mus musculus* toll-like receptor 4 (NP_067272.1), *Danio rerio* TLR 2 (NP_997977.1), *D. rerio* TLR 3 (NP_001013287.2), *D. rerio* TLR 5 (XP_001919052.2), *D. rerio* TLR 6 (NP_001124065.1), *D. rerio* TLR 7 (XP_021334735.1), *D. rerio* TLR 9 (NP_001124066.1), *Eisenia andrei* membrane pattern recognition receptor TLR (AGS14315.2), *Hirudo medicinalis* Toll-like receptor 1 (ADK94453.1) and *Drosophila melanogaster* toll protein (AAA28941.1). MyD88sequences used were from *H. sapiens* MyD88 (AAB49967.1), *Pan troglodytes* MyD88 (NP_001123935.1), *M. musculus* MyD88 (AAC53013.1), *Xenopus tropicalis* MyD88 (NP_001016837.1), *Andrias davidianus* myeloid differentiation response protein 88 (AGF25258.1), *Ictalurus punctatus* MyD88 (NP_001187207.1), *D. rerio* MyD88 (AAQ90476.1), *H. medicinalis*

doi:10.6342/NTU202000204

myeloid differentiation factor 88 (AJK90197.1), *E. andrei* MyD88 (CZQ50135.1), *Anthopleura buddemeieri* MyD88 protein (ALG40990.1), *Actinia tenebrosa* MyD88 protein (ALG40989.1), *Aulactinia veratra* MyD88 protein (ALG40991.1), *Stylophora pistillata* MyD88 (PFX20292.1), *Tribolium castaneum* Myd88 (EFA01304.1), *Spodoptera exigua* MyD88 (AYN77137.1), *Culex quinquefasciatus* myd88 (XP_001868621.1), *D. melanogaster* MyD88 adapter protein (AAL56570.1), *D. busckii* Myd88 (ALC41722.1), *Lingula anatina* myeloid differentiation primary response protein MyD88-like (XP_013416180.1), *Haliotis diversicolor* myeloid differentiation factor 88 (AHK60398.1), *Mytilus coruscus* myeloid differentiation factor 88a (AYA22345.1), *M. galloprovincialis* myeloid differentiation factor 88a (AFR54116.1), *Mizuhopecten yessoensis* MyD88 (OWF48103.1), *Pinctada fucata* myeloid differentiation factor 88 (AMQ81593.1) and *Crassostrea gigas* MyD88 (NP_001292287.1). TNF sequences used were from *H. sapiens* TNF-alpha (NP_000585.2), *M. musculus* tumor necrosis factor isoform 1 (NP_038721.1), *D. rerio* tumor necrosis factor (NP_001019618.1), *H. discus discus* tumor necrosis factor alpha (ACF75368.1), *L. anatina* protein eiger (XP_013398885.1) and *D. melanogaster* eiger, isoform A (NP_724878.2). The phylogenetic tree was constructed using the neighbor-joining method in MEGA X.

3.3 Results

doi:10.6342/NTU202000204

3.3.1 Characterization and identification of TLR in *A. viride*

In order to realize TLR-mediated innate immunity existing in *A. viride*, the major proteins including TLR, MyD88 and downstream produce TNF were cloned from cDNA. Several partial sequence of *Avi-TLR* were identified from our unpublished *A. viride* transcriptome. To extend the partial sequence of ten *Avi-TLR* genes, RACE was performed and finalized C-terminal sequencing of six sequences, *Avi*-TLR-I to VI. The other four sequences, *Avi*-TLR-a to d, were fully cloned. The amino acid sequences were annotated by SMART program. *Avi*-TLR-a and *Avi*-TLR-b have complete canonical structures of TLR, including multiple LRR, leucine-rich repeat N-terminal (LRR-NT), leucine-rich repeat C-terminal (LRR-CT), transmembrane (TM) domain and TIR domain. However, all of partial sequences and the other two full-length sequences lack TIR domain in their C-terminal (Fig. 3-1). Therefore, following experiments were conducted only on the *Avi*-TLR-a and *Avi*-TLR-b. The nucleotide sequence of *Avi*-TLR-a has 2628 nt in the coding region encoding 876 amino acids, including TM (from 617th to 639th amino acid) and TIR domain (from 676th to 872nd amino acid) with a calculated molecular weight of 99.6 kDa (Fig. 3-2A). *Avi*-TLR-b has 2364 nt in the coding region encoding 788 amino acids with TM (from 571st to 593rd amino acid) and TIR domain (from 630th to 784th amino acid) with a calculated molecular weight of 89.91 kDa (Fig. 3-2B).

doi:10.6342/NTU202000204

3.3.2 Phylogenetic analysis of TLR in *A. viride*

In the phylogenetic analysis based on protein sequence alignment, TLR 3, 4 and 5 subfamily were grouped tightly in a subgroup, whereas the TLR 1, 2, 6, 7, 8, 9, 10 and other invertebrate TLRs were more variously branched. The phylogenetic tree revealed that *Avi*-TLR-a and *Avi*-TLR-b were grouped together and clustered with vertebrate TLRs. Moreover, this phylogenetic analysis suggested *Avi*-TLR-a and *Avi*-TLR-b more conserved with vertebrate TLR 3 or TLR 5 from human and zebrafish (Fig. 3-7). Thus, the complete canonical structures of *A. viride* TLRs appear as a well-maintained phylogeny is consistent with conserved TLR signaling pathway.

3.3.3 Characterization and identification of MyD88 in *A. viride*

Based on the canonical structure of adapter protein MyD88, including death and TIR domain, two sequences of MyD88 from *A. viride* transcriptome were found. Similarly, two partial sequences of *Avi-MyD88* were extended by RACE and then their full-length sequence were analyzed with SMART program. Two *Avi*-MyD88 have a DD domain, but one of *Avi*-MyD88 lacks the TIR domain in C-terminal (Fig. 3-3B). The *Avi*-MyD88 has complete canonical structures with TIR domain named *Avi*-MyD88-a from with 1110 nt in the coding region encoding 370 amino acids with a calculated molecular weight of 41.94 kDa. The two specific domain hits of this MyD88 from the translated ORF include

doi:10.6342/NTU202000204

DD domain from residue 18 to 107, and TIR domain from residue 159 to 301 (Fig. 3-3A and 3-8A). In addition, the *Avi*-MyD88 without TIR domain named *Avi*-MyD88-i has 1374 nt in the coding region encoding 458 amino acids with a calculated molecular weight of 51.54 kDa. The only one specific domain hits of this MyD88 from the translated ORF is DD domain from residue 18 to 107 (Fig. 3-3B and 3-8A).

To compare two *Avi*-MyD88 with other species, an amino acid alignment incorporating was implemented with sequences from *Homo sapiens*, *P. troglodytes*, *M. musculus*, *X. tropicalis*, *A. davidianus*, *D. rerio*, *E. andrei*, *H. medicinalis*, *M. galloprovincialis* and *C. gigas*. First, the result revealed that *Avi*-MyD88-a and *Avi*-MyD88-i share 48% protein sequence identity with each other. Second, *Avi*-MyD88-a shares more than 30% identity from other species. The highest sequence identity of *Avi*-MyD88-a was 40% with MyD88 from annelid *H. medicinalis*, then 37% identity with those sequences from *X. tropicalis*, *A. davidianus*, *D. rerio*, *E. andrei*, 36% sequence identity with two MyD88 from *H. sapiens* and *P. troglodytes*, 34% identity with two sequences from *M. musculus* and *C. gigas*, and 30% identity with sequence from *M. galloprovincialis.* Furthermore, *Avi*-MyD88-i shares less identity from other species. The highest protein sequence identity of *Avi*-MyD88-i was 35% with MyD88 from annelid *E. andrei*, then 34% identity with MyD88 from *A. davidianus*, 31% identity with two sequences from *D. rerio* and *H. medicinalis.* Finally, *Avi*-MyD88-i shares less than 30%

doi:10.6342/NTU202000204

identity with other MyD88 from *H. sapiens*, *P. troglodytes*, *X. tropicalis, M. musculus*, *M. galloprovincialis* and *C. gigas*. Together, *Avi*-MyD88-a and *Avi*-MyD88-i share similarity with other MyD88 from Annelida, nevertheless, *Avi*-MyD88-a proportions the more identity with most protein sequences from phylum Chordata and Mollusca. The detail differences of two *Avi*-MyD88 and other MyD88 exhibited from protein alignments of DD (from residues 28 to 123) and TIR domain (box1 from residues 184 to 186, box2 from residues 220 to 226 and box3 from residues 349 to 350) are shown in Fig. 3-5. Based on the cascade of TLR signaling, the interaction between TLR and MyD88 is mediated by homo-binding of TIR domain, and the interaction between MyD88 and downstream IRAK is mediated by homo-binding of DD. Due to one of *Avi*-MyD88 without TIR domain, containing no box1 to 3 can be identified and with DD only, this MyD88 should not successfully transduce the normal TLR signaling. Therefore, it is reasonable to infer that this two MyD88 might compete each other to regulate the TLR signaling. That is why the two MyD88 were named *Avi*-MyD88-a and *Avi*-MyD88-i, respectively.

3.3.4 Phylogenetic analysis of MyD88 in *A. viride*

The phylogenetic analysis was also performed of two *Avi*-MyD88 with other species genes based on protein alignment showed that they are distinguished from all insects and molluscs MyD88. This phylogenetic tree revealed that two *Avi*-MyD88 were grouped

doi:10.6342/NTU202000204

together and closely related to other annelid *Hirudo medicinalis*, *Eisenia andrei* and all vertebrate MyD88 (Fig. 3-8B).

3.3.5 Characterization and identification of TNF in *A. viride*

To identify related gene sequences of TLR signaling pathway from *A. viride*. The downstream cytokine TNF was also found in the worm. Two partial sequence of *Avi-TNF* were identified from *A. viride* transcriptome. Again, RACE was used to extend the partial sequence of two *Avi-TNF* and then the full-length sequences were analyzed with SMART program. Both *Avi*-TNF genes have a TM and a TNF domain from canonical structures of TNF. Full-length of *Avi*-TNF-1 has 897 nt in the coding region encoding 293 amino acids including TM (from 37th to 56th amino acid) and TNF domain (from 127th to 290th amino acid) with a calculated molecular weight of 32.94 kDa (Fig. 3-4A and 3-9A). The *Avi*-TNF-2 has 855 nt in the coding region encoding 285 amino acids including TM (from 39th to 61st amino acid) and pfam TNF domain (from 152nd to 280th amino acid) with a calculated molecular weight of 32.54 kDa (Fig. 3-4B and 3-9A).

The protein sequences of *Avi*-TNF-1 and *Avi*-TNF-2 shared less identity (32%). However, the protein of *Avi*-TNF-1 shares 73% identity with Eiger from brachiopods *L. anatine*, 32% identity with *H. discus discus*, and less than 30% identity with *H. sapiens*, *M. musculus, D. rerio* and *D. melanogaster.* On the other hand, *Avi*-TNF-2 shares less

doi:10.6342/NTU202000204

identity from other species compared to *Avi*-TNF-1. The highest protein sequence identity of *Avi*-TNF-2 was 57% with TNF α from *M. musculus*, 50% identity with TNF α from *H. sapiens*, 35% identity with *D. melanogaster* Eiger, 33% identity with *L. anatine* Eiger, and less than 30% identity with two sequences from *D. rerio* and *H. discus discus.* Together, the conserved protein sequence was only observed in the TNF domain among these organisms, and detail differences of two *Avi*-TNF and other TNF, TNF α or Eiger exhibited from protein alignments of TNF domain (from residues 280 to 516) (Fig. 3-6).

3.3.6 Phylogenetic analysis of TNF in *A. viride*

In phylogenetic analysis based on protein sequence alignment, vertebrates and disk abalone *H. discus discus* were grouped in a subgroup, whereas two *Avi*-TNF genes were grouped together and closely from the Eiger of *L. anatine* and *D. melanogaster* (Fig. 3-9B).

3.4 Discussion

The TLR signaling pathway is conserved in animal kingdom that as the first line to protect host from microorganism infection, especially adaptive immunity is lacking in invertebrates (Satake & Sekiguchi, 2012; Skanta et al., 2013). However, functional and constructional divergence in all TLRs makes reach of TLR-mediated immunity and other

doi:10.6342/NTU202000204

area such as developmental biology in *Drosophila* not easy (Sasaki et al., 2009; Zhang et al., 2013). Therefore, three membranes of the TLRs signaling pathway were cloned and identified in this study, containing four fully cloned of *Avi*-TLR, six partial sequences of *Avi*-TLR, two adaptor proteins of *Avi*-MyD88 and two cytokines of *Avi*-TNF. In addition to the TLRs, all sequences of MyD88 and TNF were identified from unpublished transcriptome database in *A. viride* had been cloned in this study. The prominent structures of transmembrane TLRs including LRR for PAMPs binding, TM and TIR domain for signaling cascade (Delneste et al., 2007). Here I showed the same structures of *Avi*-TLR-a and *Avi*-TLR-b protein sequences, but other *Avi*-TLR displayed lacking of LRR, TIR or both of them even fully cloned in *Avi*-TLR-c and *Avi*-TLR-d. This diversity of structure organization also represented in *C. elagans* TOL-1 that the only one TLR without TIR domain in C-terminal. Nevertheless, *C. elagans* TOL-1 also progress in pathogen recognition same as the homologous TLRs in other organisms (Pujol et al., 2001). Based on blasting results from SMART program, two *Avi*-MyD88 sequences exhibited different structures in protein domain, one of the sequences has two regular functional domains of MyD88, namely DD and TIR domain. However, the other one lacks the TIR domain, responsible for TLR binding. One splices variant of MyD88 named MyD88s was discovered from HEK293T cell in 2002. Overexpression of MyD88s specifically inhibits downstream IL-1β and NF-κB activation (Janssens et al., 2002). This

doi:10.6342/NTU202000204

variant protein is not able to recruitment of IRAK-4 due to lack intermediate domain (ID) between DD and TIR domain (Janssens et al., 2003). However, *Avi*-MyD88-i not a variant protein of *Avi*-MyD88-a but the deficiency of TIR domain, it may act opposite function of *Avi*-MyD88-a in *A. viride*. Therefore, one of Avi-MyD88 named *Avi*-MyD88-a which might activate the TLR signaling pathway, and the other named *Avi*-MyD88-i which might be involved to inactive the TLR pathway. Following this opinion, the gene expression and regulation of *Avi*-MyD88-a and *Avi*-MyD88-i were be track during regenerative processes in chapter 4.

doi:10.6342/NTU202000204

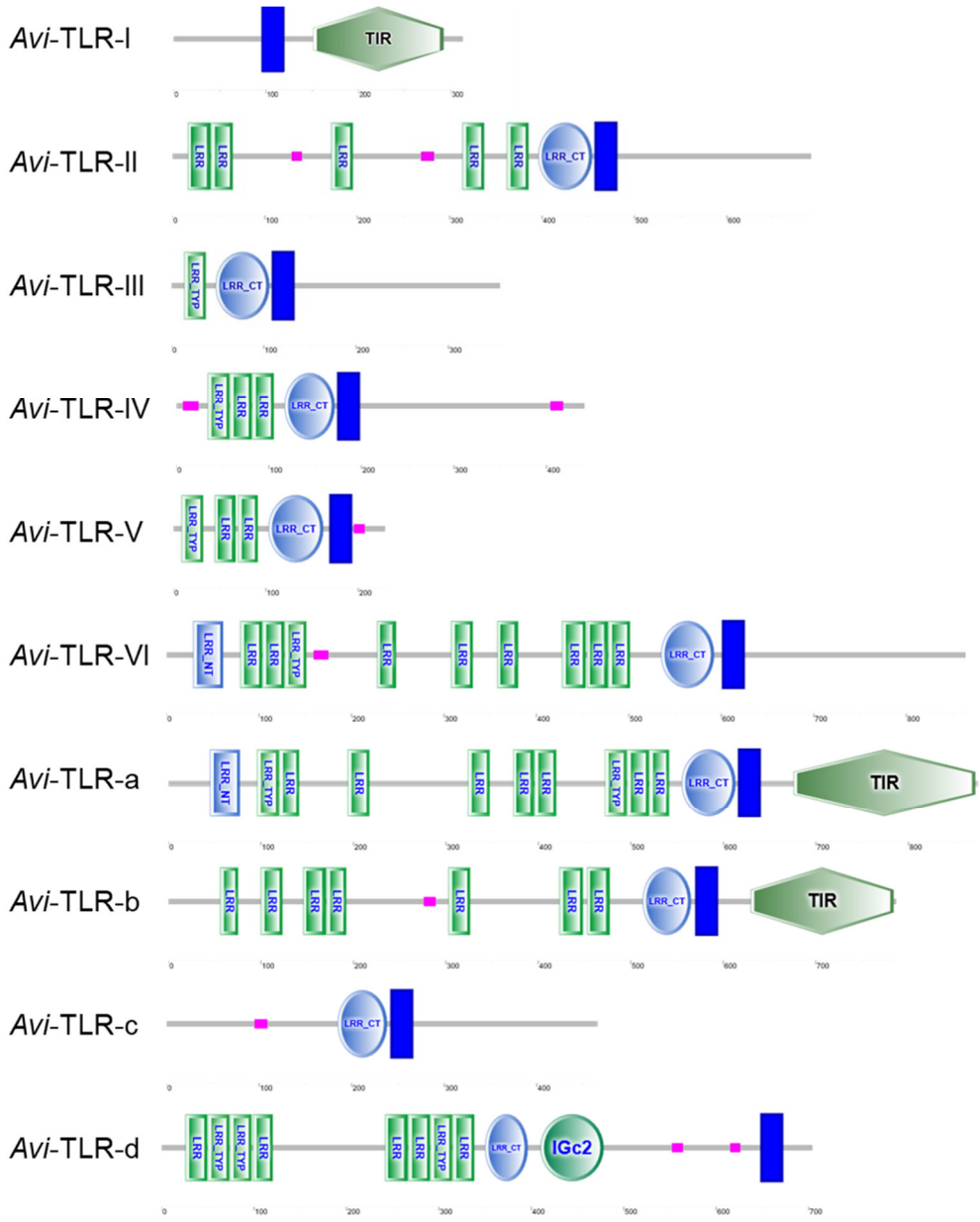

Figure 3-1. The structural organization of ten *Avi*-TLR protein sequence. The partial sequences of *Avi*-TLR-I to VI and full sequences of *Avi*-TLR-a to b were analyzed with SMART program. Both of *Avi*-TLR-a and *Avi*-TLR-b have canonical structure of TLRs, including LRR, TM and TIR domain but not N-terminal signal peptide. LRR-NT: leucine-rich repeat N-terminal; LRR: leucine-rich repeat; LRR-CT: leucine-rich repeat C-terminal; Blue rectangle: TM; TIR: Toll-interleukin 1 receptor domain.

doi:10.6342/NTU202000204

A

```
1 ATGACGAACTTCAAAGCATTAGCTGTCGTTATTATTTTAATCTGCTCATCAGTTAGCTTCGCAGAAAAGAACAAACCTGTTTTAGAAGCG
  M__T__N__F__K__A__L__A__V__V__I__I__L__I__C__S__S__V__S__F__A__E__K__N__K__P__V__L__E__A__
91 ACAAGCAAGTTGGCTAAAAAAACGAGCAAAAGAAACTTTGCCGAATGTCCGTCGAAATGTTCCTGTTCAAACAGCTCCGTTGACTGTTCG
  T__S__K__L__A__K__K__T__S__K__R__N__F__A__E__C__P__S__K__C__S__C__S__N__S__S__V__D__C__S__
181 AATCACCAGTTGTCCAGAGTACCACGTGGTTTTGCAGTTTCAACTACATCAATCGATCTCAGCTTCAATTCCATTGACGAAATTACAAGC
  N__H__Q__L__S__R__V__P__R__G__F__A__V__S__T__T__S__I__D__L__S__F__N__S__I__D__E__I__T__S__
271 ACTAGTTTTAGTAACTTGATCAATCTGCAAAGACTCGACTTATCTCACAATGATATCTCAACGATTGATTATAAAGCGTTTATTGATCTT
  T__S__F__S__N__L__I__N__L__Q__R__L__D__L__S__H__N__D__I__S__T__I__D__Y__K__A__F__I__D__L__
361 GCTAACTTGACATGGCTCAGCCTGTCATCGAATTATCTGTCGACTATTTCGAACGATGATTTCGTTGGATCAACTAACATACGCCATCTT
  A__N__L__T__W__L__S__L__S__S__N__Y__L__S__T__I__S__N__D__D__F__V__G__S__T__N__I__R__H__L__
451 GATCTCAGTTACAACGATAGATTATCGAGTCGTGGTTTTCCTAATATTAGTTCCTTGGAAAAATTGGAGCTGCTTGACATATCTGGCACT
  D__L__S__Y__N__D__R__L__S__S__R__G__F__P__N__I__S__S__L__E__K__L__E__L__L__D__I__S__G__T__
541 GGACTGACTGCTACTAAGTTTCCTCCCAGTTATGGAACTTTGTCAAATTTACGAACACTTAAAATGAGTTTTAATCAGTTGTCGAAGATT
  G__L__T__A__T__K__F__P__P__S__Y__G__T__L__S__N__L__R__T__L__K__M__S__F__N__Q__L__S__K__I__
631 TACAATGAATATTTTACGAACATTCATCGCGAAAGTATTTTCAGATTTGAATGCGCTGTTTGTAGTTTAACATTTATAGAGGCAGGCTTC
  Y__N__E__Y__F__T__N__I__H__R__E__S__I__F__R__F__E__C__A__V__C__S__L__T__F__I__E__A__G__F__
721 TTTTCTTATTGGAAAAAATTAACATATATCAACTTATCTGGCAACGCTTTAGATTTTGGTCAGGTACAGAGCGTATTAATGGGTCTAGAG
  F__S__Y__W__K__K__L__T__Y__I__N__L__S__G__N__A__L__D__F__G__Q__V__Q__S__V__L__M__G__L__E__
811 AAAAATAGTGGTCCGCTCGAAGCGCTTGATTTCACTGGTTATACCGATCATTCTCTGTTCTCTGATACTCTTGATTCCATAAAAAATCGG
  K__N__S__G__P__L__E__A__L__D__F__T__G__Y__T__D__H__S__L__F__S__D__T__L__D__S__I__K__N__R__
901 GCATTATTGTGGCTATCCTTCGCGTGTAGTTCTAATTATGGACCATTACGCGCTAATACGTTTCGTCAGTTAAATGCACTGAAATTCTTA
  A__L__L__W__L__S__F__A__C__S__S__N__Y__G__P__L__R__A__N__T__F__R__Q__L__N__A__L__K__F__L__
991 AATCTTAGCTTTAGTAAAATTTCTTCAATAGAATTGCACGCTTTTGACGGTCTATACAATTTGACAGAACTACACATCGAAAAGATTGTT
  N__L__S__F__S__K__I__S__S__I__E__L__H__A__F__D__G__L__Y__N__L__T__E__L__H__I__E__K__I__V__
1081 GAAGTAAAATGGTCAATTCCAGCAAATATGTTTCCACCAAGCTTACTGACTTTAAATCTGAATAATAATAATCTCGGTGAAATCAATCAA
  E__V__K__W__S__I__P__A__N__M__F__P__P__S__L__L__T__L__N__L__N__N__N__N__L__G__E__I__N__Q__
1171 GACGCATTTGCTAATCTGATCAATTTAAAATCATTATCTTTAAGTAAATGTGTCATAAATTGGATAAGTGATGCGATATTTGCAACTGAA
  D__A__F__A__N__L__I__N__L__K__S__L__S__L__S__K__C__V__I__N__W__I__S__D__A__I__F__A__T__E__
1261 AATTCTTTGACATATTTAGATCTATCCTATAATGAATTAAATAAACAGATAAATTTCTTAAGTTTATTTCATGATTTGAAAAAATTAACA
  N__S__L__T__Y__L__D__L__S__Y__N__E__L__N__K__Q__I__N__F__L__S__L__F__H__D__L__K__K__L__T__
1351 ATTTTGGATATGTCATATTGCATTAAATTTAATTTGATAAACAACCAGGATATGTTCAAAAGTCTTGTATCTCTCACAAATTTATCATTA
  I__L__D__M__S__Y__C__I__K__F__N__L__I__N__N__Q__D__M__F__K__S__L__V__S__L__T__N__L__S__L__
1441 GCAGGAAATAAAATAAAAACATTACCAATTGAACTGTTTGCAAGTGTATCTGACCTTCAGAATCTGAATCTTAGCGATAATAATGTGGAA
  A__G__N__K__I__K__T__L__P__I__E__L__F__A__S__V__S__D__L__Q__N__L__N__L__S__D__N__N__V__E__
1531 GACTGGGACGATCAGACTTTTATGTCAGTTTCTCATTTAAAAAGCATTTCATTAGCTAGCAATAAAATTCAGATCATTAAACCATCTTTT
  D__W__D__D__Q__T__F__M__S__V__S__H__L__K__S__I__S__L__A__S__N__K__I__Q__I__I__K__P__S__F__
```


doi:10.6342/NTU202000204

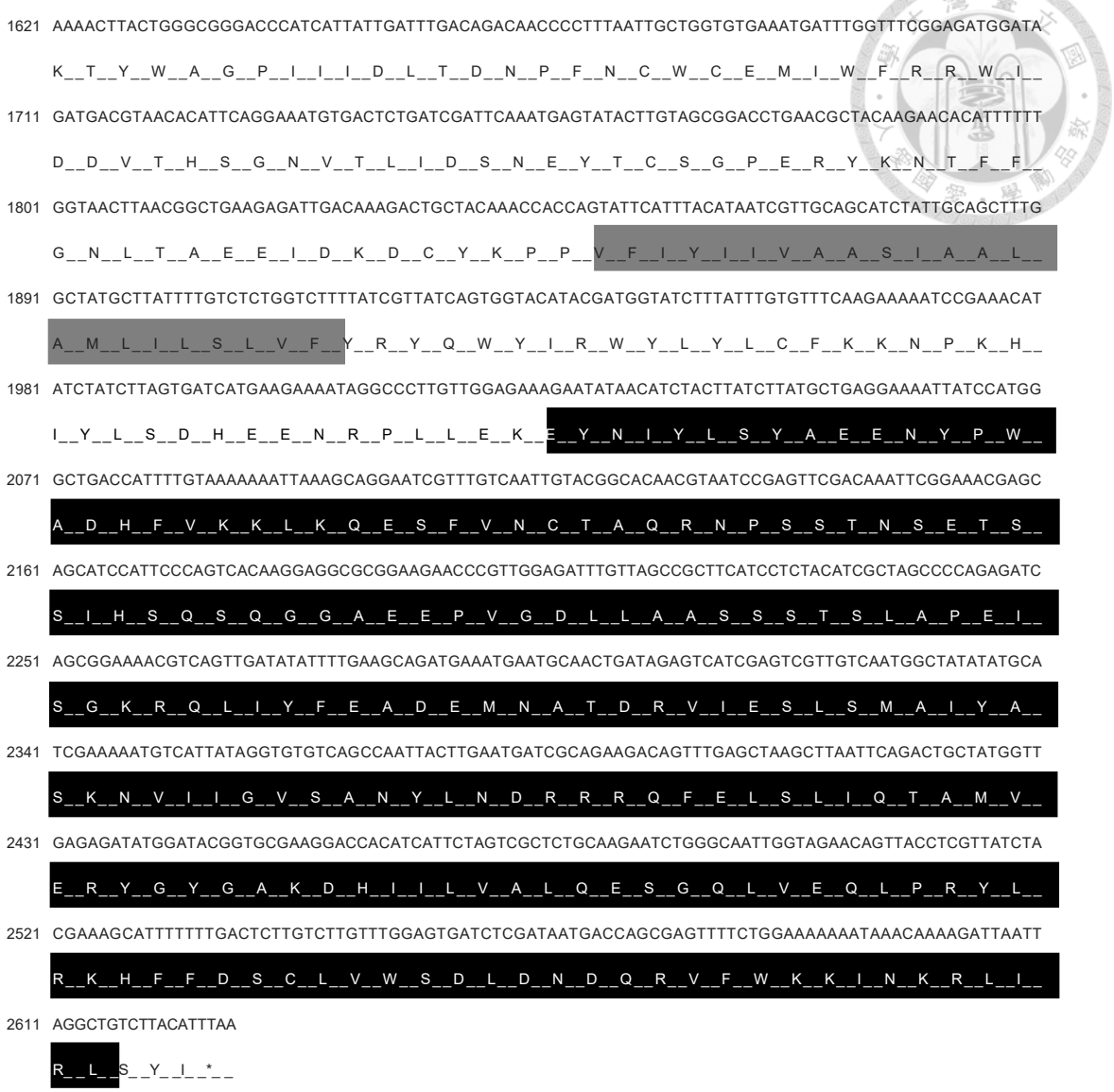

B

doi:10.6342/NTU202000204

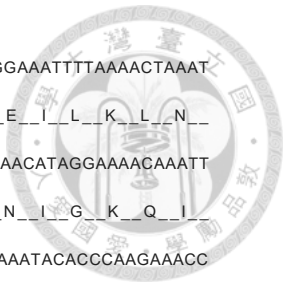

451 TTATTGGATTTATCTAATAATAAACTCAGCGAAGCAATATTTCCTTCCAGTTATTCGTCAATGGGGCAGCTGGAAATTTTAAAACTAAAT

L__L__D__L__S__N__N__K__L__S__E__A__I__F__P__S__S__Y__S__S__M__G__Q__L__E__I__L__K__L__N__

541 TGCAACGGGATTACTCAGATAAATATGATAAATCTACATGCCACTTCGATTAAAGTTTTCGAGCTAATGCAAAACATAGGAAAACAAATT

C__N__G__I__T__Q__I__N__M__I__N__L__H__A__T__S__I__K__V__F__E__L__M__Q__N__I__G__K__Q__I__

631 TGTGTTCAAAGTGAAGGCGATTGGTGGTTTTCTTCATTCAAAAATCTTGCGATACTGAAATTATCTGGAAATAAATACACCCAAGAAACC

C__V__Q__S__E__G__D__W__W__F__S__S__F__K__N__L__A__I__L__K__L__S__G__N__K__Y__T__Q__E__T__

721 TTGCAAAAGATTATAACCAGTTTGAATGGGACGAAGTTTTTAACTCACTTGTATTTAGATGGAGTTATTAGTGGGTATTCAATAACTCCT

L__Q__K__I__I__T__S__L__N__G__T__K__F__L__T__H__L__Y__L__D__G__V__I__S__G__Y__S__I__T__P__

811 AGCATTTTCCAAACTCTATCTTCTAGTCGGCTCAAGTTTCTTTCTCTATCTTGGAGTCAGTACATCGAAAAAATTGAAGATAAAGCATTT

S__I__F__Q__T__L__S__S__S__R__L__K__F__L__S__L__S__W__S__Q__Y__I__E__K__I__E__D__K__A__F__

901 ATTGCGTTATCACAATTGACAGAATTAAATTTAAAGTACTCACGTATAACGCAAATAGGTAATGACGCTTTAGCTGGATTAGATAAGCTG

I__A__L__S__Q__L__T__E__L__N__L__K__Y__S__R__I__T__Q__I__G__N__D__A__L__A__G__L__D__K__L__

991 CAATTACTTAATATGGATTGTGCATACGCGGGAGATCAAATGAATCTGTCGAAAGACTTTTTCCCAAAAAGTTTGAAGTCAATAAATTTA

Q__L__L__N__M__D__C__A__Y__A__G__D__Q__M__N__L__S__K__D__F__F__P__K__S__L__K__S__I__N__L__

1081 TCCCGGAATAAAATCCTTATTTCATCAGATGCATTTCAAAATTTAATTAATTTAACCGAGCTGTCATTATGTAACATTGGGTTAAACGCG

S__R__N__K__I__L__I__S__S__D__A__F__Q__N__L__I__N__L__T__E__L__S__L__C__N__I__G__L__N__A__

1171 TTTAATTCTTCACTATTATTTCATCAAAACGTATCTCTAAGATATCTAGATTTATCTAAAAATAAACTTTATGGTGGTTCCTTAAATCTA

F__N__S__S__L__L__F__H__Q__N__V__S__L__R__Y__L__D__L__S__K__N__K__L__Y__G__G__S__L__N__L__

1261 ACGAGGTTAACAAGTCTACAGGTTCTTAATATAAGTTGCAATAAACTTGGAGATTCGTATGTAGGATTTTCTACGTTTCTAGAAAATATT

T__R__L__T__S__L__Q__V__L__N__I__S__C__N__K__L__G__D__S__Y__V__G__F__S__T__F__L__E__N__I__

1351 TGTCTTCTCACAGCCCTACAAAAGTTAGATCTTAGCAGTAATACGATAAATTATTGGAACGTAGCCACTCAATTCCAGTACATGCGTTTC

C__L__L__T__A__L__Q__K__L__D__L__S__S__N__T__I__N__Y__W__N__V__A__T__Q__F__Q__Y__M__R__F__

1441 TTTTCATTGGCTAATAACAGCATCATTGCACTCGATGAGTCATTCAGCACTAGTTGGGGATCAACGAATGTTGAAACCATTATTGATTTA

F__S__L__A__N__N__S__I__I__A__L__D__E__S__F__S__T__S__W__G__S__T__N__V__E__T__I__I__D__L__

1531 AGAGCCAATAAATTTGATTGCAATTGCACAATGGAATGGTTTCGTAAGTGGATGGAAAATACTAAAGAAAATTACGTAATCTTAATTGGT

R__A__N__K__F__D__C__N__C__T__M__E__W__F__R__K__W__M__E__N__T__K__E__N__Y__V__I__L__I__G__

1621 TGGGAGGAGTACAGATGTTCTGATGGTAGGTTGTATAAAAATATCAGCAACTCTGAACTTGAAGCGTATTGTCACTTATCAGTATCCCAG

W__E__E__Y__R__C__S__D__G__R__L__Y__K__N__I__S__N__S__E__L__E__A__Y__C__H__L__S__V__S__Q__

1711 GCCGCTGTTATAATTACTATCATTGTTGTAGTAGTGGTAACGTTAATATTAGCTGCACTAGGTAACGTTATGTACTCGAAATATAAATGG

A__A__V__I__I__T__I__I__V__V__V__V__V__T__L__I__L__A__A__L__G__N__V__M__Y__S__K__Y__K__W__

1801 CAATTAATGTATTGGTGTTATCGTACTTTCTGTTTGGAGCAACAACAGATGAATGGCGAACTAGAGTCTTTGCGGCAGAATTATTACATA

Q__L__M__Y__W__C__Y__R__T__F__C__L__E__Q__Q__Q__M__N__G__E__L__E__S__L__R__Q__N__Y__Y__I__

1891 AGAGATTTTTACATATCATATGCAGCAAATGATGAAATTATAGCCACACAATTGAACGCGAAGACTGAACAACAACAAAATGCAAACGAT

R__D__F__Y__I__S__Y__A__A__N__D__E__I__I__A__T__Q__L__N__A__K__T__E__Q__Q__Q__N__A__N__D__

1981 TTGAATCGTTGCAATAGAACTTATTTCGAAGGCAGAGACGCCACGGGAGATGAATGGGAAATCGAAAGTCTAGCGCAAGCAATTCACTTC

L__N__R__C__N__R__T__Y__F__E__G__R__D__A__T__G__D__E__W__E__I__E__S__L__A__Q__A__I__H__F__

doi:10.6342/NTU202000204

Figure 3-2. Sequence identification of two *Avi*-TLR. Nucleotide sequence and amino acid sequence of *Avi*-TLR-a and *Avi*-TLR-b were identified by degenerate primer and 3'/5' RACE. (A) The protein sequence of *Avi*-TLR-a has 2628 nt in the coding region encoding 876 amino acids, including TM (label by grey background) and TIR domain (label by black background). (B) The *Avi*-TLR-b has 2364 nt in the coding region encoding 788 amino acids with TM and TIR domain.

doi:10.6342/NTU202000204

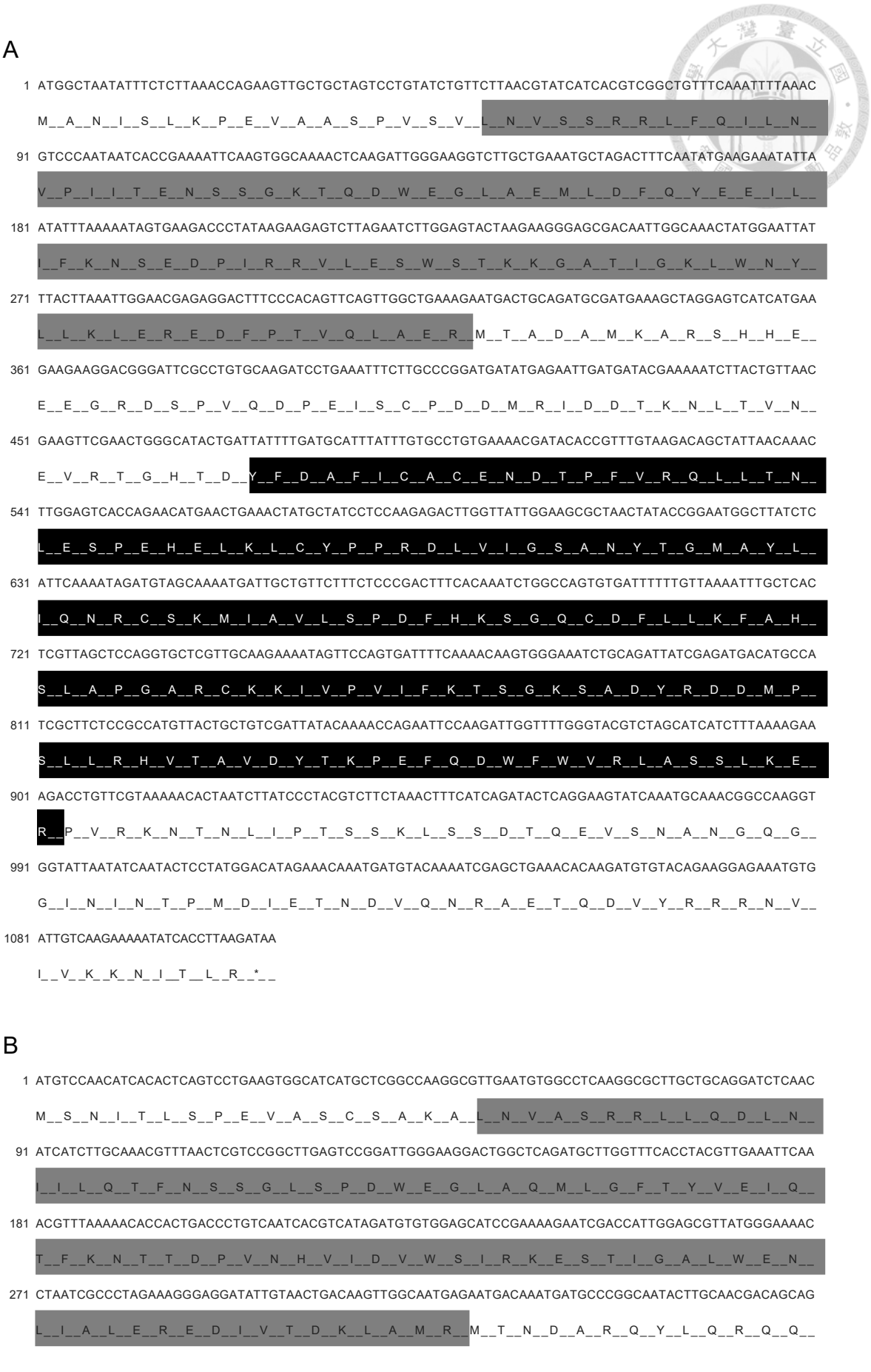

doi:10.6342/NTU202000204

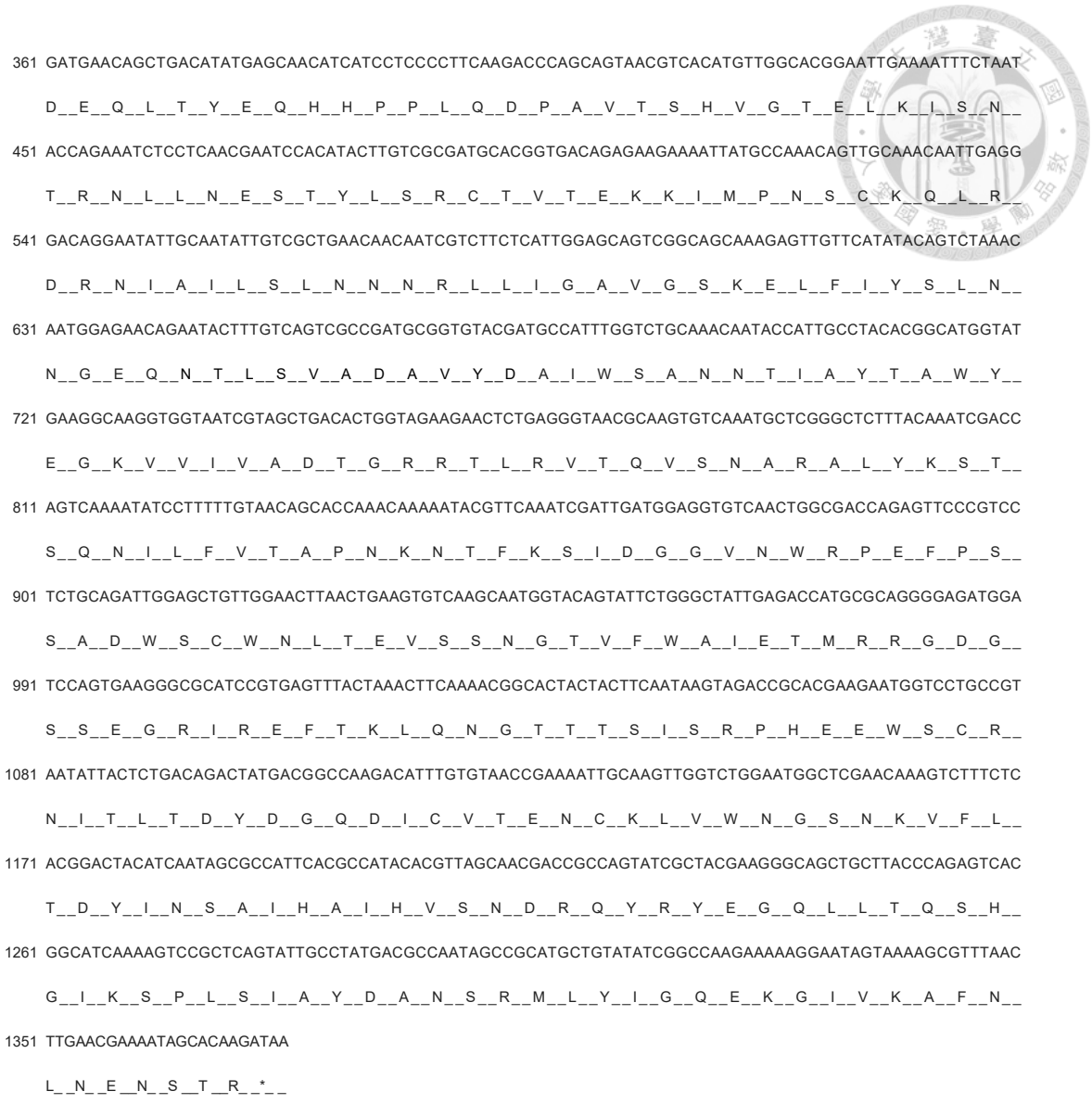

Figure 3-3. Sequence identification of two *Avi*-MyD88. Nucleotide sequence and amino acid sequence of *Avi*-MyD88-a and *Avi*-MyD88-i were identified by RACE PCR. (A) The protein sequence of *Avi*-MyD88-a from with 1110 nt in the coding region encoding 370 amino acids, including DD (label by grey background) and TIR domain (label by black background). (B) The *Avi*-MyD88-i has 1374 nt in the coding region encoding 458 amino acids with DD but not TIR domain.

doi:10.6342/NTU202000204

A

```
1 ATGAATGAAGCGAGGAAAACCCCGGGATTTTTTTCCGTTGCGAATGGTGGTGATAGAGTGATAAAGCCGGCAGAAGAAGCACGACAGTTG
  M__N__E__A__R__K__T__P__G__F__F__S__V__A__N__G__G__D__R__V__I__K__P__A__E__E__A__R__Q__L__
91 TGCACATCGTCAGGAAAGTTGACAGTCGCTTTCTTCGTACTTTGCATTTGTTTTGACGTGTTAGTTGTCGTATACGTGAAAAGCTTACAC
  C__T__S__S__G__K__L__T__V__A__F__F__V__L__C__I__C__F__D__V__L__V__V__V__Y__V__K__S__L__H__
181 TTGAAAATTGAACGTATTCAAAGCTCAGCTGCATTTTCGCAAAATGATGACTGCGAAATAAACTCACTGAATTCTCACAATGAAGGATCT
  L__K__I__E__R__I__Q__S__S__A__A__F__S__Q__N__D__D__C__E__I__N__S__L__N__S__H__N__E__G__S__
271 CTGTCTCGGCGTAGAAGGCAAACATGCAACGGAAGAGCTACCATAGATGACCTGCATAGCTTAGAGGACAAATTTCATGAAGAGTTACAA
  L__S__R__R__R__R__Q__T__C__N__G__R__A__T__I__D__D__L__H__S__L__E__D__K__F__H__E__E__L__Q__
361 AAACATCGTTACAATCATCAATCAGCACATGTTGGCCTGGAACAAAGCAAAATACCGTCAGCAGTTACGAATGCATCGTCTTTTACATGG
  K__H__R__Y__N__H__Q__S__A__H__V__G__L__E__Q__S__K__I__P__S__A__V__T__N__A__S__S__F__T__W__
451 ACTCTCAATCGTGGTGCTCATTTTGCTCTTCACAATCACATGGAATTTGAAGAATCCAATAAAAAGCTGTCTGTTATCGGCAGTGGCTAT
  T__L__N__R__G__A__H__F__A__L__H__N__H__M__E__F__E__E__S__N__K__K__L__S__V__I__G__S__G__Y__
541 TACTTTGTTTATGCTCAAGTAACATCTAAACGAGTTACAACTGCGTCGTATGCTGATTGCTATTTTACTATTTGGATTGAGAGGATTGAG
  Y__F__V__Y__A__Q__V__T__S__K__R__V__T__T__A__S__Y__A__D__C__Y__F__T__I__W__I__E__R__I__E__
631 AGGCCTGGCAAAACGAAACATATTCATTTGCTTACAATGCAACCGTCATCTGCTGTGAACAGTACGTATAAGAGAACTCAACGACAAGTG
  R__P__G__K__T__K__H__I__H__L__L__T__M__Q__P__S__S__A__V__N__S__T__Y__K__R__T__Q__R__Q__V__
721 GGGAGCCAGTCCTCCACCAACGAAAGCGTCTTCAGCGGAGGAATTTTCCTATTAGAGAGTTCTGATCGCATCTTTTTAAAGAACCACGAA
  G__S__Q__S__S__T__N__E__S__V__F__S__G__G__I__F__L__L__E__S__S__D__R__I__F__L__K__N__H__E__
811 TATCGTGTTTGCCAAGTGCTGACTGCGCCTGACAAAACTTTCCTCGGTGCAGTAAAATTGCAATCATAG
  Y__R__V__C__Q__V__L__T__A__P__D__K__T__F__L__G__A__V__K__L__Q__S__*__
```

B

```
1 ATGAGTTTAAATTTGTTACCATCTCATGAGATCGAAGTGAAAAATACTGACAAGACGGCAGATGATAAAAAAAGAAATTCTAAGAATGCT
  M__S__L__N__L__L__P__S__H__E__I__E__V__K__N__T__D__K__T__A__D__D__K__K__R__N__S__K__N__A__
91 TCAAAAAATTGGCAAGTGGGCGATGTTGTCAGCCTTCTGTTCTTGCTGTGTGGGCAAGTAGTTATCATAATTCTGGTCGTGCAGCTTCAT
  S__K__N__W__Q__V__G__D__V__V__S__L__L__F__L__L__C__G__Q__V__V__I__I__I__L__V__V__Q__L__H__
181 TTCGAAGTGGACGAGCTGGAACGTTCAAACTTGGCCAAGTTGCAGTTGAAAGCAGACCAAGCAAAGCAACATTTAAACGATGTTGGTGTG
  F__E__V__D__E__L__E__R__S__N__L__A__K__L__Q__L__K__A__D__Q__A__K__Q__H__L__N__D__V__G__V__
271 TTTCGGCAACGAGAGAAGCGAGGCACAAATCTAGCTCGAAATGAAGAGTTTGATAAGTTGAAAGGAAATATTATGAGTTATTTTCAATTT
  F__R__Q__R__E__K__R__G__T__N__L__A__R__N__E__E__F__D__K__L__K__G__N__I__M__S__Y__F__Q__F__
361 TTGCATGCGTCAGCTCATTTGTGCCTCAACGAAAACTACACGAGAAGAATGAACGAACATTTCGATAGTAATTTCCGCTGGTCAGGGGGG
  L__H__A__S__A__H__L__C__L__N__E__N__Y__T__R__R__M__N__E__H__F__D__S__N__F__R__W__S__G__G__
451 CGGAGTCATTGTTCAGGAACTTCTAACATCAATCACGACAATCTGGAACTAAGGACGGCTCACTCAAGCGGTTTGGAATTATCTAGAACT
  R__S__H__C__S__G__T__S__N__I__N__H__D__N__L__E__L__R__T__A__H__S__S__G__L__E__L__S__R__T__
541 GGTCACTACTTCATATACTTACAAATGACTGTAAATGGCACTGATCCACAGGCTGCGCGGACCAATCCACATTGTGTCTTCTTCATTGAG
  G__H__Y__F__I__Y__L__Q__M__T__V__N__G__T__D__P__Q__A__A__R__T__N__P__H__C__V__F__F__I__E__
```


doi:10.6342/NTU202000204

Figure 3-4. Sequence identification of two *Avi*-TNF. Nucleotide sequence and amino acid sequence of *Avi*-TNF-1 and *Avi*-TNF-2 were identified. (A) The protein sequence of *Avi*-TNF-1 has 897 nt in the coding region encoding 293 amino acids, including TM (label by grey background) and TNF domain (label by black background). (B) The *Avi*-TNF-2 has 855 nt in the coding region encoding 285 amino acids with TM and pfam TNF domain (label by black background).

doi:10.6342/NTU202000204

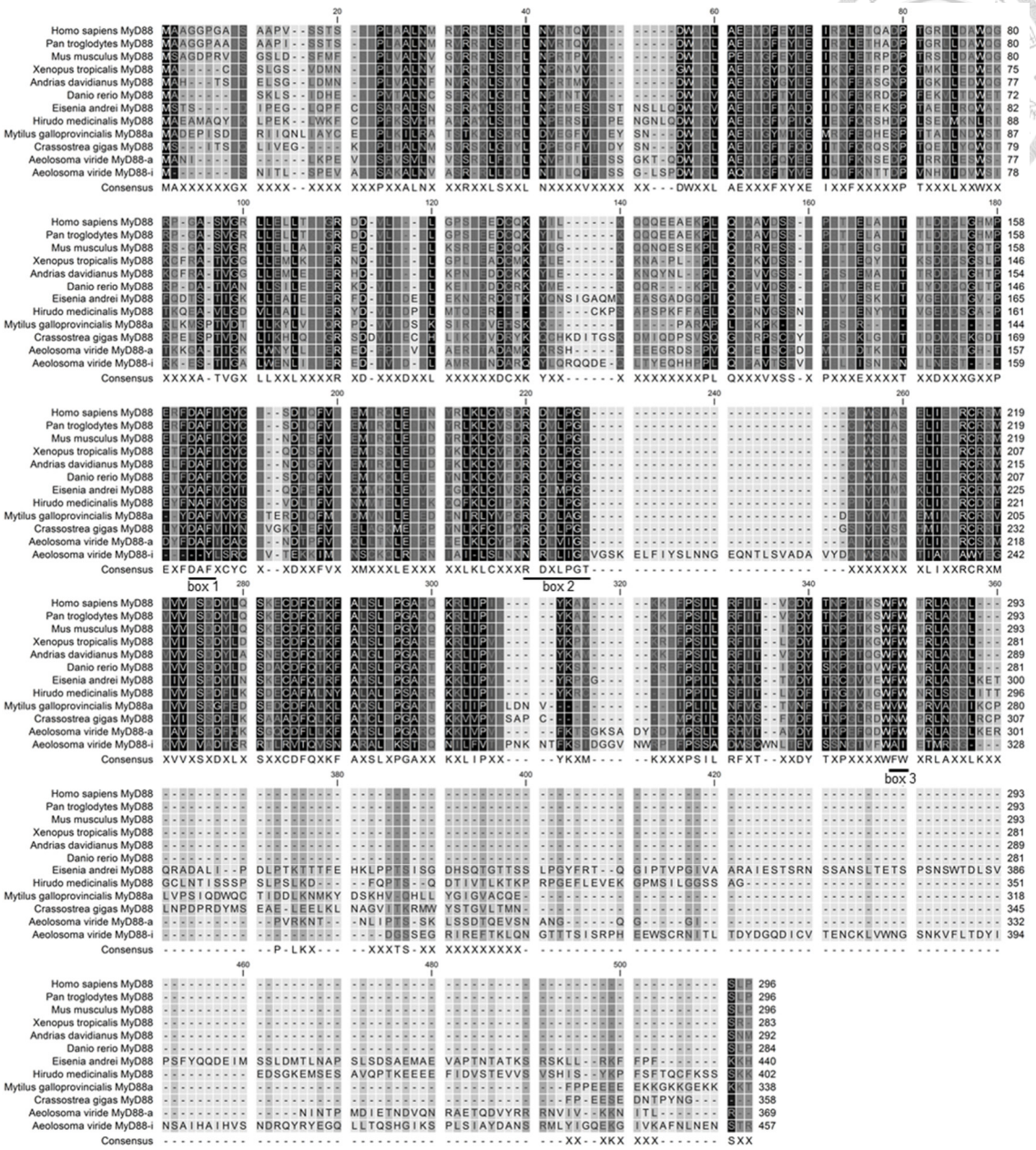

Figure 3-5. Protein sequence alignment of *Avi*-MyD88-a and *Avi*-MyD88-i with other species from GenBank. Multiple ORF alignment of MyD88 from 10 representative species, including human (*H. sapiens*), chimpanzee (*P. troglodytes*), mouse (*M. musculus*), clawed frog (*X. tropicalis*), salamander (*A. davidianus*), zebrafish (*D. rerio*), leech (*H. medicinalis*), earthworm *(E. andrei*), mussel (*M. galloprovincialis*) and oyster (*C. gigas*).

doi:10.6342/NTU202000204

Consensus residues (>60% identity) are shown in the bottom row of the alignment. Box 1-3 motifs are conserved between TIR domains of MyD88 but not including *Avi*-MyD88-i.

doi:10.6342/NTU202000204

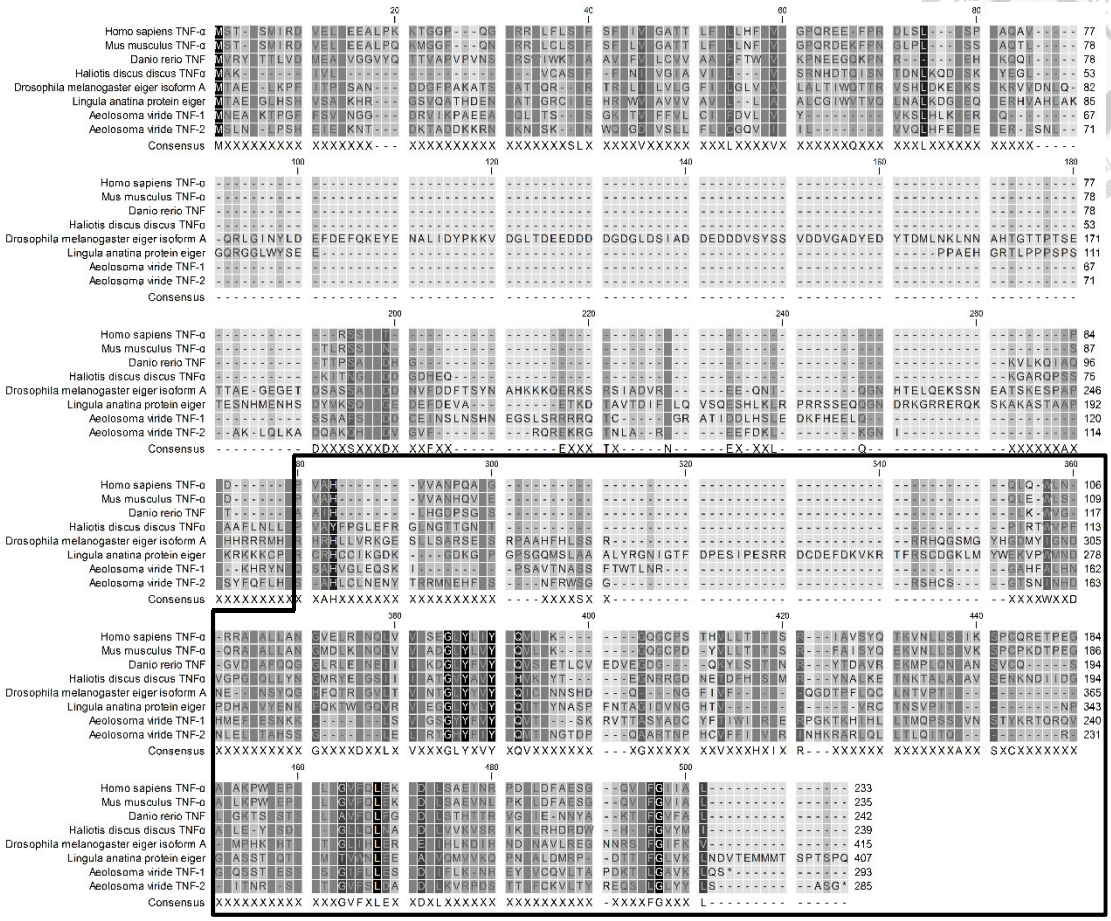

Figure 3-6. Protein alignment of *Avi*-TNF-1 and *Avi*-TNF-2 with other species from GenBank. Multiple ORF alignment of TNF superfamily, including TNF, TNF α or Eiger from six species, including human (*Homo sapiens*), mouse (*Mus musculus*), zebrafish (*D. rerio*), disk abalone *H. discus discus*, Lingula *L. anatine* and fly *D. melanogaster*. Consensus residues (>60% identity) are shown in the bottom row of the alignment. Black box area revealed TNF domain in ORF

doi:10.6342/NTU202000204

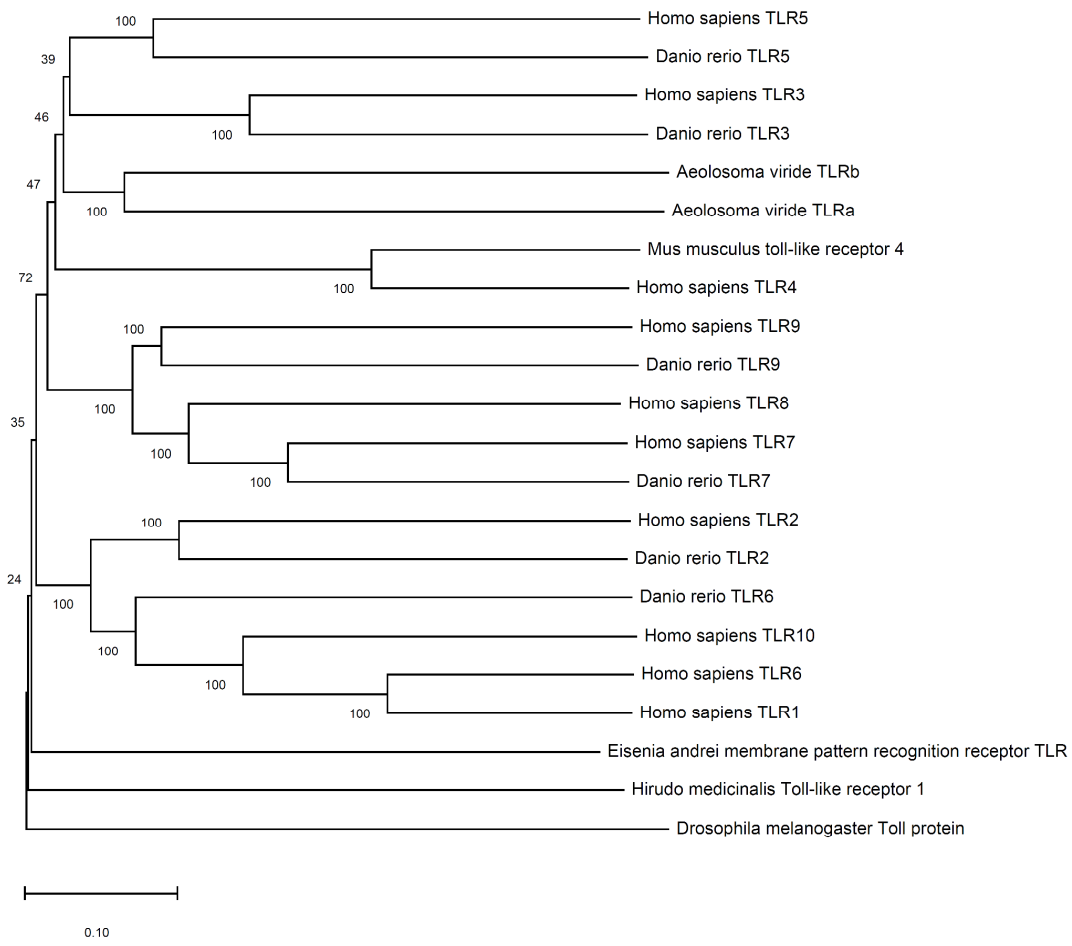

Figure 3-7. The structural organization and phylogenic analysis of two *Avi*-TLR. B Phylogenetic analysis of the two *Avi*-TLR deduced from a protein alignment by MEGA-X. The phylogenetic tree showed that *Avi*-TLR-a and *Avi*-TLR-b are conserved with TLR3 and TLR5 from human *H. sapiens* and zebrafish *D. rerio*.

doi:10.6342/NTU202000204

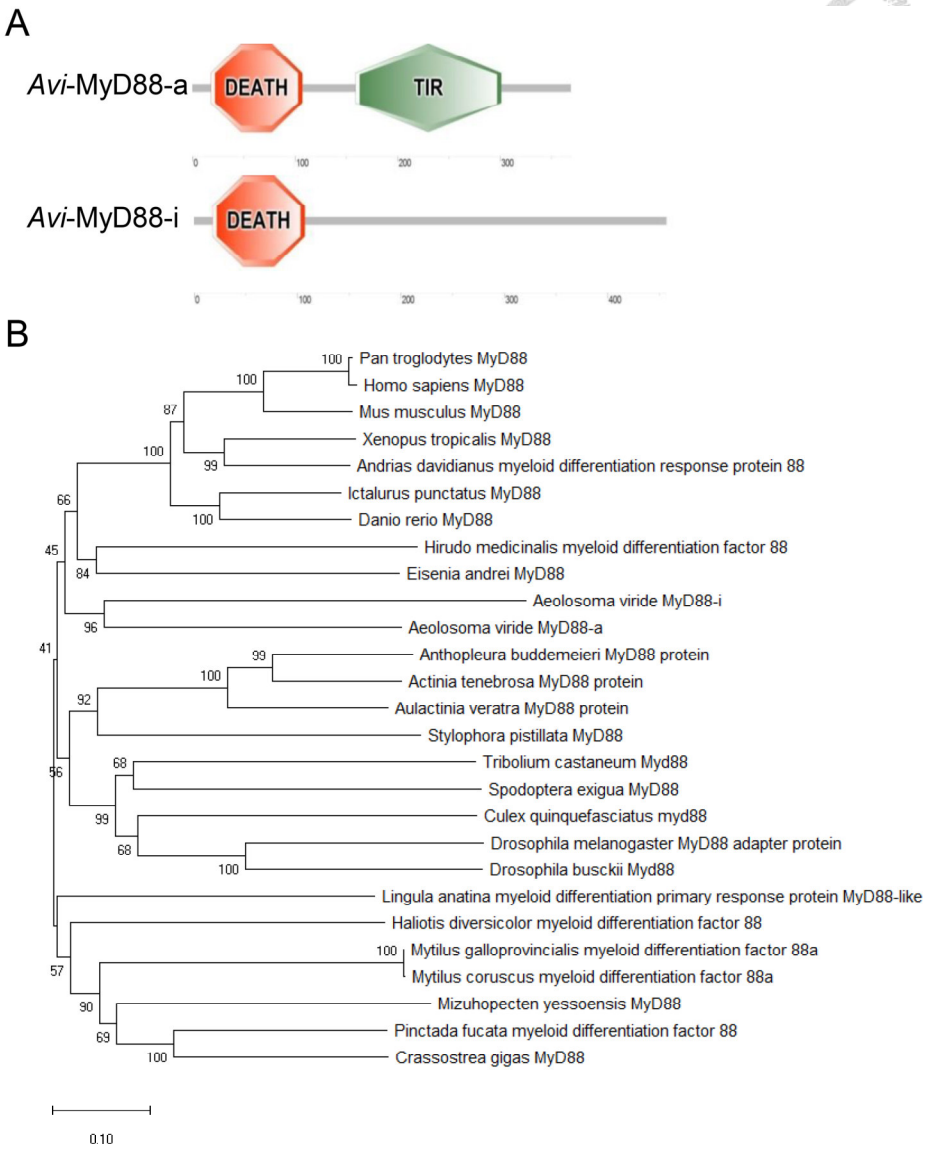

Figure 3-8. The structural organization and phylogenic analysis of two *Avi*-MyD88.

(A) *Avi*-Myd88-a and *Avi*-Myd88-i were identified and analyzed with SMART program. Both *Avi*-MyD88 genes have death domain, but *Avi*-MyD88-i lacks the TIR domain in C-terminal. TIR: Toll-interleukin 1 receptor domain. (B) Phylogenetic analysis of the two *Avi*-MyD88 deduced from a protein alignment by MEGA-X. *Avi*-MyD88-a and *Avi*-MyD88-i were grouped closed to leech *H. medicinalis* and earthworm *E. andrei*, then can be distinguished with other species MyD88 from Chordata, Arthropoda and Mollusca.

doi:10.6342/NTU202000204

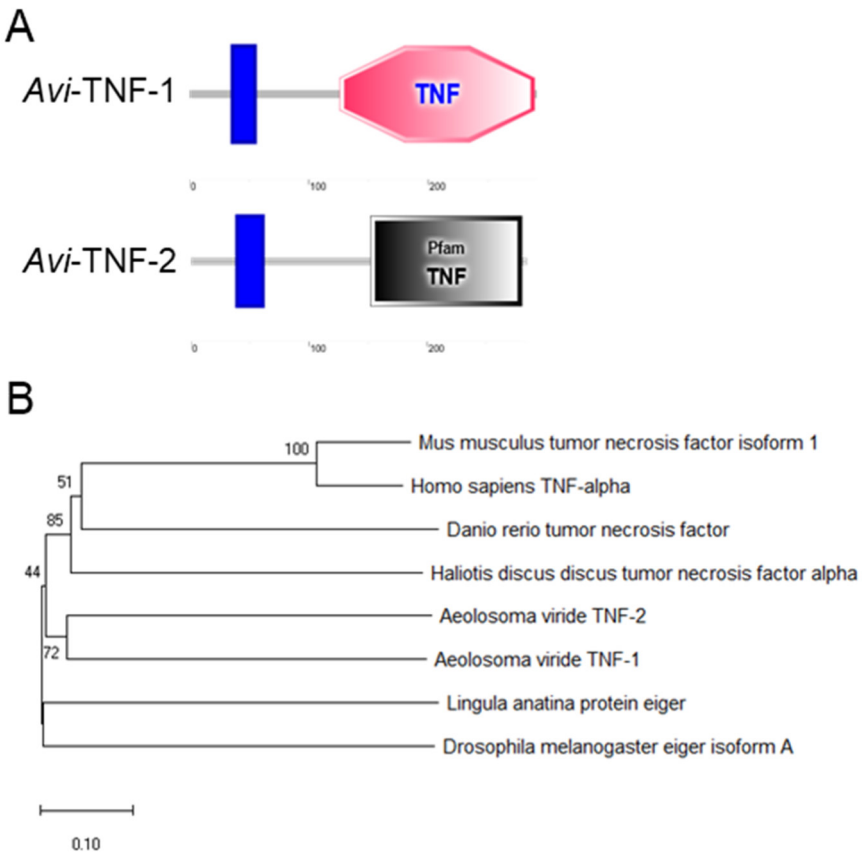

Figure 3-9. The structural organization and phylogenic analysis of two *Avi*-TNF. (A) *Avi*-TNF-1 and *Avi*-TNF-2 were identified and analyzed with SMART program. Both of two *Avi*-TNF have TM and TNF domain. (B) Phylogenetic analysis of the two *Avi*-TNF deduced from a protein alignment by MEGA-X. Both of two *Avi*-TNF can be grouped with other TNF sequences from *D. rerio*, *H. discus discus*, *H. sapiens* and *M. musculus*, and also close to protein Eiger of *L. anatine* and *D. melanogaster.*

doi:10.6342/NTU202000204

Chapter 4

Immune regulation of toll-like receptor (TLR) signaling pathway during anterior regeneration in *Aeolosoma viride*

doi:10.6342/NTU202000204

4.1 Introduction

The immune system and inflammatory responses that prevent deadly infections have been implicated as playing critical roles during wound healing and regeneration (Aderem & Ulevitch, 2000; Kyritsis et al., 2012). Wound healing in animals after injury is one of the most complex processes which are not fully understood. Infection and injury may share similar inflammatory cascades that are activated by pathogens invasion of the wound during regeneration. The process involves the spatial and temporal synchronization of a variety of cell types that are triggered by cytokines or chemokines with different roles in the squirted stages of inflammation, hemostasis, growth, and remodeling. Therefore, inflammation as a first defense line which is to be proved the highly conserved event in both vertebrates and invertebrates (Ashley et al., 2012; Vizzini, 2017).

One of crucial topics in host inflammation is how pathogen recognition by pattern recognition receptors (PRR). And ancient function of toll-like receptors (TLRs) is the interesting issue in immunology. TLR signaling pathway is evolutionarily conserved across species of vertebrate and invertebrate, given that can insight of comparative studies on evolution of innate immunity (Ausubel, 2005; Satake & Sekiguchi, 2012). TLR signaling pathway is activated by recognized conserved microbial structures or products of microbial metabolism that trigger immune responses to invaded pathogens (Aderem &

doi:10.6342/NTU202000204

Ulevitch, 2000). This pathway initiates by ligand (pathogen-associated molecular patterns (PAMPs) binding to the receptors and then recruits myeloid differentiation factor 88 (MyD88) to serve as an adaptor molecule to activate the transcription factor NF-κB. Then, the activated NF-κB translocates into the nucleus to serve as a transcription factor to promote pro-inflammatory cytokine production, like tumor necrosis factor (TNF) and interleukin (IL). After cytokine production and the releasing of costimulatory molecules on macrophage, several kinds of naïve immune cells can be activated to perform the following defense responses (Hallman et al., 2001; Yamamoto et al., 2003).

Nowadays, some scientists have proposed that the immune response might be trade-off with the capacity of regeneration (Aurora & Olson, 2014; Forbes & Rosenthal, 2014; Mescher & Neff, 2005). Several evidences were showed that the regenerative ability is improved by through inhibited the immunity and the regenerative ability is suppressed by through promoted the immunity. Martin *et al.* reported that different distribution of immune cells in wild type and PU.1 null mice post-wounding, null mice shows an absence of macrophage and neutrophil aggregation at wound site. And the processes of skin repair result in more mature epithelial layer in null mice (Martin et al., 2003). On the other hand, *Xenopus laevis* tadpole has stronger ability with tail regeneration excluding for a refractory period. The significantly restored regenerative ability by knockdown of *PU.1* gene that cause immune suppression during the refractory period (Fukazawa et al., 2009).

doi:10.6342/NTU202000204

In addition, neutrophil clearance by macrophage pre-depletion in zebrafish have been reported to inhibit the regeneration (Lai et al., 2017). However, opposite results were also published, Toll knockout fly and TLR2/TLR4- deficient (TLR2/4$^{(-/-)}$) mice had bigger wound area than wild-type group after skin injury (Carvalho et al., 2014; Suga et al., 2014). Here I introduced a new model of invertebrate, *Aeolosoma viride* is a fresh water annelid that can regenerate whole body after head or tail removing (Brace, 1901; Chen et al., 2018a). As this worm always exposed to water that is an environment rich in microorganisms, it has advanced an effective system to defense pathogens. In addition, the previous work on the chapter 3 characterized the TLR signaling pathway in *A. viride*, making it a suitable model for investigating the interactions between immune responses and regeneration.

The aim of this study is to verify the involvement of TLR signaling pathway in anterior regeneration of *A. viride*, a 3 mm long freshwater annelid with a stronger regenerative ability. In the previous study, members of TLR signaling pathway showed different motifs of protein sequences, especially between *Avi*-MyD88-a and *Avi*-MyD88-i. In this study, expression pattern of TLR related genes were documented during anterior regenerative process, the major divergence of transcript level that has been observed was down-regulation of *Avi-MyD88-a* and up-regulation of *Avi-MyD88-i.* Therefore, PAMPs was used to conform the influence of inflammation and regeneration afterwards. And

doi:10.6342/NTU202000204

demonstrating the importance of both positive and negative regulation from TLR signaling pathway are critical to success anterior regeneration in *A. viride*.

4.2 Materials and Methods

4.2.1 Animal cultures and regeneration procedure

Worms were maintained similarly with materials and methods of chapter 2, *A. viride* was cultured in ASW at 25°C under 12 hours of day-night cycles and was fed with grounded oat. Animal preparation and basic experimental procedures were as described in our previous study (Chen et al., 2018a; Chen et al., 2020). Briefly, worms were dissected at the site anterior to the fission zone and zooid for synchronization, and transferred into fresh ASW for 3 days to recovery. In pre-treatment experiment, worms were transferred into fresh ASW containing antibiotic cocktail (125 ng/ml fungizone, 100 μg/ml penicillin G and 50 μg/ml kanamycin sulfate in the ASW) or C34 (250 or 500 μM in the ASW). To minimize the influence of microorganisms from the alimentary canal, worms were bisected at the segment anterior to the peristomium. After amputation, ten worms of each group were transferred into fresh ASW, antibiotic cocktail, C34 or 150 μg/ml PAMPs which including LPS (Cayman), peptidoglycan (PGN, InvivoGen), poly I:C (TOCRIS) and zymosan (InvivoGen), and then renew every 24 hours for subsequent regenerative experiments. In gene expression or cell proliferation assay, the regenerating

doi:10.6342/NTU202000204

tissue (first segment) or whole body of worms were collected for the following 0 to 7 days after amputation. Specimens were examined fixed in 4% paraformaldehyde (PFA) using dissecting microscope (WILD M8, Leica) for detail morphological observation, or were extracted by Trizol® (Invitrogen) for mRNA transcript level analysis. At least 10 individuals were examined for all observations and experiments and at different time points.

4.2.2 RNA exaction for quantitative real-time RT-PCR (qRT-PCR)

The total RNAs were extracted from five intact worms or 25 specimens of regenerating tissue by using TRIzol and reverse-transcribed to cDNA using SuperScript III Kit (Invitrogen). Transcriptional levels were determined by Bio-Rad iCycler™ using SYBR green system (Bio-Rad). The following primers used to amplify *Avi-TLR-a* were 5'-CAACTTATCTGGCAACGCTTTAG-3' and 5'-CTTCGAGCGGACCACTATTT-3', *Avi-TLR-b* were 5'-ACTTTGGCTTGGTTACGGATAC-3' and 5'-CTCTGTGAAGATCCATGCTAGAAC-3', *Avi-MyD88-a* were 5'-TCCCGACTTTCACAAATCTGG-3' and 5'-GAGAAGCGATGGCATGTCAT-3', *Avi-MyD88-i* were 5'-TCTCCTCAACGAATCCACATACT-3' and 5'-CTGCCGACTGCTCCAATG-3', *Avi-TNF-1* were 5'-GCTACCATAGATGACCTGCATAG-3' and 5'-ATTCGTAACTGCTGACGGTATT-3',

doi:10.6342/NTU202000204

and *Avi-TNF-2* were 5'-CACTCAAGCGGTTTGGAATTATC-3' and 5'-CCGGGCTCGCTTATGATTTA-3'. *Avi-actin* was used as internal control with specific primers: 5'-ATGGAGAAGATCTGGCATCA-3' and 5'-GGAGTACTTGCGCTCAGGTG-3' designed from *Avi-actin* (NCBI # KY079092.1). Relative quantification of gene expression was calculated by the $\Delta\Delta C_T$ method. Three technical replicates were performed in each real-time PCR reaction, and a no-template blank was served as negative control.

4.2.3 Whole mount *in situ* hybridization (WISH)

Worms were treated same with materials and methods of chapter 2. Total 20 worms of each group were collected every time points following specific experiments and fixed in 4% PFA at 4 °C. After wash with phosphate buffered saline with 0.1 % Triton X-100 (PBS-T, pH 7.4) for five times, sample were treated with 10 mg/ml proteinase K in PBS-T for 10 minutes then re-fixed in 4% PFA for 20 minutes. After worms were washed with PBS-T to remove PFA, samples were then pre-hybridized in HYB^- buffer (50% formamide, 5X SSC, 9.2 mM citric acid, and 0.1% Tween-20 in DEPC-H_2O) for 3 hours at 65°C, then divided to two groups and hybridized in HYB^+ buffer (HYB^- containing yeast tRNA and heparin) contains digoxigenin (DIG)-conjugated antisense riboprobes for *Avi-TLR*, *Avi-MyD88* and *Avi-TNF* or sense-strand riboprobes for 16 hours at 65°C. After

doi:10.6342/NTU202000204

overnight hybridization, samples were washed with HYB$^-$ buffer at 65°C to remove excessive RNA probe, and transferred through a wash HYB$^-$dilution series (66%, 33% and 0% in 2X SSC-tw, 0.1% tween-20 in 2X SSC buffer) at 65°C, then washed once with 0.2X SSC-tw at 65°C, and transferred into 0.2X SSC-TW for 15 minutes at 65 °C twice. And gradually changed to a series 0.2X SSC-tw dilution (66%, 33% and 0% in PBS-T) at room temperature. After final wash with PBS-T, blocking buffer (5% bovine serum albumin (BSA, Sigma- Aldrich)) in PBS-T) was added for two hours at room temperature. The sample was transferred into antibody solution, which contained 1:5000 diluted anti-DIG antibody conjugated to alkaline phosphatase (AP) (Roche) in blocking buffer. Samples were then incubated at 4 °C overnight. After antibody incubation, samples were washed 10 times with PBS-T, then transferred into staining buffer (0.1 M Tris-Cl, 0.05 M $MgCl_2$, 0.1 M NaCl, and 0.1% tween-20 in DEPC-H_2O). Finally, signal detection was developed using NBT/BCIP in staining buffer at 25°C for 2 hr and then 4°C for overnight. The sample were kept away from light during the staining process. To stop the colorization reaction, the samples were washed five times with PBS-T, and mounted with Fluoromount-G^{TM} (eBioscience). The images were taken on an Olympus DP80 microscope.

4.2.4 Labeling with 5-ethynyl-2′-deoxyuridine for cell proliferation and migration

doi:10.6342/NTU202000204

Cell proliferation was monitored by *in vivo* labeling with EdU in the same way of chapter 2. Total five worms of each group were exposed to 100 μg/ml of EdU (Invitrogen) in ASW for 12 hours, and 5 specimens of each group was then fixed in 4% PFA at 24, 36 or 48 hours post-amputation (hpa). EdU incorporated during S-phase of mitosis was detected by immunohistochemistry (IHC) using the Click-it EdU Alexa Fluor 488 Imaging Kit (Invitrogen) according to the manufacturer's instructions. Specimens were mounted in Fluoromount-G^{TM} and images were taken on an Olympus DP80 microscope.

4.2.5 Plasmid DNA constructs for RNA interference (RNAi)

The RNAi protocol was modified as described previously (Kamath et al., 2001). Partial sequence about 300 base pairs (bp) of yellow fluorescent protein (*YFP*, as control group), *Avi-MyD88-a* or *Avi-MyD88-i* were constructed with L4440 vector and transformed into an RNase III deficient strain competent cell HT115 (DE3). Worms was fed with 1×10^8 cfu/ml containing double-stranded (dsRNA) for five consecutive days and renew every day. Worms were then collected for RNA extraction or regeneration study.

4.2.6 Statistics

Data were test for significance using Mann Whitney U test. Probability values of *p*

doi:10.6342/NTU202000204

≤ 0.05 were regarded as statistically significant.

4.3 Results

4.3.1 The effect of antibiotic cocktail treatment during anterior regeneration in *A. viride*

For characterization and functional analysis of related genes in TLR signaling pathway, expression level of *Avi-TLR*, *Avi-MyD88*, and *Avi-TNF* were evaluated by RT-qPCR after pre-treatment of antibiotic cocktail. These expression profiles were normalized with *Avi-actin.* The mRNA expression level of all genes decreased significantly at 3 days post-synchronization (dps) (0.3 to 0.7 fold) after antibiotic cocktail treatment compared to that in the ASW control group (Fig. 4-1). Furthermore, WISH of *Avi-MyD88* were conducted to visualize mRNA in intact worm. The localization of *Avi-MyD88-a* expression extended over the whole body, especially in alimentary canal. By contrast, *Avi-MyD88-i* only expressed in the middle of alimentary canal in intact worm. Consistent with the RT-qPCR data, WISH of *Avi-MyD88-a* and *Avi-MyD88-i* were not significant alteration after antibiotic cocktail treatment as showed in Fig. 4-2A and B.

To verify the possible roles of TLR signaling pathway in anterior regeneration, and previous results revealed that the pre-inflammatory cytokines including *Avi-TNF-1* and *Avi-TNF-2* can be inhibit by antibiotics (Fig. 4-1E and F). I tried to perform regenerative

doi:10.6342/NTU202000204

experiment by cocktail treatment to prevent pathogen growth in the ASW from mix solution of fungizone, penicillin G and kanamycin sulfate. The immersion protocol with drugs during anterior regenerative process showed in Fig. 4-3A. The pre-treatment of antibiotic cocktail showed significant affect after *A. viride* amputation. Besides, the percentage of successful regenerates was increased to around 85% compared with 60% in the control group at 5 dpa (Fig. 4-3B). Also, the morphological difference were observed from 1 to 7 dpa. The most of difference is the regenerating prostomium gradually bulged wider than control group at 5 dpa (Fig. 4-3C). These results indicate that anterior regeneration processes can be improved through down-regulation of TLR signaling pathway before head amputation by antibiotic cocktail treatment in *A. viride.* Otherwise, the improved regeneration also conformed through cell proliferation by EdU labeling at 36 hpa (Fig. 4-4).

4.3.2 The expression and regulation of TLR signaling pathway during *A. viride* anterior regeneration

To verify the expression patterns of *Avi-TLR*, *Avi-MyD88* and *Avi-TNF* genes during anterior regeneration, RT-qPCR was performed from the regenerated tissues. These relative profiles were normalized with *Avi-actin* and then normalized with the control group (collection from intact head). In the first 24 hours, the gene transcript level of *Avi-*

doi:10.6342/NTU202000204

TLR-b, *Avi-MyD88-a*, *Avi-TNF-1* and *Avi-TNF-2* decreased at the regenerative tissues, then backed to the normal expression level (Fig. 4-5B, C, E and F). In addition, *Avi-TLR-a* had similar pattern but increased of the first 3 hours after amputation (Fig. 4-5A). However, only the gene expression level of *Avi-MyD88-i* quickly increased from 0 and maintained the high level to 120 hpa (Fig. 4-5D).

Furthermore, the difference profile appeared in two *Avi*-TLR, *Avi*-MyD88 and *Avi*-TNF. The data showed that the RNA transcript level of *Avi-TLR-a* was higher than the control group during whole regenerative processes but expression of *Avi-TLR-b* decreased then returns to basal level from 72 to 120 hpa (Fig. 4-5A and B). On the other hand, the expression of *Avi-MyD88-i* was induced immediately to average eight-folds following amputation and then was exhibited higher level expression until 5 dpa, suggesting an important role that either this adaptor protein is critical or it appears a suppressive effect on the whole regenerative events (Fig. 4-5D). By contract, unlike *Avi-MyD88-i*, a decreasing of the *Avi-MyD88-a* was observed at first 24 hours, suggesting that either this adaptor protein is not essential or it applies a suppressive effect on the regenerative process (Fig. 4-5C). Finally, the mainly difference was observed between *Avi-TNF-1* and *Avi-TNF-2* due to their expression reduced in varied period of regenerative process. The gene expression of *Avi-TNF-1* decreased from 3 hpa to 120 hpa after head amputation (Fig. 4-5E). Conversely, *Avi-TNF-2* only decreased from 6 hpa to 48 hpa and then

doi:10.6342/NTU202000204

increased after 72 hpa (Fig. 4-5F).

To define the localization of TLR signaling pathway during *A. viride* regeneration, WISH was conducted to imagine these TLR related genes in regenerating worms. The results showed in Fig. 4-6, *Avi-TLR-a* and *Avi-TLR-b* mRNA expression patterns were observed similar results by the anti-sense probe at 6 and 48 hpa, non-significant differences at the regenerative areas (Fig. 4-6A and B). By contrast, *Avi-MyD88-a* displayed slight up-regulation of expression inside of blastema at 48 hpa (Fig. 4-6C). Furthermore, the mRNA transcript level of *Avi-MyD88-i* presented consisted with previous RT qPCR data (Fig. 4-5D), and was induced in the regenerative areas at 12 hpa and decreased at 48 hpa (Fig. 4-6D). Moreover, the downstream cytokine genes, *Avi-TNF-1* and *Avi-TNF-2*, also represented similar patterns with RT qPCR results which peaked at 48 hpa (Fig. 4-6E and F).

4.3.3 The effect of PAMPs on the *A. viride* regeneration processes through TLR signaling pathway

According to previous results, TLR signaling pathway has be known to be involved in regulation of anterior regeneration in *A. viride*. Furthermore, some PAMPs including LPS, PGN, poly I:C and zymosan were used to confirm the relationship between TLR signaling pathway and regeneration in this worm. An immersion protocol with drugs

doi:10.6342/NTU202000204

during anterior regenerative process (Fig. 4-7A). Three PAMPs, LPS, PGN and zymosan, showed no significant effect on *A. viride* regeneration at 7 dpa (Fig. 4-7B). However, poly I:C, an immunostimulant on TLR3 in mammal immune system, was significantly decreased the percentage of successful regenerates from 5 to 7 dpa (Fig. 4-8A at 150 μg/ml concentration). None of bulged prostomium in the regenerating *A. viride* after 150 μg/ml poly I:C treatment at 7 dpa (Fig. 4-8B). Also, cell proliferation assay was performed after poly I:C treatment, EdU^+ cells in the blastema were apparently reduced under poly I:C treated at 36 and 48 hpa (Fig. 4-9).

In addition, the gene expression of TLR signaling pathway related genes after poly I:C treatment was also analyzed from the regenerative tissues. These profiles were normalized with the control group (ASW). Obviously, each group of two *Avi-TLR, Avi-Myd88* and *Avi-TNF* genes exhibited total different profiles after poly I:C treatment. The transcript level of *Avi-TLR-a* was significantly increased at 3 and 6 hpa (Fig. 4-10A), but *Avi-TLR-b* was significantly decreased at 1 and 6 hpa (Fig 4-10B). Similarly, *Avi-Myd88-a* was significantly amplified from 1 to 6 hpa (Fig. 4-10C), but *Avi-Myd88-i* was only slightly change at 1 hpa (Fig 4-10D). Additionally, the gene of *Avi-TNF-1* presented similar patterns with that of *Avi-TLR-a* and *Avi-MyD88-a*. The highest expression was revealed at 3 hpa (Fig. 4-10E). However, *Avi-TNF*-2 showed decreased pattern dependent time points from 1 to 6 hpa (Fig. 4-10F). These results indicated that two types of

doi:10.6342/NTU202000204

regulation on TLR signaling pathway after poly I:C treatment during *A. viride* regeneration.

4.3.4 The effect of C34, an inhibitor of TLR signaling pathway on *A. viride* regeneration

To approve the essential roles of TLR signaling pathway involved in the anterior regeneration, the TLR4 inhibitor C34 was used in further experiment. First, the activity of this drug was confirmed by RT-qPCR of *Avi-TNF-1* and *Avi-TNF-2* from intact worms after C34 treatment. The gene expressions of two *Avi-TNF* were similarly reduced after C34 treatment (Fig. 4-11). Therefore, the 250 μM of C34 was used in following *A. viride* regenerative test. The immersion protocol with drugs during anterior regenerative process presented in Fig. 4-12A. The pre-treatment of C34 showed no effect on *A. viride* regeneration after amputation. Nevertheless, the percentage of successful regenerates in the poly I:C+C34 group was synergistically increased two folds (around 70%) compared with the poly I:C group (around 35%) at 5 dpa (Fig. 4-12B). Correspondingly, the morphology of regenerative head were observed difference in these two groups at 7 dpa (Fig. 4-12C). Moreover, the transcript levels of two *Avi-TNF* also showed opposite expression level in poly I:C treatment at 3 hpa. Compared with only poly I:C treatment, down-regulation of *Avi-TNF-1* and up-regulation of *Avi-TNF-2* in the poly I:C+C34 group

doi:10.6342/NTU202000204

(Fig. 4-13). Together, these data suggested that the inhibitory effect of anterior regeneration in *A. viride* can be rescued by the suppression of *Avi-TNF-1*or activation of *Avi-TNF-2* at early stage of regeneration.

4.3.5 The roles of *Avi-MyD88-i* in anterior regeneration

In order to precisely distinguish the roles of *Avi-MyD88* in anterior regeneration, dsRNA RNAi was performed to knockdown experiment. Both relative gene expression and the percentage of successful regeneration were estimated after treated with *Avi-MyD88-a* or *Avi-MyD88-i* RNAi by feeding method. The immersion protocol with bacteria during anterior regenerative process showed in Fig. 4-14A. The gene expression of *Avi-MyD88-a* and *Avi-MyD88-i* were measured by RT-qPCR. The groups of *Avi-MyD88-a* RNAi showed no significant effects on the gene expression of *Avi-MyD88-a* (Fig. 4-14B). By contrast, *Avi-MyD88-i* RNAi showed significant effect on the *Avi-MyD88-i* knock-down expression (Fig. 4-14C). These results exhibited that only *Avi-MyD88-i* dsRNA successfully reduced the mRNA expression of *Avi-MyD88-i.* Furthermore, to test if *Avi-MyD88-i* is crucially required for anterior regeneration, worms were amputated after fed with bacteria. The RNAi of *Avi-MyD88-i* successfully reduced the percentage of successful regeneration from around 80% to 50% compared to control and *Avi-MyD88-a* RNAi group at 5 dpa (Fig. 4-15A). Morphologically, most worms

doi:10.6342/NTU202000204

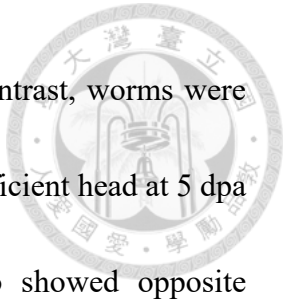

treated with *YFP* dsRNA regenerated normally at 5 to 7 dpa. By contrast, worms were treated with *Avi-MyD88-i* dsRNA showed significantly smaller or deficient head at 5 dpa (Fig. 4-15B). Moreover, the transcript levels of *Avi-TNF-1* also showed opposite expression level in poly I:C treatment at 3 hpa. Compared with *YFP* RNAi, the down-regulation of *Avi-TNF-1* was represented in *Avi-MyD88-i* RNAi group after poly I:C treatment (Fig. 4-16A). However, there were no significant differences with *Avi-TNF-2* expression between *YFP* and *Avi-MyD88-i* RNAi (Fig. 4-16B). To conclude with transcript level in Fig. 4-5D, the up-regulation of *Avi-MyD88-i* gene expression is required for anterior regeneration that may play a competition role with *Avi-MyD88-a* in *A. viride.*

4.4 Discussion

TLR signaling pathway have been demonstrated as an evolutionarily conserved mechanism immune response (Lu et al., 2020). These recognition receptors display an important and efficient innate immunity tool for debris removal or infection decline in vertebrates and invertebrates (Akira et al., 2006; Prochazkova et al., 2020). Also, regulation of this pathway can be linked with advantageous for wound repair or regeneration (Zhang & Schluesener, 2006). A rising evidence from vertebrates on the involvement of TLR signaling pathway in tissue injury prominently extends this

doi:10.6342/NTU202000204

knowledge from innate immunity, and delivers the concept of important insights between immunology and regenerative medicine (Huebener & Schwabe, 2013; Macedo et al., 2007).

In this study, the modulation of TLR related genes at transcript level and the effect on regeneration were established in the freshwater annelid, *A. viride*. TLR signaling pathway was found to be involved and essential for complete regeneration through opposite regulation of cytokine production in this pathway. Two transcript profiles of *Avi-MyD88* and *Avi-TNF* were detected during the process of anterior regeneration from 0 to 48 hpa. This phenomenon is similar with six CgMyD88 genes from oyster (*C. gigas*) responses to heat-killed *V. splendidus* challenge. The mRNA transcript levels of two CgMyD88 genes (*CgMyD88-A* and *CgMyD88-D*, were denoted as "down inducible" negative MyD88s) first decreased quickly to the lowest level at 6 hours post bacteria treatment. While the other two truncated CgMyD88 genes (*CgMyD88-T1* and *CgMyD88-T2*, both of them lack DD domain in N-terminal that was denoted as "up inducible" negative MyD88s) increased rapidly and peaked at 6 hours. Moreover, *CgMyD88-B* and *CgMyD88-C* were slowly up-regulated at the beginning and then back to normal expression level after bacteria challenge, were denoted as positive MyD88s. The authors speculated that CgMyD88-T1 and CgMyD88-T2 might mainly function in inflammation to defense from pathogen but as a negative modulator in the activation of NF-κB. And

doi:10.6342/NTU202000204

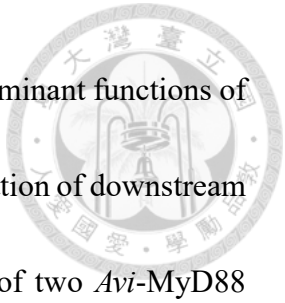

"down inducible" negative MyD88s should serve as a partner with dominant functions of positive MyD88s. The positive MyD88s lead to most efficiently activation of downstream signaling (Xin et al., 2016). That does not consist with the events of two *Avi*-MyD88 genes against poly I:C in this study. Two expression patterns of *Avi-MyD88* and *Avi-TNF* were consisted with each other that *Avi-MyD88-a* and *Avi-TNF-a* increased rapidly and *Avi-MyD88-i* and *Avi-TNF-2* not to change or decreased quickly (Fig. 4-10C-F). Therefore, *Avi-MyD88-a* and *Avi-TNF-a* are classified as the positive factors of TLR signaling pathway in *A. viride.* And *Avi-MyD88-i* and *Avi-TNF-2* are grouped into the negative factors. Their coordination regulate this pathway to success anterior regeneration in *A. viride*. In my study, up-regulation of *Avi-MyD88-a* or knock-down of *Avi-MyD88-i* leads to fail of regeneration. Therefore, both *Avi-MyD88-a* and *Avi-MyD88-i* were concluded that have important roles of dominant regulation in this research. Based on the cross-talk concept of signaling, it should not only one way to control immune responses in animals. The LPS-inducible MyD88s was discovered that splices variant of MyD88 from HEK293T cell in 2002. Overexpression of MyD88s specifically inhibits IL-1β and NF-κB activation (Janssens et al., 2002). This variant protein is not able to recruitment of IRAK-4 due to lack intermediate domain (ID) between DD and TIR domain (Janssens et al., 2003). However, *Avi*-MyD88-i not a variant protein of *Avi*-MyD88-a but the deficiency of TIR domain, it should act opposite function of *Avi*-MyD88-a during anterior

doi:10.6342/NTU202000204

regeneration.

The inflammatory reaction can be induced by PAMPs from various microorganisms (Medzhitov & Janeway, 2000). For example, the poly I:C has been known as an agonist of TLR 3 in mammalian system. The cytokine *Avi*-TNF belong to pre-inflammatory signaling proteins that had been demonstrated opposite regulations after poly I:C treatment. The result of incomplete or failed regeneration that were caused by up-regulation the canonical molecules of TLR signaling pathway, including *Avi-TLR-a, Avi-MyD88-a* and *Avi-TNF-1*. And inhibition of the non-canonical molecules of same pathway that contains *Avi-TLR-b* and *Avi-TNF-2*. Therefore, PAMP would affect to *A. viride* through production of inflammatory cytokine and also decrease the percentage of cell proliferation. However, incomplete regeneration can be rescue by C34 that thought down-expression of *Avi-TNF-1*and up-expression of *Avi-TNF-2* after poly I:C treatment (Fig. 4-13). Unexpectedly, the universal PAMPs including LPS, PGN and zymosan showed no significant effect in this study. Similarly, some comparable studies on invertebrates had no significant effect to stimulate cells, organs or whole body have been published including Atlantic salmon (*Salmo salar*), chicken (Gallus domesticus), disk abalone (*Haliotis discus discus*), flatworm (*Dugesia japonica*), leech (*H. medicinalis*), mussel (*Mytilus. gallopro vincialis*), nematode (*C. elegans*), oyster (*C. gigas*), and sea cucumber (*Apostichopus japonicus*) (Gao et al., 2017; Karnati et al., 2015; Priyathilaka

doi:10.6342/NTU202000204

et al., 2018; Pujol et al., 2001; Rodet et al., 2015; Schikorski et al., 2009; Skjaeveland et al., 2009; Toubiana et al., 2013; Zhang et al., 2015; Zhang et al., 2013). One of the possible reason to explain is that the water environments of most above species living in which fill with aquatic microorganisms. The condition leads hosts to maintain their regular level of innate immune responses and even tolerant to some kinds of microorganisms all the time (Zhang et al., 2013). In summary, this worm can sense and then identification of specific pathogen component after injury.

In the present day, the relationship between the regenerative ability and the immune competence have been trusted by contraries depend on development or evolution. Therefore, it has been proposed that development of adaptive immunity causes the capacity of regeneration lost during vertebrate evolution (Aurora & Olson, 2014; Mescher et al., 2013). However, some publications reported the opposite relationship between immune responses and regenerative capacity in amphibian, mammalian and teleost (Godwin et al., 2017; Petrie et al., 2014; Simkin et al., 2017). Recently, no correlated data has been reported from invertebrate models. The well-known non-bilaterian metazoan regenerative model namely *Hydra*, reveals induced immune responses of reactive oxygen species (ROS) and MAPK pathway but not altered transcript levels in TLR singling pathway (Wenger et al., 2014). Planarian is another famous model of regenerative study, also shows up-regulation of ROS in both of head and tail regeneration (Pirotte et al., 2015).

doi:10.6342/NTU202000204

However, no MyD88-like protein has been identified from *Schmidtea mediterranea*, only one TIR domain containing protein represents down-regulation of mRNA expression from 10 to 72 hpa (Peiris et al., 2014). It means that some important immune responses should be necessary for regeneration, but neither *Hydra* nor planarian have the correlative research about the trade-off between innate immunity and regeneration.

The ability of regeneration is irregular distributed among annelid. My previous work (in chapter 2) has confirmed the excellent capacity in *A. viride.* I also identified the innate immunity related TLR signaling pathway from this worm (in chapter 3). By contrast with regenerative capacity, only a few of PRRs has been characterized in phylum Annelida (Prochazkova et al., 2020). In this chapter, the mRNA expression profile of TLR signaling pathway was conducted and showed down-regulation of canonical molecules in this pathway after amputation. This phenomenon is not identical with other regenerative study, including repair of *Drosophila* intestine, human and mice skin, *Xenopus* tadpole tail and zebrafish fin (Feiken et al., 1995; Franchini & Bertolotti, 2012; Grellner, 2002; Nguyen-Chi et al., 2017; Xu et al., 2011). Moreover, both of the activator and inhibitor in TLR signaling pathway were tested in the new regenerative model *A. viride* that revealed opposite regulation in the anterior regeneration. To conclude, this model conforms the requirement of immune responses in TLR signaling pathway for anterior regeneration. These results supports the trade-off theory between immunity and regeneration, and

doi:10.6342/NTU202000204

insights the possible therapeutic strategies in regenerative medicine.

doi:10.6342/NTU202000204

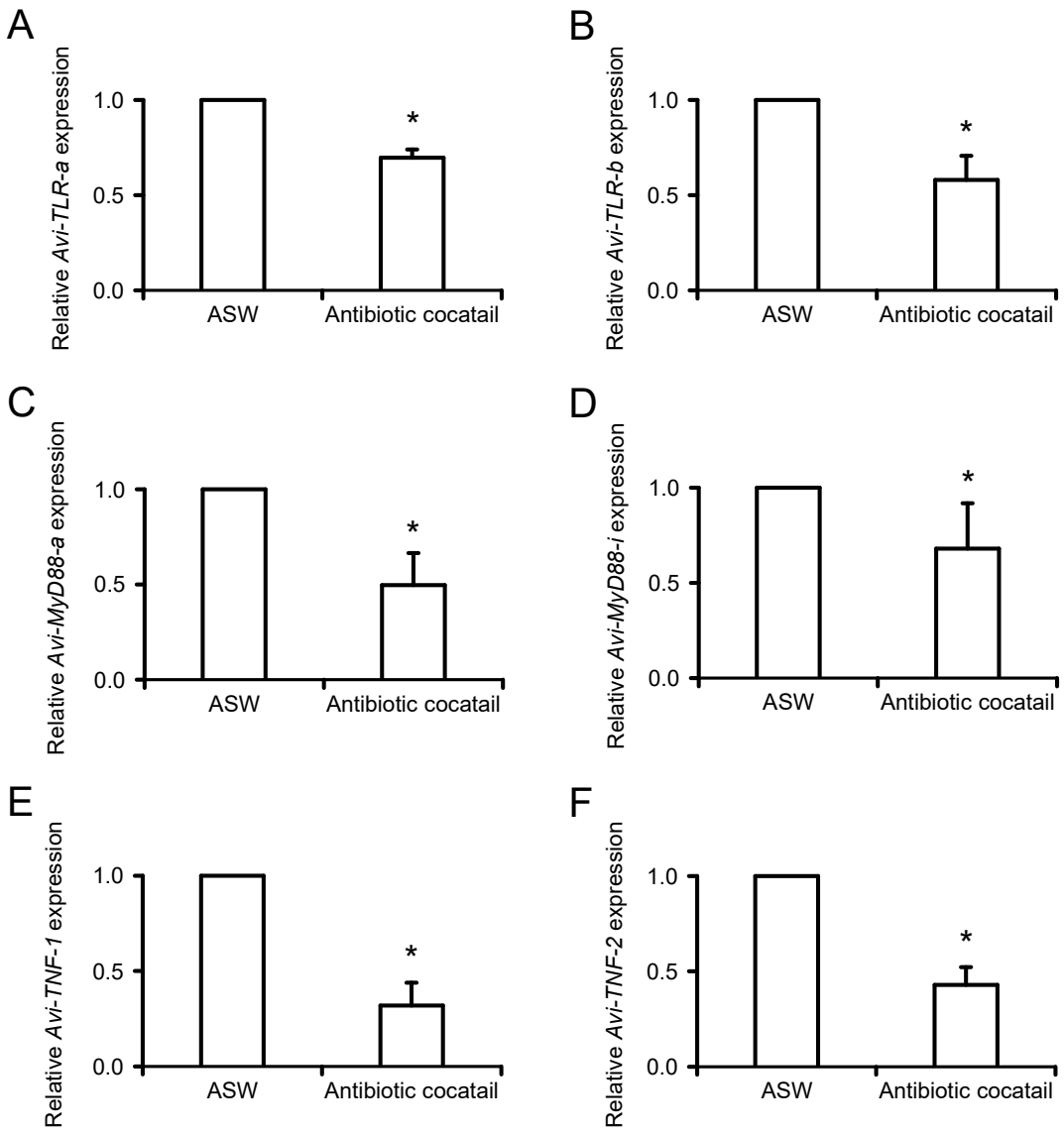

Figure 4-1. The expression level of TLR signaling pathway related genes at the intact worms were treated with antibiotic cocktail. Gene expression level of *Avi-TLR-a* (A), *Avi-TLR-b* (B), *Avi-MyD88-a* (C), *Avi-MyD88-i* (D), *Avi-TNF-1* (E) and *Avi-TNF-2* (F) were evaluated by RT-qPCR. These profiles were normalized with *Avi-actin.* All data represented the mean ± s.d. from three independent duplicate experiments (n = 3 biological replicates). Significant differences relative to ASW group are denoted by *. *: $p \leq 0.05$ using the Mann Whitney U test.

doi:10.6342/NTU202000204

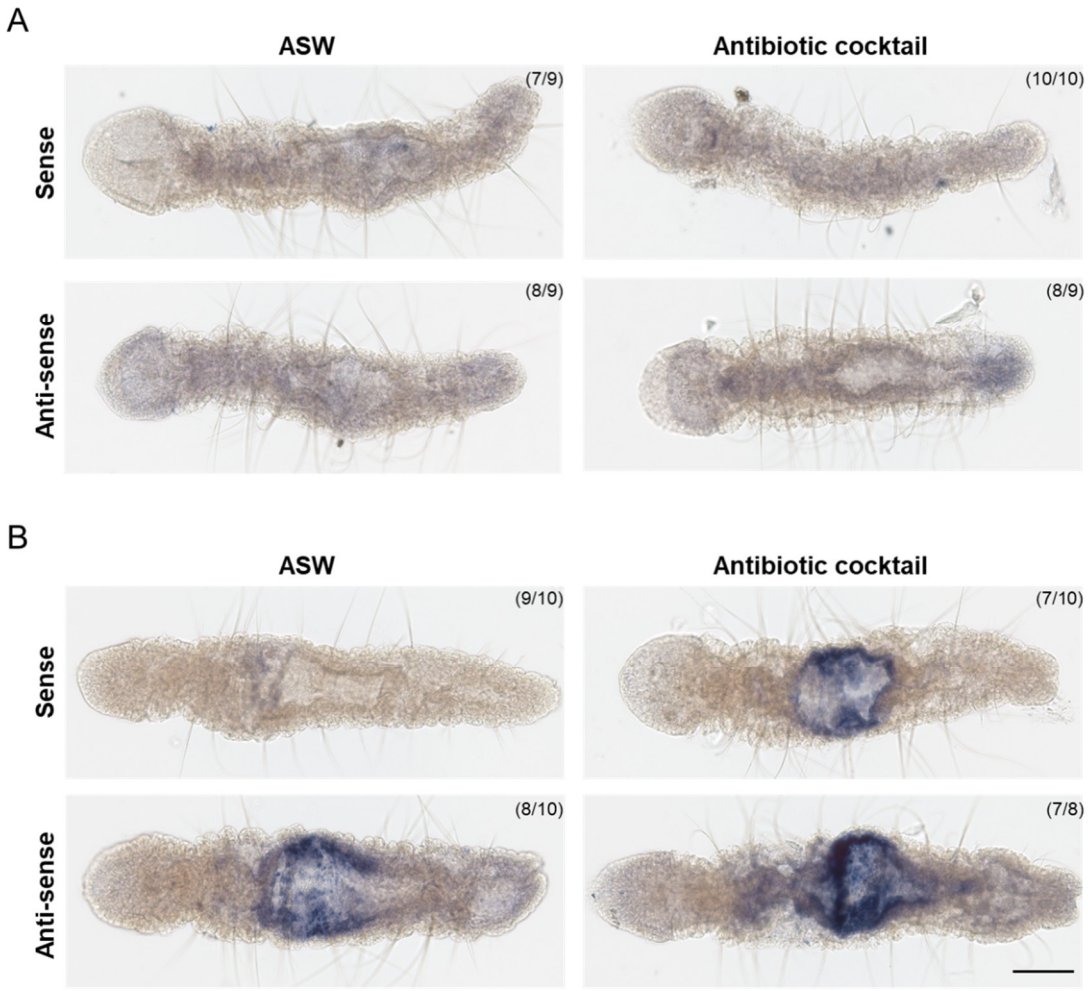

Figure 4-2. Localization of *Avi-myD88* in intact worms. WISH of *Avi-MyD88-a* (A) and *Avi-MyD88-i* (B) were performed on intact animals, with sense probe used as negative control. The numbers of worms showing the expression pattern out of the total number of inspect worms were labeled in the right side of each picture. Black dotted line indicated the amputation site. Scale bar: 100 μm.

doi:10.6342/NTU202000204

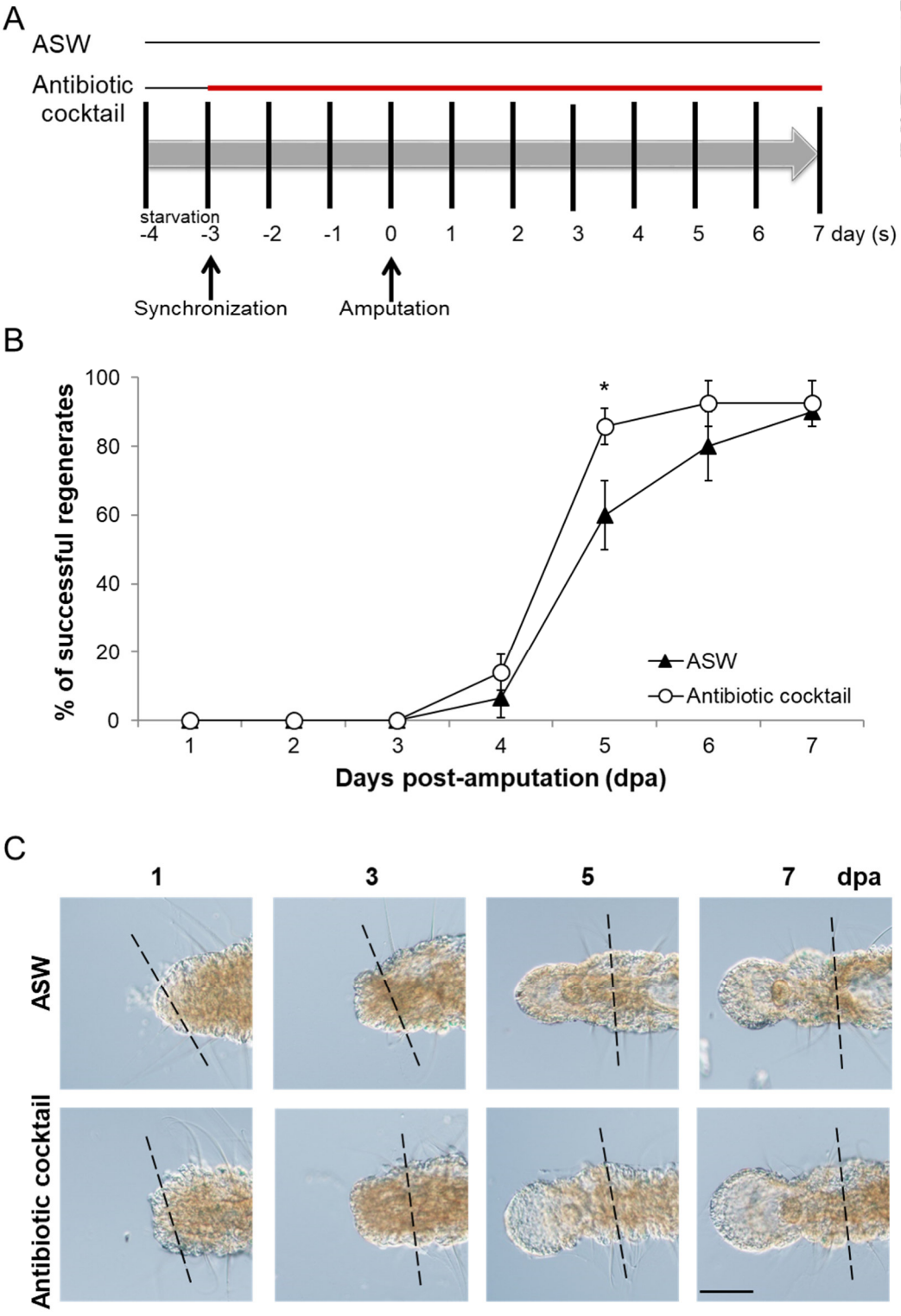

Figure 4-3. The antibiotic cocktail promotes anterior regenerative process. (A) Worms were treated with antibiotics from synchronization to regeneration. The drug was

doi:10.6342/NTU202000204

renewed every 24 hours and anterior regeneration was observed for 7 days after amputation. (B) The antibiotic cocktail treated worms showed increased successful regeneration compare to the control group at 5 dpa. (C) The head morphology of regenerating worms was affected by the antibiotic cocktail treatment. The amputation site was labeled by black dotted line. Scale bar: 100 μm. Data represented the mean ± s.d. in figure B from three independent duplicate experiments (n = 3 biological replicates). Significant differences relative to control group (ASW) at each day were denoted by *. *: $p \leq 0.05$ using the Mann Whitney U test.

doi:10.6342/NTU202000204

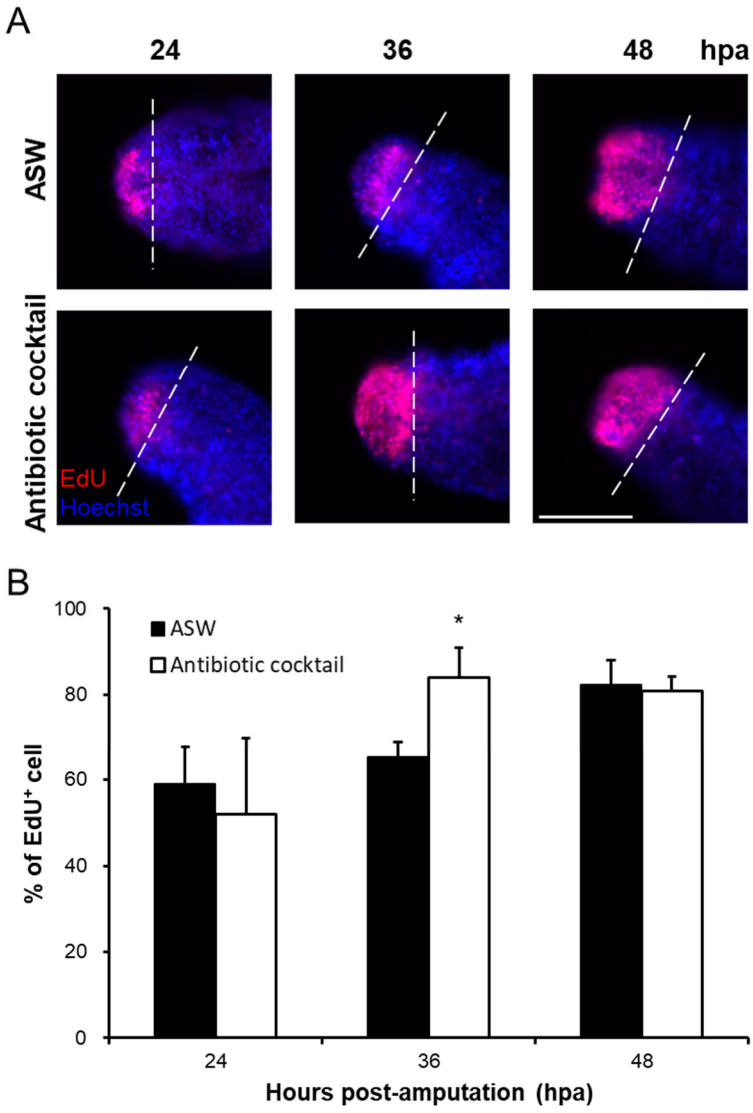

Figure 4-4. Cell proliferation was promoted by antibiotic cocktail during the stage of blastema formation. (A) The profile of proliferating cells increased after antibiotics treatment at 36 hpa. The amputation site was labeled by white dotted line. Scale bar: 100 μm. (B) Statistical analysis of the EdU^+ cells at 24 to 48 dpa in regenerating area. Data represented the mean ± s.d. from three independent duplicate experiments (n = 3 biological replicates). Significant differences relative to control group (ASW) at each time point were denoted by *. *: $p \leq 0.05$ using the Mann Whitney U test.

doi:10.6342/NTU202000204

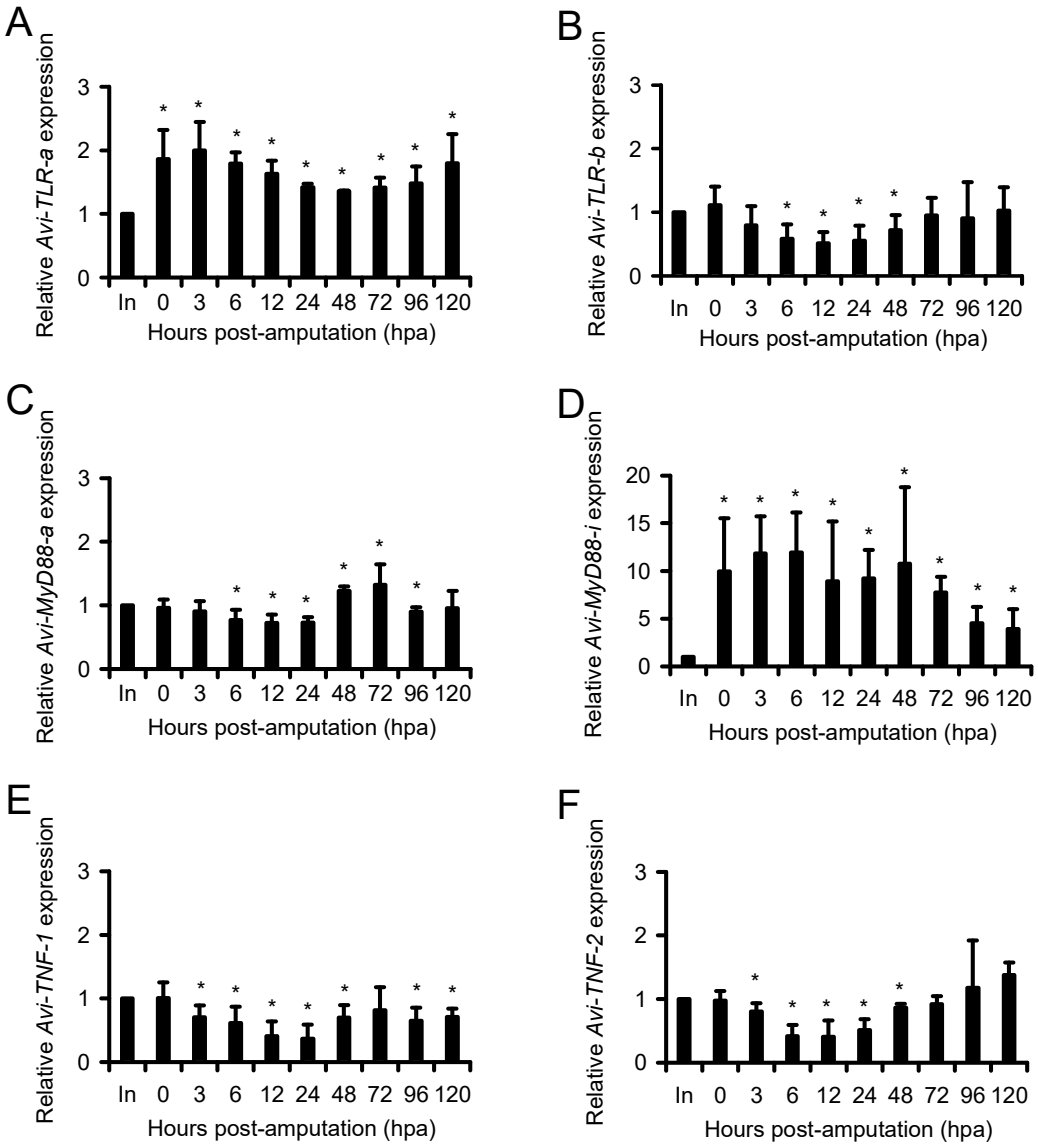

Figure 4-5. Gene expressions of TLR signaling pathway at the regenerating tissue during anterior regeneration in *A. viride*. The expression level of *Avi-TLR-a* (A), *Avi-TLR-b* (B), *Avi-MyD88-a* (C), *Avi-MyD88-i* (D), *Avi-TNF-1* (E) and *Avi-TNF-2* (F) were evaluated by RT-qPCR. These profiles were normalized with *Avi-actin* and then to normalized value of the intact head (IH) group. All data represented the mean ± s.d. from three independent duplicate experiments (n = 3). Significant differences relative to IH group were denoted by *. *: $p \leq 0.05$ using the Mann Whitney U test.

doi:10.6342/NTU202000204

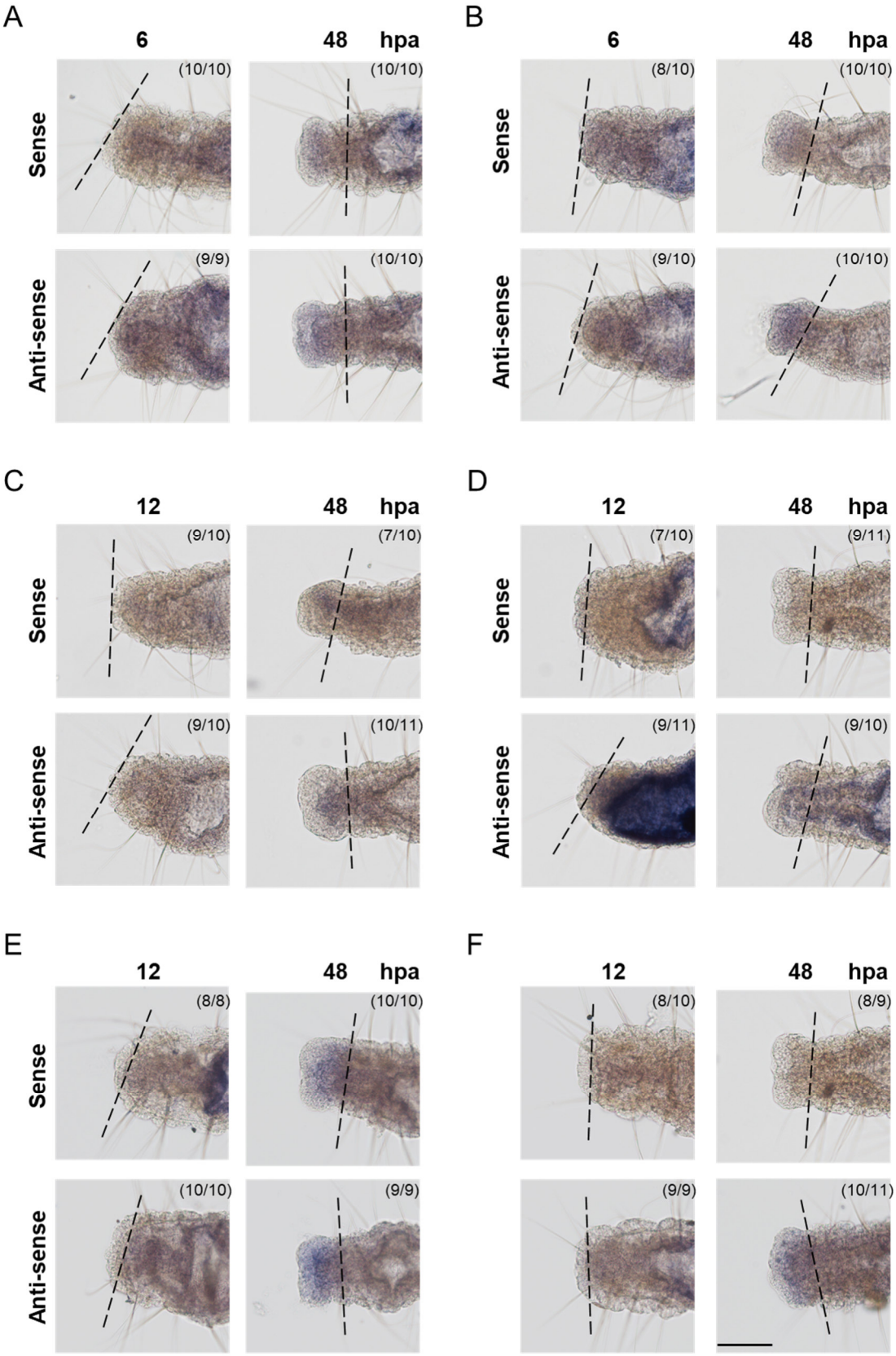

Figure 4-6. Localization of TLR signaling pathway related genes in anterior

doi:10.6342/NTU202000204

regenerating worm. The mRNA expression profile of *Avi-TLR-a* (A), *Avi-TLR-b* (B), *Avi-MyD88-a* (C), *Avi-MyD88-i* (D), *Avi-TNF-1* (E) and *Avi-TNF-2* (F) were assessed by WISH. The numbers of worms showing the expression pattern out of the total number of inspect worms were labeled in the right side of each picture. The amputation site was labeled by black dotted line. Scale bar: 100 μm.

doi:10.6342/NTU202000204

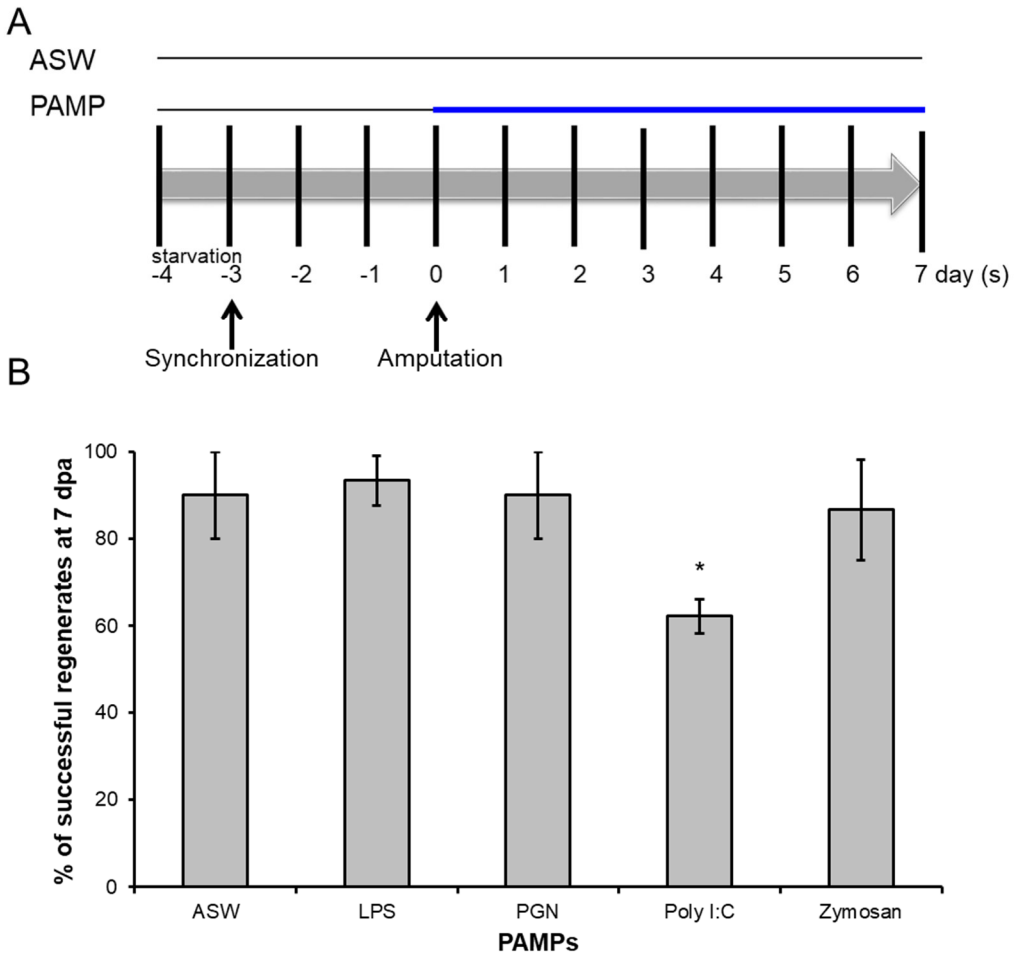

Figure 4-7. The effect of PAMPs during anterior regeneration in *A. viride*. (A) Worms were treated with PAMP including LPS, PGN, poly I:C or zymosan from amputation to regeneration. The drug was renewed every 24 hours and anterior regeneration was observed for 7 days after amputation. (B) The percentage of successful regenerates under 150 μg/ml PAMP treatment was calculated at 7 dpa. Worms were presented significantly inhibited regeneration after poly I:C treatment. Data represented the mean ± s.d. in figure B from three independent duplicate experiments (n = 3). Significant differences relative to control group (ASW) were denoted by *. *: $p \leq 0.05$ using the Mann Whitney U test.

doi:10.6342/NTU202000204

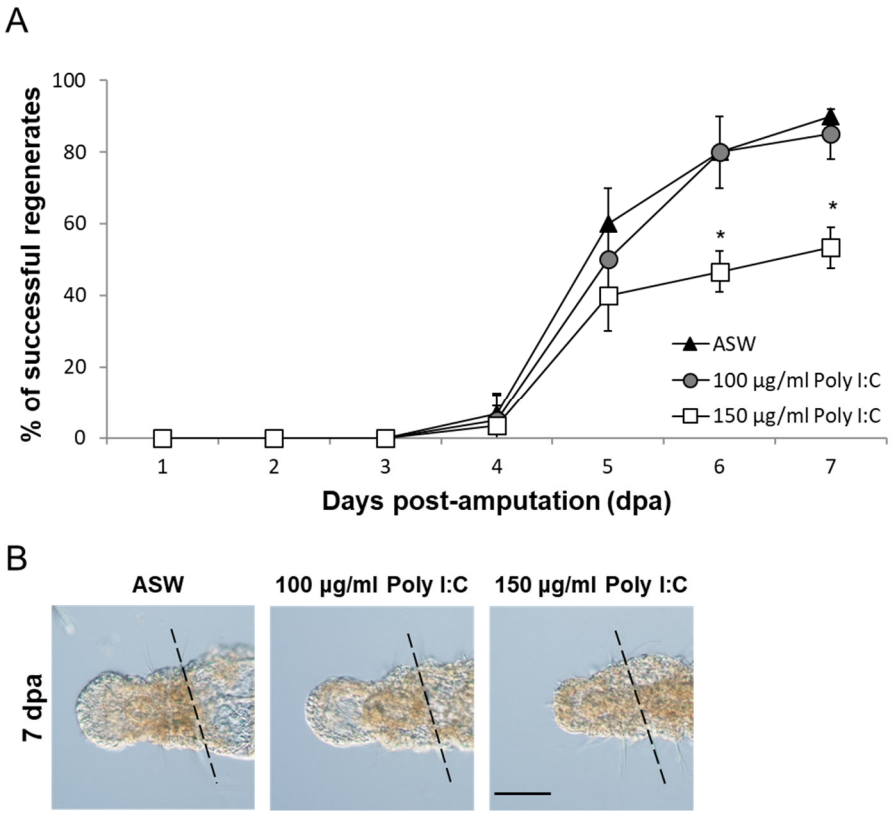

Figure 4-8. The inhibition of anterior regeneration after poly I:C treatment. (A) Poly I:C treated worms showed decreased successful regeneration compare to the control group from 5 to 7 dpa. (B) The head morphology of regenerating worms was obviously affected by 150 µg/ml poly I:C treatment. The amputation site was labeled by black dotted line. Scale bar: 100 µm. Data represented the mean ± s.d. in figure A from three independent duplicate experiments (n = 3 biological replicates). Significant differences relative to control group (ASW) at each day were denoted by *. *: $p \leq 0.05$ using the Mann Whitney U test.

doi:10.6342/NTU202000204

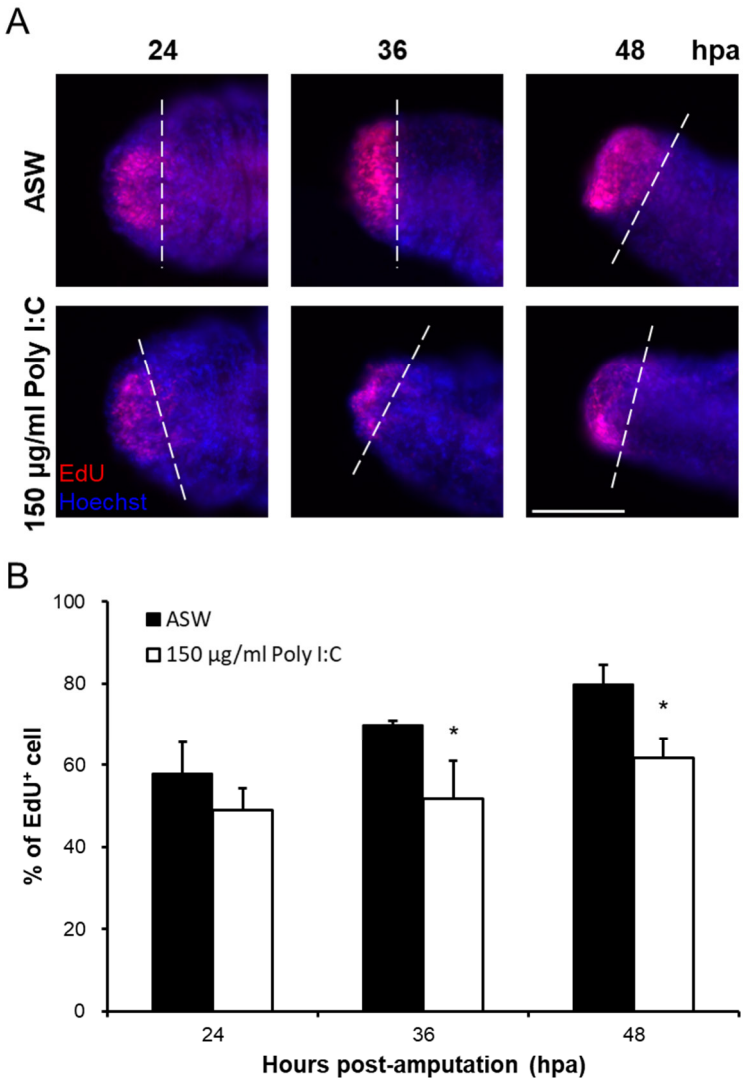

Figure 4-9. Cell proliferation was inhibited by poly I:C during the stage of blastema formation. (A) The number of proliferating cells at the blastema was decreased after poly I:C treatment at 36 to 48 hpa. The amputation site was labeled by white dotted line. Scale bar: 100 µm. (B) Statistical analysis of the EdU^+ cells at 24 to 48 dpa in regenerating area. Data represented the mean ± s.d. from three independent duplicate experiments (n = 3 biological replicates). Significant differences relative to control group (ASW) at each time point were denoted by *. *: $p \leq 0.05$ using the Mann Whitney U test.

doi:10.6342/NTU202000204

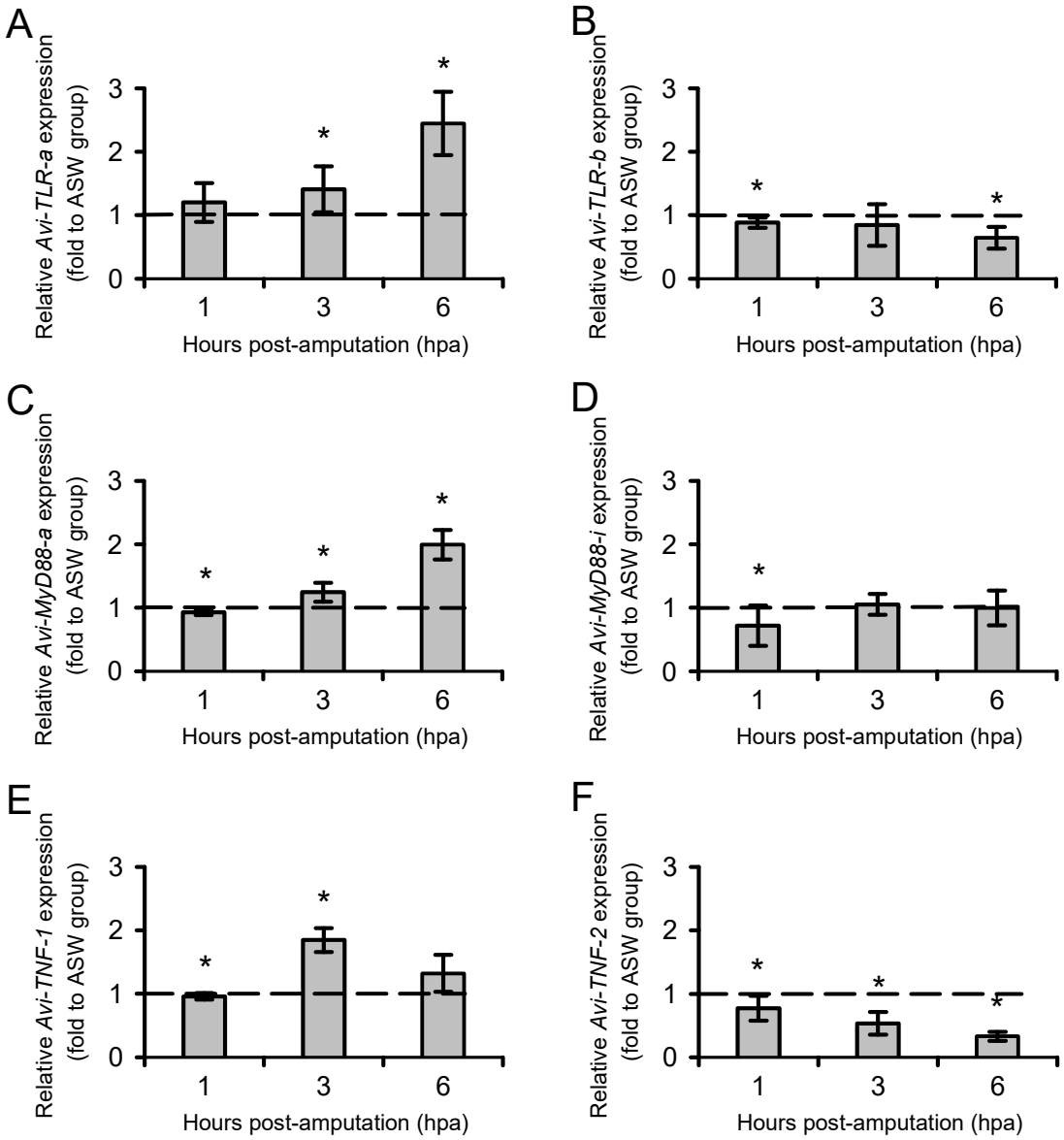

Figure 4-10. The effect of poly I:C on gene expressions of TLR signaling pathway-related genes at the regenerating tissue. The expression level of *Avi-TLR-a* (A), *Avi-TLR-b* (B), *Avi-MyD88-a* (C), *Avi-MyD88-i* (D), *Avi-TNF-1* (E) and *Avi-TNF-2* (F) were evaluated by RT-qPCR. These profiles were normalized with *Avi-actin* then normalized to control group at each time point. The relative expression level of genes in the ASW group is equal to 1.0 and is marked with a black dashed line. All data represented the

doi:10.6342/NTU202000204

mean ± s.d. from three independent duplicate experiments (n = 3 biological replicates). Significant differences relative to control group (ASW) at each time point were denoted by *. *: $p \leq 0.05$ using the Mann Whitney U test.

doi:10.6342/NTU202000204

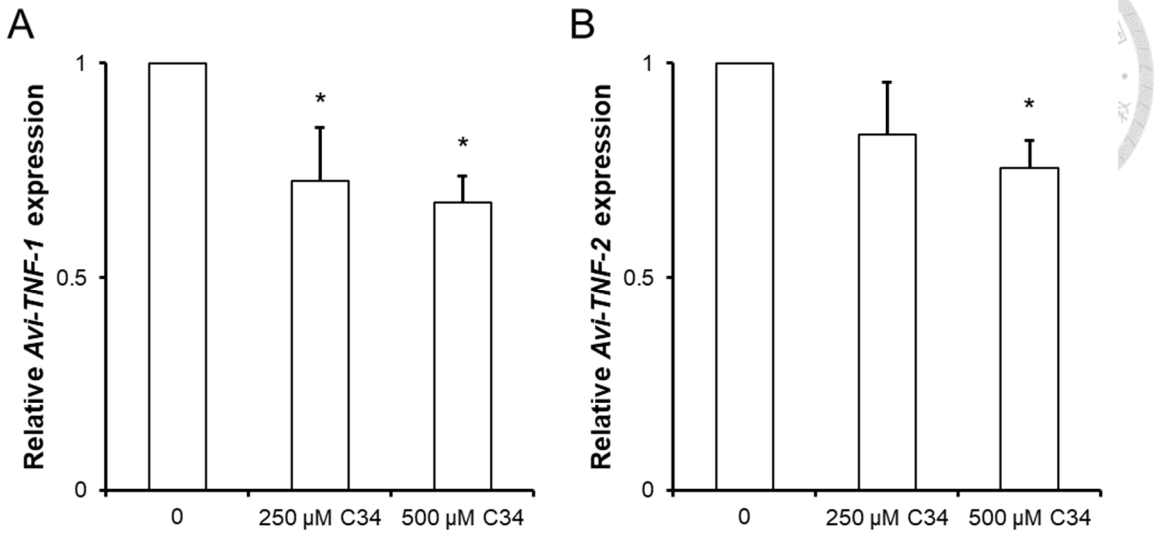

Figure 4-11. The gene expression of *Avi-TNF-1* and *Avi-TNF-2* were down-regulated by the TLR inhibitor C34. The gene expression of *Avi-TNF-1* (A) and *Avi-TNF-2* (B) from intact worms were measured after C34 treatment for continuous five days. All data represented the mean ± s.d. from three independent duplicate experiments (n = 3 biological replicates). Significant differences relative to control group were denoted by *. *: $p \leq 0.05$ using the Mann Whitney U test.

doi:10.6342/NTU202000204

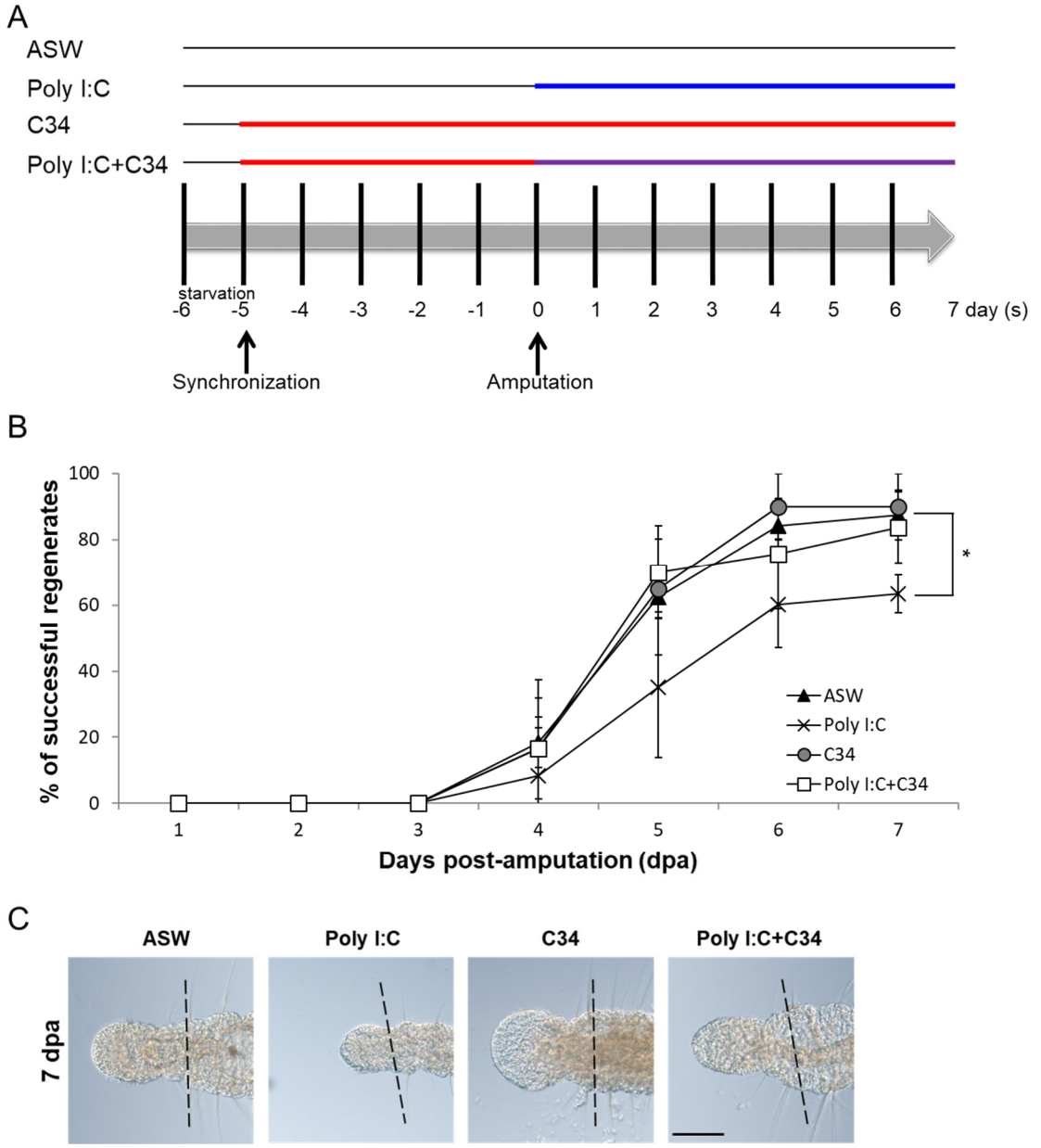

Figure 4-12. The rescue regenerative experiment of TLR inhibitor C34. (A) Worms were treated with C34 from synchronization to regeneration. The drugs were renewed every 24 hours and anterior regeneration was observed for 7 days after amputation. (B) The percentage of successful regeneration was measured from 0 to 7 dpa. (C) The head morphology of regenerating worms was visibly rescued by C34 at 7 dpa. The amputation site was labeled by black dotted line. Scale bar: 100 μm. Data represented the mean ± s.d.

doi:10.6342/NTU202000204

in figure B from three independent duplicate experiments (n = 3 biological replicates). Significant differences in the poly I:C group relative to control group (ASW) at each day were denoted by *. *: $p \leq 0.05$ using the Mann Whitney U test.

doi:10.6342/NTU202000204

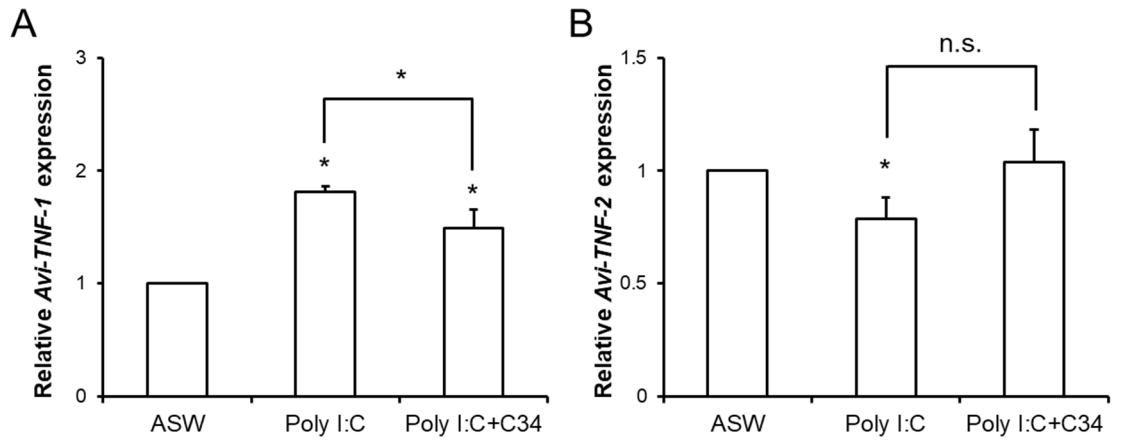

Figure 4-13. The regulation effect of *Avi-TNF-1* and *Avi-TNF-2* from C34 treatment in anterior regeneration. The gene expression of *Avi-TNF-1* (A) and *Avi-TNF-2* (B) from regenerative tissue were measured after poly I:C, or poly I:C+C34 treatment at 3 hpa. All data represented the mean ± s.d. from three independent duplicate experiments (n = 3 biological replicates). Significant differences relative to control (ASW) or poly I:C group were denoted by *. *: $p \leq 0.05$ using the Mann Whitney U test. n.s.: no significant.

doi:10.6342/NTU202000204

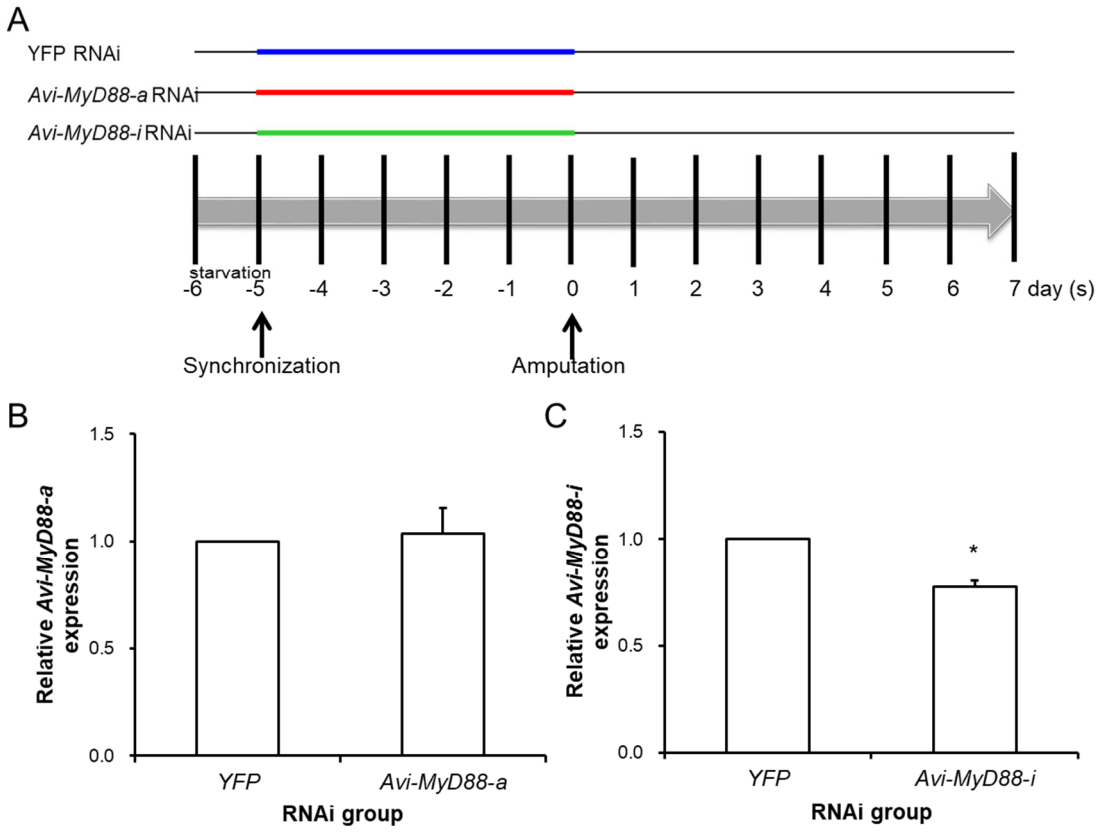

Figure 4-14. Knockdown experiment procedure of *Avi-MyD88-a* and *Avi-MyD88-i* by RNAi. (A) Worms were treated with dsRNA by feeding method from synchronization to regeneration. The heat-killed bacteria was renewed every 24 hours and anterior regeneration was observed for 7 days after amputation. The gene expression of *Avi-MyD88-a* (B) and *Avi-MyD88-i* (C) from intact worms were measured after dsRNA treatment for continuous five days. All data represented the mean ± s.d. in figure B and C from three independent duplicate experiments (n = 3). Significant differences relative to control group (*YFP*) were denoted by *. * $p \leq 0.05$ using the Mann Whitney U test.

doi:10.6342/NTU202000204

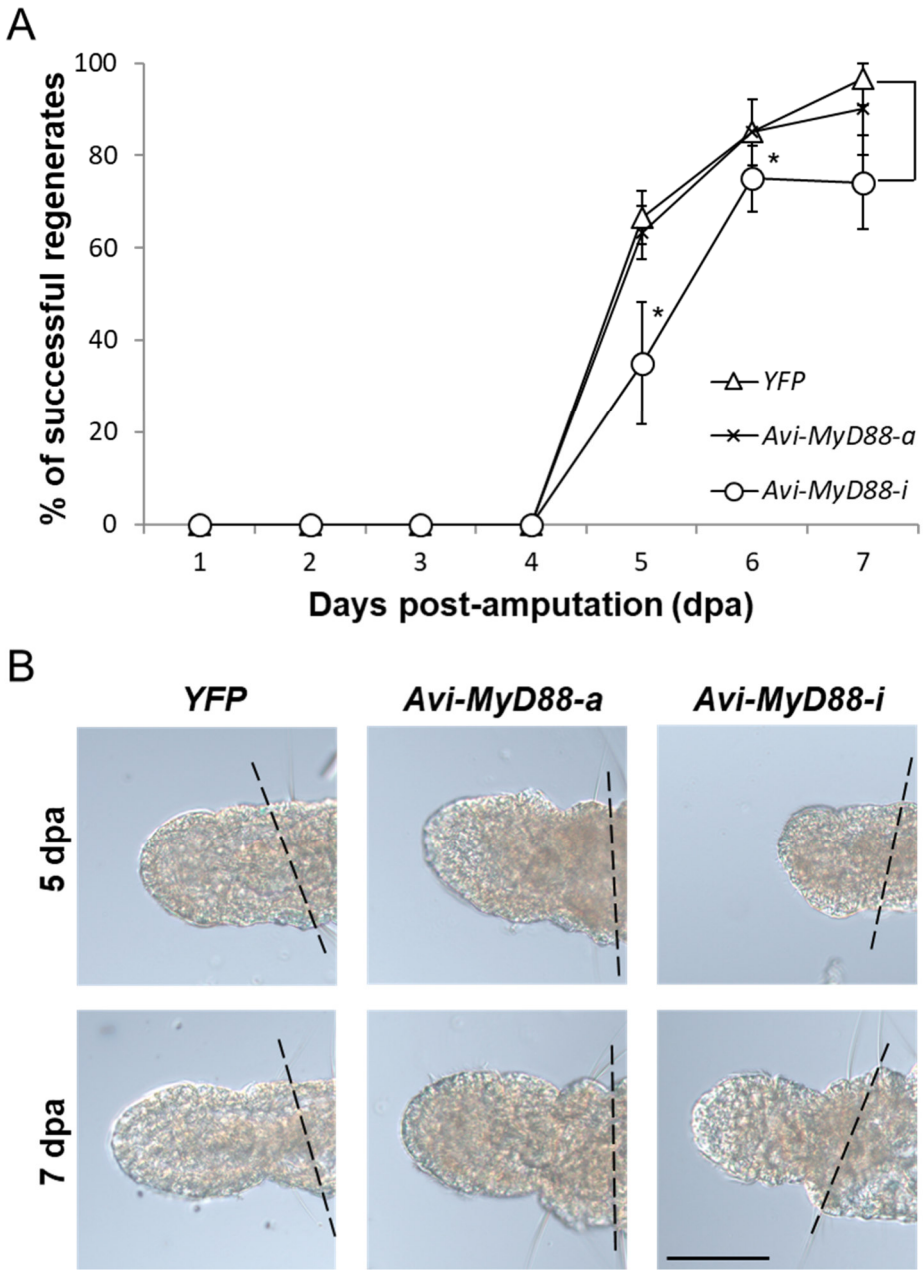

Figure 4-15. The efficiency of *Avi-MyD88-a* and *Avi-MyD88-i* knockdown experiment by feeding RNAi. (A) The percentage of successful regeneration was measured from 0 to 7 dpa, RNAi of *Avi-MyD88-i* represented inhibition of regeneration at 5 and 7 dpa. (B) The head morphology of regenerating worms were not regenerate by *Avi-MyD88-i* RNAi at 5 dpa. The amputation site was labeled by black dotted line. Scale bar: 100 μm. Data

doi:10.6342/NTU202000204

represented the mean ± s.d. in figure A from three independent duplicate experiments (n = 3 biological replicates). Significant differences in *Avi-MyD88-i* RNAi group relative to control group (*YFP*) at each day were denoted by *. * $p \leq 0.05$ using the Mann Whitney U test.

doi:10.6342/NTU202000204

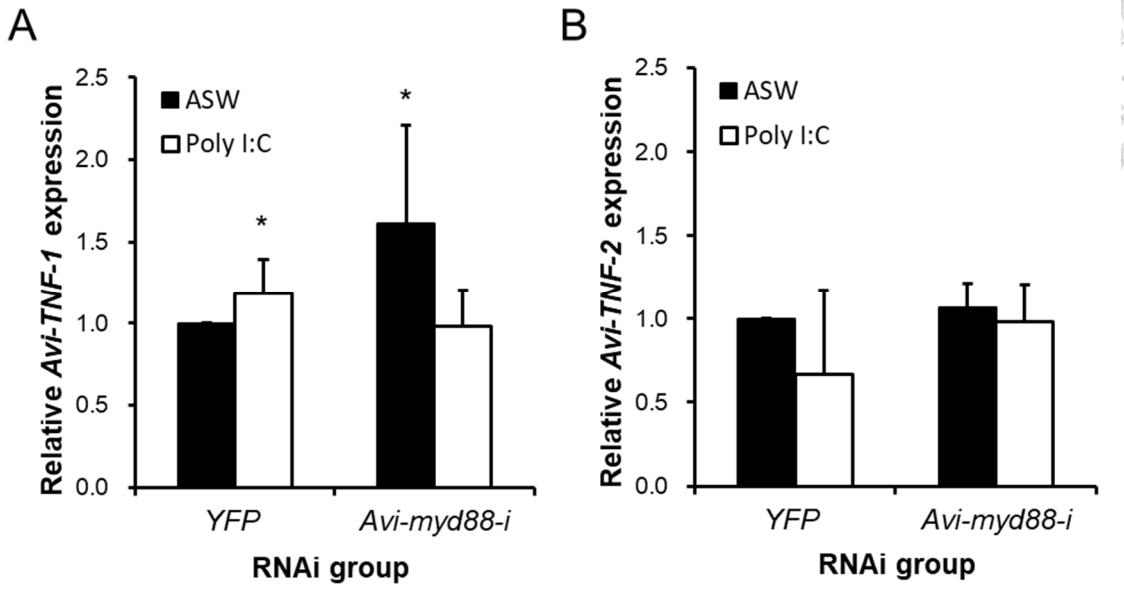

Figure 4-16. The efficiency of *Avi-MyD88-i* RNAi after poly I:C treatment during anterior regeneration. The gene expression of *Avi-TNF-1* (A) and *Avi-TNF-2* (B) from regenerative tissue were measured after poly I:C treatment at 3 hpa. All data represented the mean ± s.d. from three independent duplicate experiments (n = 3 biological replicates). Significant differences relative to control (*YFP* RNAi) or *Avi-MyD88-i* group were denoted by *. *: $p \leq 0.05$ using the Mann Whitney U test.

doi:10.6342/NTU202000204

Discussion and Conclusion

doi:10.6342/NTU202000204

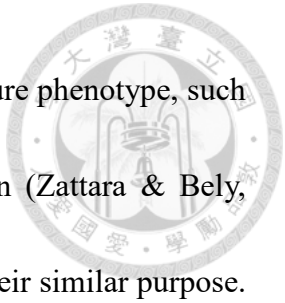

Animals have several developmental strategies to establish mature phenotype, such as embryogenesis, regeneration, and agametic asexual reproduction (Zattara & Bely, 2016). There are many similarities between these processes due to their similar purpose. Regeneration is considered a conventional asexual development according to the essential and specific developing complement to asexual reproduction (Brockes & Kumar, 2008). On the other hand, based on the widespread but variable distribution of regeneration and asexual reproduction among the animal kingdom, the evolutionary relationships between this two processes are still unclear (Bely & Nyberg, 2010; Brockes & Kumar, 2008). Therefore, the emphasis of many studies is to find out the close relation with fission and regeneration processes due to comparative strategies. Asexual reproduction such as paratomic fission or budding that reproduce from the reproduction zone in the middle of worm is highly associated with strong regenerative abilities (Bely, 1999; Berrill, 1952; Galloway, 1899). Most annelids such as *O. notoglandulata*, *A. raptisae*, and *S. benedicti* have been documented that the regenerative ability to regenerate posterior segments is better than to regenerate anterior segments (Bely, 2006; Bely & Sikes, 2010; Pfannenstiel, 1974). Regeneration like the growth of annelids can add new segments from the segment addition zone (SAZ) located near the pygidium or the last segment (Bely & Wray, 2001; Ribeiro et al., 2019). This study has confirmed that *A. viride* can completely restore lost body parts within 5 days in response to either anterior or posterior amputation. These

doi:10.6342/NTU202000204

findings are similar to the study on the other worms with paratomic fission in Naidinae, for example, *Dero digitate* and *P. leidyi* (Bely, 2006; Drewes & Fourtner, 1991; Zattara & Bely, 2011). Therefore, the capacity of regeneration in *A. viride* provides another positive insight between asexual reproduction and regeneration in Annelida.

In addition to regeneration, this study also focused on immune response. Immune cells play crucial roles to prevent deadly infection after injury (Godwin et al., 2013; Petrie et al., 2014). The inflammatory inducers are recognized by PRRs including conserved TLRs, which are expressed on tissue-resident immune cells and can induce the production of pro-inflammatory cytokines and chemokines that involve in the processes of wound healing (Medzhitov & Janeway, 2000; O'Neill et al., 2013; Satake & Sekiguchi, 2012). The TLR signaling pathway conserved in the animal kingdom is served as the first line to protect the host from microorganism infection, especially in invertebrates which are lacking adaptive immunity (Satake & Sekiguchi, 2012; Skanta et al., 2013). However, both functional and constructional divergence in all TLRs make the reach of TLR-mediated immunity and other areas such as developmental biology in *Drosophila* not so easy (Sasaki et al., 2009; Zhang et al., 2013). This study not only focused on TLR, but also paid attend to other molecules in the related signaling. Three members of TLR signaling pathway were cloned and identified in this study including TLR, MyD88, and TNF. The identification of these three members that including canonical and non-

doi:10.6342/NTU202000204

canonical molecules suggested this conserved pathway also exists in this worm. Similarly, in many vertebrates and invertebrates, this pathway plays very important role in innate immunity (Akira et al., 2001; Anthoney et al., 2018; Cuvillier-Hot et al., 2011; Inamori et al., 2000; Janssens et al., 2002; Kadowaki et al., 2001; O'Neill et al., 2013; Xu et al., 2018; Zhang et al., 2013).

The results of the chapter 3 showed diversity of protein motif in *Avi*-TLR and *Avi*-MyD88. Some *Avi*-TLR lack either LRR or TIR, and *Avi*-MyD88-i lacks TIR domain. This diversity of structure organization also represents in *C. elagans* only TLR, TOL-1, has no TIR domain in C-terminal. TOL-1 still has the function of pathogen recognition same as other TLR homologues in other organisms (Pujol et al., 2001). Excepted in *C. elagans*, more than one TLR or MyD88 have been identified in other invertebrates. For example, four TLRs and six MyD88s are identified and present different immune functions in *C. gigas* (Xin et al., 2016; Zhang et al., 2013). In leech *H. medicinalis*, two adaptor protein of TLR signaling pathway named *Hm*-MyD88 and *Hm*-SARM are characterized (Rodet et al., 2015). Those studies demonstrated that there are diverse roles of this signaling pathway, just like MyD88-dependant and –independent pathogens in vertebrates (Janssens et al., 2003; Karnati et al., 2015).

In addition to demonstrated both the regenerative ability and the TLR signaling pathway in *A. viride*, this study has the other aim to realize the trade-off hypothesis

doi:10.6342/NTU202000204

between regeneration capacity and immune responses. In the past decade, several published articles points out that regenerative ability seems to be has been lost gradually during animal evolution (Brockes et al., 2001; Sánchez Alvarado, 2000). By contrast, the evolution of innate and adaptive immunity becomes more specialized and complex through mammalian ontogeny (Godwin & Brockes, 2006; Mescher & Neff, 2005). The involvement and regulation of injury-induced inflammatory responses with regeneration remain poorly understood in invertebrates. In this study, five data strongly support the trade-off hypothesis. First, the antibiotic cocktail served as inflammatory inhibitor significantly promotes the anterior regeneration. Second, the opposed gene expression pattern after amputation between *Avi-MyD88-a* and *Avi-MyD88-i*. The increased gene expression of *Avi-MyD88-i* should inhibit inflammation during the anterior regeneration in *A. viride*. Third, the anterior regeneration was inhibit when the TLR signaling pathway were activated by poly I:C treated. Fourth, a TLR inhibitor successfully rescued the anterior regeneration after poly I:C treatment. And the last, the anterior regeneration was inhibited when the TLR signaling pathway were activated by knock-down of *Avi-MyD88-i.* Those data showed that regenerative ability could be improved through inhibition of immunity and the regenerative ability was suppressed by promoted immunity. Several shreds of evidence have presented previously in vertebrates, Martin *et al.* reported that null mice absences both macrophage and neutrophil aggregation at the wound site. And

doi:10.6342/NTU202000204

the processes of skin repair result in the more mature epithelial layer in null mice (Martin et al., 2003). Similarly, *X. laevis* tadpole has a stronger ability with tail regeneration excluding at a refractory period. Knockdown of *PU.1* gene significantly restores regenerative ability which causes immune suppression during the refractory period. (Fukazawa et al., 2009). In addition, neutrophil clearance by macrophage pre-depletion can inhibit the regeneration in zebrafish. Also, PAMP injection would promote medaka heart regeneration (Lai et al., 2017). So far, no related research works on the trade-off hypothesis in invertebrate model. Therefore, here I introduced a new invertebrate model, *A. viride*, a freshwater annelid that can regenerate the lost body parts after anterior or posterior amputation (Brace, 1901; Chen et al., 2018a). Due to this worm always living in fresh water that is rich in microorganisms, it has advanced with an effective system to defense putative pathogens. Besides, this work characterized the TLR signaling pathway in *A. viride* and provided five strong data support the trade-off hypothesis, making it a suitable model for investigating the interactions between immune responses and regeneration. Finally, this model conforms the requirement of the TLR signaling pathway to regulate immune responses in for anterior regeneration. This comparative research supports the trade-off hypothesis between immunity and regeneration, and insights into the possible therapeutic strategies in regenerative medicine.

doi:10.6342/NTU202000204

References

doi:10.6342/NTU202000204

Aderem A & Ulevitch R. (2000). Toll-like receptors in the induction of the innate immune response. *Nature, 406*(6797), 782-787.

Akira S, Takeda K & Kaisho T. (2001). Toll-like receptors: critical proteins linking innate and acquired immunity. *Nat Immunol, 2*(8), 675-680.

Akira S, Uematsu S & Takeuchi O. (2006). Pathogen recognition and innate immunity. *Cell, 124*(4), 783-801.

Anderson KV, Jurgens G & Nusslein-Volhard C. (1985). Establishment of dorsal-ventral polarity in the *Drosophila* embryo: genetic studies on the role of the Toll gene product. *Cell, 42*(3), 779-789.

Anthoney N, Foldi I & Hidalgo A. (2018). Toll and Toll-like receptor signalling in development. *Development, 145*(9).

Ashley NT, Weil ZM & Nelson RJ. (2012). Inflammation: mechanisms, costs, and natural variation. *Annu Rev Ecol Evol Syst, 43*(1), 385-406.

Aurora AB & Olson EN. (2014). Immune modulation of stem cells and regeneration. *Cell stem cell, 15*(1), 14-25.

Ausubel FM. (2005). Are innate immune signaling pathways in plants and animals conserved? *Nat Immunol, 6*(10), 973-979.

Beffagna G. (2019). Zebrafish as a smart model to understand regeneration after heart injury: how fish could help humans. *Front Cardiovasc Med, 6*, 107-107.

doi:10.6342/NTU202000204

Bely AE. (1999). Decoupling of fission and regenerative capabilities in an asexual oligochaete. *Hydrobiologia, 406*, 243-251.

Bely AE. (2006). Distribution of segment regeneration ability in the Annelida. *Integr Comp Biol, 46*(4), 508-518.

Bely AE & Nyberg KG. (2010). Evolution of animal regeneration: re-emergence of a field. *Trends Ecol Evol, 25*(3), 161-170.

Bely AE & Sikes JM. (2010). Latent regeneration abilities persist following recent evolutionary loss in asexual annelids. *PNAS, 107*(4), 1464.

Bely AE & Wray GA. (2001). Evolution of regeneration and fission in annelids: insights from *engrailed*- and *orthodenticle*-class gene expression. *Development, 128*(14), 2781-2791.

Berrill NJ. (1952). Regeneration and budding in worms. *Biol Rev, 27*(4), 401-438.

Bertolotti E, Malagoli D & Franchini A. (2013). Skin wound healing in different aged *Xenopus laevis*. *J Morphol, 274*(8), 956-964.

Bode HR. (2003). Head regeneration in *Hydra*. *Dev Dyn, 226*(2), 225-236.

Bosch TC. (2007). Why polyps regenerate and we don't: towards a cellular and molecular framework for *Hydra* regeneration. *Dev Biol, 303*(2), 421-433.

Brace EM. (1901). Notes on *Aeolosoma tenebrarum*. *J Morphol, 17*(2), 177-184.

Brockes JP & Kumar A. (2008). Comparative aspects of animal regeneration. *Annu Rev*

doi:10.6342/NTU202000204

Cell Dev Biol, 24, 525-549.

Brockes JP, Kumar A & Velloso CP. (2001). Regeneration as an evolutionary variable. *J Anat, 199*(Pt 1-2), 3-11.

Brusselle G & Bracke K. (2014). Targeting immune pathways for therapy in asthma and chronic obstructive pulmonary disease. *Ann Am Thorac Soc, 11 Suppl 5*, S322-328.

Buchmann K. (2014). Evolution of innate immunity: clues from invertebrates via fish to mammals. *Front Immunol, 5*, 459-459.

Caamaño J & Hunter CA. (2002). NF-kappaB family of transcription factors: central regulators of innate and adaptive immune functions. *Clin Microbiol Rev, 15*(3), 414-429.

Carty M, Goodbody R, Schroder M, Stack J, Moynagh PN & Bowie AG. (2006). The human adaptor SARM negatively regulates adaptor protein TRIF-dependent toll-like receptor signaling. *Nat Immunol, 7*(10), 1074-1081.

Carvalho L, Jacinto A & Matova N. (2014). The Toll/NF-kappaB signaling pathway is required for epidermal wound repair in *Drosophila*. *PNAS, 111*(50), E5373-5382.

Chen CF, Sung TL, Chen LY & Chen JH. (2018a). Telomere maintenance during anterior regeneration and aging in the freshwater annelid *Aeolosoma viride*. *Sci*

doi:10.6342/NTU202000204

Rep, 8(1), 18078.

Chen CH & Poss KD. (2017). Regeneration genetics. *Annu Rev Genet, 51*, 63-82.

Chen CP, Fok SKW, Hsieh YW, Chen CY, Hsu FM, Chang YH & Chen JH. (2020). General characterization of regeneration in *Aeolosoma viride* (Annelida, Aeolosomatidae). *Invertebr Biol, 00*, e12277.

Chen L, Deng H, Cui H, Fang J, Zuo Z, Deng J, . . . Zhao L. (2018b). Inflammatory responses and inflammation-associated diseases in organs. *Oncotarget, 9*(6), 7204-7218.

Clark KF, Acorn AR & Greenwood SJ. (2013). A transcriptomic analysis of American lobster (*Homarus americanus*) immune response during infection with the bumper car parasite *Anophryoides haemophila*. *Dev Comp Immunol, 40*(2), 112-122.

Coscia MR, Giacomelli S & Oreste U. (2011). Toll-like receptors: an overview from invertebrates to vertebrates. *Invert Surviv J, 8*(2), 210-226.

Cuvillier-Hot V, Boidin-Wichlacz C, Slomianny C, Salzet M & Tasiemski A. (2011). Characterization and immune function of two intracellular sensors, *Hm*TLR1 and *Hm*NLR, in the injured CNS of an invertebrate. *Dev Comp Immunol, 35*(2), 214-226.

De Gregorio E, Spellman PT, Rubin GM & Lemaitre B. (2001). Genome-wide analysis

doi:10.6342/NTU202000204

of the *Drosophila* immune response by using oligonucleotide microarrays. *PNAS, 98*(22), 12590-12595.

De Zoysa M, Jung S & Lee J. (2009). First molluscan TNF-α homologue of the TNF superfamily in disk abalone: molecular characterization and expression analysis. *Fish Shellfish Immunol, 26*(4), 625-631.

Delneste Y, Beauvillain C & Jeannin P. (2007). [Innate immunity: structure and function of TLRs]. *Med Sci, 23*(1), 67-73.

Dinsmore CE. (1991). *A history of regeneration research: milestones in the evolution of a science*.

Doyle SE, O'Connell RM, Miranda GA, Vaidya SA, Chow EK, Liu PT, . . . Cheng G. (2004). Toll-like receptors induce a phagocytic gene program through p38. *J Exp Med, 199*(1), 81-90.

Drewes CD & Fourtner CR. (1991). Reorganization of escape reflexes during asexual fission in an aquatic oligochaete, *Dero digitata*. *J Exp Zool, 260*(2), 170-180.

Erickson JR & Echeverri K. (2018). Learning from regeneration research organisms: the circuitous road to scar free wound healing. *Dev Biol, 433*(2), 144-154.

Essink K & Kleef HL. (1993). Distribution and life cycle of the North American Spionid polychaete *Marenzelleria viridis* (Verrill, 1873) in the Ems estuary. *Aquat Ecol, 27*(2), 237-246.

doi:10.6342/NTU202000204

Falconi R, Gugnali A & Zaccanti F. (2015). Quantitative observations on asexual reproduction of *Aeolosoma viride* (Annelida, Aphanoneura). *Invertebr Biol, 134*, 151-161.

Falconi R, Renzulli T & Zaccanti F. (2006). Survival and reproduction in *Aeolosoma viride* (Annelida, Aphanoneura). *Hydrobiologia, 564*(1), 95-99.

Feiken E, Romer J, Eriksen J & Lund LR. (1995). Neutrophils express tumor necrosis factor-alpha during mouse skin wound healing. *J Invest Dermatol, 105*(1), 120-123.

Fernando WA, Leininger E, Simkin J, Li N, Malcom CA, Sathyamoorthi S, . . . Muneoka K. (2011). Wound healing and blastema formation in regenerating digit tips of adult mice. *Dev Biol, 350*(2), 301-310.

Fleischer B & Schrezenmeier H. (1988). T cell stimulation by Staphylococcal enterotoxins. Clonally variable response and requirement for major histocompatibility complex class II molecules on accessory or target cells. *J Exp Med, 167*(5), 1697-1707.

Forbes SJ & Rosenthal N. (2014). Preparing the ground for tissue regeneration: from mechanism to therapy. *Nat Med, 20*(8), 857-869.

Foulkes RH. (1953). Regeneration of the anterior end of *Aulophorus furcatus* (Naididae) with special reference to effect of X-rays. *Biol Bull, 105*(1), 80-86.

doi:10.6342/NTU202000204

Franchi L, Warner N, Viani K & Nuñez G. (2009). Function of Nod-like receptors in microbial recognition and host defense. *Immunol Rev, 227*(1), 106-128.

Franchini A & Bertolotti E. (2012). The thymus and tail regenerative capacity in *Xenopus laevis* tadpoles. *Acta Histochem, 114*(4), 334-341.

Fukazawa T, Naora Y, Kunieda T & Kubo T. (2009). Suppression of the immune response potentiates tadpole tail regeneration during the refractory period. *Development, 136*(14), 2323-2327.

Gaete M, Muñoz R, Sánchez N, Tampe R, Moreno M, Contreras EG, . . . Larraín J. (2012). Spinal cord regeneration in *Xenopus* tadpoles proceeds through activation of Sox2-positive cells. *Neural Dev, 7*(1), 13.

Galloway TW. (1899). Observations on non-sexual reproduction in *Dero vaga*. *Bull Mus compo Zool, 35*, 115-140.

Gao L, Han Y, Deng H, Hu W, Zhen H, Li N, . . . Pang Q. (2017). The role of a novel C-type lectin-like protein from planarian in innate immunity and regeneration. *Dev Comp Immunol, 67*, 413-426.

Geijtenbeek TBH & Gringhuis SI. (2009). Signalling through C-type lectin receptors: shaping immune responses. *Nat Rev Immunol, 9*(7), 465-479.

Gibson GD & Paterson IG. (2003). Morphogenesis during sexual and asexual reproduction in *Amphipolydora vestalis* (Polychaeta: Spionidae). *New Zeal J*

doi:10.6342/NTU202000204

Mar Fresh, 37(4), 741-752.

Gierer A, Berking S, Bode H, David CN, Flick K, Hansmann G, . . . Trenkner E. (1972). Regeneration of from *Hydra* reaggregated cells. *Nat New Biol, 239*(91), 98-101.

Glasby CJ & Timm T. (2008). Global diversity of polychaetes (Polychaeta; Annelida) in freshwater. *Hydrobiologia, 595*(1), 107-115.

Glasby CJ, Timm T, Muir AI & Gil J. (2009). Catalogue of non-marine Polychaeta (Annelida) of the world. *Zootaxa, 52*, 1-52.

Godwin JW & Brockes JP. (2006). Regeneration, tissue injury and the immune response. *J Anat, 209*(4), 423-432.

Godwin JW, Debuque R, Salimova E & Rosenthal NA. (2017). Heart regeneration in the salamander relies on macrophage-mediated control of fibroblast activation and the extracellular landscape. *NPJ Regen Med, 2*, 22.

Godwin JW, Pinto AR & Rosenthal NA. (2013). Macrophages are required for adult salamander limb regeneration. *PNAS, 110*(23), 9415-9420.

Godwin JW & Rosenthal N. (2014). Scar-free wound healing and regeneration in amphibians: immunological influences on regenerative success. *Differentiation, 87*(1-2), 66-75.

Goss RJ. (1969). *Principles of Regeneration*: Academic Press, New York.

doi:10.6342/NTU202000204

Grellner W. (2002). Time-dependent immunohistochemical detection of proinflammatory cytokines (IL-1beta, IL-6, TNF-alpha) in human skin wounds. *Forensic Sci Int, 130*(2-3), 90-96.

Guo B, Liu S, Li J, Liao Z, Liu H, Xia H & Qi P. (2018). Identification and functional characterization of three myeloid differentiation factor 88 (MyD88) isoforms from thick shell mussel *Mytilus coruscus*. *Fish Shellfish Immunol, 83*, 123-133.

Hallman M, Ramet M & Ezekowitz RA. (2001). Toll-like receptors as sensors of pathogens. *Pediatr Res, 50*(3), 315-321.

Hashimoto C, Hudson KL & Anderson KV. (1988). The *Toll* gene of drosophila, required for dorsal-ventral embryonic polarity, appears to encode a transmembrane protein. *Cell, 52*(2), 269-279.

Herlant-Meewis H. (1951). Les lois de la scissiparite´ chez les Aeolosomatidae: *Aeolosoma viride*. *Ann Soc r Zool Belg, 82*, 231-284.

Herlant-Meewis H. (1953). Contribution a l'étude de la régénération chez les oligochètes Aeolosomatidae. *Ann Soc r Zool Belg, 84*, 117-161.

Herlant-Meewis H. (1964). Regeneration in annelids. *Advances in Morphogenesis, 4*, 155-215.

Heyland A, Schuh N & Rast J. (2018). Sea urchin larvae as a model for postembryonic development. *Results Probl Cell Differ, 65*, 137-161.

doi:10.6342/NTU202000204

Hibino T, Loza-Coll M, Messier C, Majeske AJ, Cohen AH, Terwilliger DP, . . . Rast JP. (2006). The immune gene repertoire encoded in the purple sea urchin genome. *Dev Biol, 300*(1), 349-365.

Holmblad T & Söderhäll K. (1999). Cell adhesion molecules and antioxidative enzymes in a crustacean, possible role in immunity. *Aquaculture, 172*(1), 111-123.

Huebener P & Schwabe RF. (2013). Regulation of wound healing and organ fibrosis by Toll-like receptors. *Biochimica et biophysica acta, 1832*(7), 1005-1017.

Hyman LH. (1938). The fragmentation of *Nais paraguayensis*. *Physiol Zool, 11*(2), 126-143.

Inamori K, Koori K, Mishima C, Muta T & Kawabata S. (2000). A horseshoe crab receptor structurally related to *Drosophila* Toll. *J Endotoxin Res, 6*(5), 397-399.

Janeway CA, Jr. (1989). Approaching the asymptote? Evolution and revolution in immunology. *Cold Spring Harb Symp Quant Biol, 54 Pt 1*, 1-13.

Janeway CA, Jr. & Medzhitov R. (2002). Innate immune recognition. *Annu Rev Immunol, 20*, 197-216.

Jang IH, Chosa N, Kim SH, Nam HJ, Lemaitre B, Ochiai M, . . . Lee WJ. (2006). A Spatzle-processing enzyme required for toll signaling activation in *Drosophila* innate immunity. *Dev Cell, 10*(1), 45-55.

Janssens S, Burns K, Tschopp J & Beyaert R. (2002). Regulation of interleukin-1- and

doi:10.6342/NTU202000204

lipopolysaccharide-induced NF-kappaB activation by alternative splicing of MyD88. *Curr Biol, 12*(6), 467-471.

Janssens S, Burns K, Vercammen E, Tschopp J & Beyaert R. (2003). MyD88S, a splice variant of MyD88, differentially modulates NF-kappaB- and AP-1-dependent gene expression. *FEBS letters, 548*(1-3), 103-107.

Kadowaki N, Ho S, Antonenko S, Malefyt RW, Kastelein RA, Bazan F & Liu YJ. (2001). Subsets of human dendritic cell precursors express different toll-like receptors and respond to different microbial antigens. *J Exp Med, 194*(6), 863-869.

Kalidas RM, Raja SE, Mydeen SAKNM, Samuel SCJR, Durairaj SCJ, Nino GD, . . . Sudhakar S. (2015). Conserved lamin A protein expression in differentiated cells in the earthworm *Eudrilus eugeniae*. *Cell Biol Int, 39*(9), 1036-1043.

Kamath RS, Martinez-Campos M, Zipperlen P, Fraser AG & Ahringer J. (2001). Effectiveness of specific RNA-mediated interference through ingested double-stranded RNA in *Caenorhabditis elegans*. *Genome Biol, 2*(1), research0002.0001-research0002.0010.

Karnati HK, Pasupuleti SR, Kandi R, Undi RB, Sahu I, Kannaki TR, . . . Gutti RK. (2015). TLR-4 signalling pathway: MyD88 independent pathway up-regulation in chicken breeds upon LPS treatment. *Vet Res Commun, 39*(1), 73-78.

doi:10.6342/NTU202000204

Kawai T, Adachi O, Ogawa T, Takeda K & Akira S. (1999). Unresponsiveness of MyD88-deficient mice to endotoxin. *Immunity, 11*(1), 115-122.

Kawai T & Akira S. (2005). Toll-like receptor downstream signaling. *Arthritis Res Ther, 7*(1), 12-19.

Kawai T & Akira S. (2010). The role of pattern-recognition receptors in innate immunity: update on Toll-like receptors. *Nat Immunol, 11*(5), 373-384.

Kharin AV, Zagainova IV & Kostyuchenko RP. (2006). Formation of the paratomic fission zone in freshwater oligochaetes. *Russ J Dev Biol, 37*(6), 354-365.

Kimbrell DA & Beutler B. (2001). The evolution and genetics of innate immunity. *Nat Rev Genet, 2*(4), 256-267.

Kozin VV & Kostyuchenko RP. (2015). Vasa, PL10, and Piwi gene expression during caudal regeneration of the polychaete annelid *Alitta virens*. *Dev Genes Evol, 225*(3), 129-138.

Kumagai Y & Akira S. (2010). Identification and functions of pattern-recognition receptors. *J Allergy Clin Immunol, 125*(5), 985-992.

Kyritsis N, Kizil C, Zocher S, Kroehne V, Kaslin J, Freudenreich D, . . . Brand M. (2012). Acute inflammation initiates the regenerative response in the adult zebrafish brain. *Science, 338*(6112), 1353-1356.

Lai SL, Marin-Juez R, Moura PL, Kuenne C, Lai JKH, Tsedeke AT, . . . Stainier DY.

doi:10.6342/NTU202000204

(2017). Reciprocal analyses in zebrafish and medaka reveal that harnessing the immune response promotes cardiac regeneration. *Elife, 6*.

LeibundGut-Landmann S, Gross O, Robinson MJ, Osorio F, Slack EC, Tsoni SV, . . . Reis e Sousa C. (2007). Syk- and CARD9-dependent coupling of innate immunity to the induction of T helper cells that produce interleukin 17. *Nat Immunol, 8*(6), 630-638.

Lemaitre B, Nicolas E, Michaut L, Reichhart JM & Hoffmann JA. (1996). The dorsoventral regulatory gene cassette spatzle/Toll/cactus controls the potent antifungal response in *Drosophila* adults. *Cell, 86*(6), 973-983.

Li L, Yan B, Shi YQ, Zhang WQ & Wen ZL. (2012). Live imaging reveals differing roles of macrophages and neutrophils during zebrafish tail fin regeneration. *J Biol Chem, 287*(30), 25353-25360.

Loo Y-M & Gale M. (2011). Immune signaling by RIG-I-like receptors. *Immunity, 34*(5), 680-692.

Lu Y, Li C, Zhang P, Shao Y, Su X, Li Y & Li T. (2013). Two adaptor molecules of MyD88 and TRAF6 in *Apostichopus japonicus* Toll signaling cascade: molecular cloning and expression analysis. *Dev Comp Immunol, 41*(4), 498-504.

Lu Y, Su F, Li Q, Zhang J, Li Y, Tang T, . . . Yu XQ. (2020). Pattern recognition receptors in *Drosophila* immune responses. *Dev Comp Immunol, 102*, 103468.

doi:10.6342/NTU202000204

Macedo L, Pinhal-Enfield G, Alshits V, Elson G, Cronstein BN & Leibovich SJ. (2007). Wound healing is impaired in MyD88-deficient mice: a role for MyD88 in the regulation of wound healing by adenosine A2A receptors. *Am J Pathol, 171*(6), 1774-1788.

MacEwan DJ. (2002). TNF ligands and receptors--a matter of life and death. *Br J Pharmacol, 135*(4), 855-875.

Maden M. (2018). The evolution of regeneration - where does that leave mammals? *Int J Dev Biol, 62*(6-7-8), 369-372.

Marotta R, Ferraguti M & Martin P. (2003). Spermiogenesis and seminal receptacles in *Aeolosoma singulare* (Annelida, Polychaeta, Aeolosomatidae). *Ital J Zool, 70*(2), 123-132.

Martin P, D'Souza D, Martin J, Grose R, Cooper L, Maki R & McKercher SR. (2003). Wound healing in the PU.1 null mouse--tissue repair is not dependent on inflammatory cells. *Curr Biol, 13*(13), 1122-1128.

Martinez VG, Reddy PK & Zoran MJ. (2006). Asexual reproduction and segmental regeneration, but not morphallaxis, are inhibited by boric acid in *Lumbriculus variegatus* (Annelida: Clitellata: Lumbriculidae). *Hydrobiologia, 564*, 73-86.

Martinon F & Tschopp J. (2007). Inflammatory caspases and inflammasomes: master switches of inflammation. *Cell Death Differ, 14*(1), 10-22.

doi:10.6342/NTU202000204

McCusker C, Bryant SV & Gardiner DM. (2015). The axolotl limb blastema: cellular and molecular mechanisms driving blastema formation and limb regeneration in tetrapods. *Regeneration, 2*(2), 54-71.

Medzhitov R. (2010). Inflammation 2010: new adventures of an old flame. *Cell, 140*(6), 771-776.

Medzhitov R & Janeway C, Jr. (2000). The Toll receptor family and microbial recognition. *Trends Microbiol, 8*(10), 452-456.

Medzhitov R, Preston-Hurlburt P & Janeway CA, Jr. (1997). A human homologue of the *Drosophila* Toll protein signals activation of adaptive immunity. *Nature, 388*(6640), 394-397.

Mekata T, Sudhakaran R, Okugawa S, Inada M, Kono T, Sakai M & Itami T. (2010). A novel gene of tumor necrosis factor ligand superfamily from kuruma shrimp, *Marsupenaeus japonicus*. *Fish Shellfish Immunol, 28*(4), 571-578.

Mescher AL. (2017). Macrophages and fibroblasts during inflammation and tissue repair in models of organ regeneration. *Regeneration (Oxf), 4*(2), 39-53.

Mescher AL & Neff AW. (2005). Regenerative capacity and the developing immune system. *Adv Biochem Eng Biotechnol, 93*, 39-66.

Mescher AL, Neff AW & King MW. (2013). Changes in the inflammatory response to injury and its resolution during the loss of regenerative capacity in developing

doi:10.6342/NTU202000204

Xenopus limbs. *PLoS One, 8*(11), e80477.

Mescher AL, Neff AW & King MW. (2017). Inflammation and immunity in organ regeneration. *Dev Comp Immunol, 66*, 98-110.

Midwood KS, Williams LV & Schwarzbauer JE. (2004). Tissue repair and the dynamics of the extracellular matrix. *Int J Biochem Cell Biol, 36*(6), 1031-1037.

Mitashov VI, Panova IG & Koussoulakos S. (2004). Transdifferentiation potential of ciliary and pigment epithelial cells in lower vertebrates and mammals. *Biol Bull, 31*(4), 324-331.

Moreno E, Yan M & Basler K. (2002). Evolution of TNF signaling mechanisms: JNK-dependent apoptosis triggered by Eiger, the *Drosophila* homolog of the TNF superfamily. *Curr Biol, 12*(14), 1263-1268.

Morgan TH. (1901). Regeneration and liability to injury. *Science, 14*(346), 235-248.

Muller MCM & Henning L. (2004). Ground plan of the polychaete brain--I. Patterns of nerve development during regeneration in *Dorvillea bermudensis* (Dorvilleidae). *J Comp Neurol, 471*(1), 49-58.

Murry CE, Soonpaa MH, Reinecke H, Nakajima H, Nakajima HO, Rubart M, . . . Field LJ. (2004). Haematopoietic stem cells do not transdifferentiate into cardiac myocytes in myocardial infarcts. *Nature, 428*(6983), 664-668.

Nechiporuk A & Keating MT. (2002). A proliferation gradient between proximal and

doi:10.6342/NTU202000204

msxb-expressing distal blastema directs zebrafish fin regeneration. *Development, 129*(11), 2607-2617.

Newmark PA, Reddien PW, Cebrià F & Sánchez Alvarado A. (2003). Ingestion of bacterially expressed double-stranded RNA inhibits gene expression in planarians. *PNAS, 100*(Suppl 1), 11861-11865.

Nguyen-Chi M, Laplace-Builhe B, Travnickova J, Luz-Crawford P, Tejedor G, Lutfalla G, . . . Djouad F. (2017). TNF signaling and macrophages govern fin regeneration in zebrafish larvae. *Cell Death Dis, 8*(8), e2979.

Nye HL, Cameron JA, Chernoff EA & Stocum DL. (2003). Regeneration of the urodele limb: a review. *Dev Dyn, 226*(2), 280-294.

O'Neill LA & Bowie AG. (2007). The family of five: TIR-domain-containing adaptors in toll-like receptor signalling. *Nat Rev Immunol, 7*(5), 353-364.

O'Neill LA, Golenbock D & Bowie AG. (2013). The history of Toll-like receptors - redefining innate immunity. *Nat Rev Immunol, 13*(6), 453-460.

Olson JK & Miller SD. (2004). Microglia initiate central nervous system innate and adaptive immune responses through multiple TLRs. *J Immunol, 173*(6), 3916-3924.

Özpolat BD & Bely AE. (2015). Gonad establishment during asexual reproduction in the annelid *Pristina leidyi*. *Dev Biol, 405*(1), 123-136.

doi:10.6342/NTU202000204

Özpolat BD & Bely AE. (2016). Developmental and molecular biology of annelid regeneration: a comparative review of recent studies. *Curr Opin Genet Dev, 40*, 144-153.

Palm NW & Medzhitov R. (2009). Pattern recognition receptors and control of adaptive immunity. *Immunol Rev, 227*(1), 221-233.

Pasare C & Medzhitov R. (2005). Toll-like receptors: linking innate and adaptive immunity. *Adv Exp Med Biol, 560*, 11-18.

Passamaneck YJ & Martindale MQ. (2012). Cell proliferation is necessary for the regeneration of oral structures in the anthozoan cnidarian *Nematostella vectensis*. *BMC Dev Biol, 12*, 34.

Paulus T & Müller MCM. (2006). Cell proliferation dynamics and morphological differentiation during regeneration in *Dorvillea bermudensis* (Polychaeta, Dorvilleidae). *J Morphol, 267*(4), 393-403.

Pecchi E, Dallaporta M, Jean A, Thirion S & Troadec JD. (2009). Prostaglandins and sickness behavior: old story, new insights. *Physiol Behav, 97*(3-4), 279-292.

Peiris TH, Hoyer KK & Oviedo NJ. (2014). Innate immune system and tissue regeneration in planarians: an area ripe for exploration. *Semin Immunol, 26*(4), 295-302.

Petrie TA, Strand NS, Yang CT, Rabinowitz JS & Moon RT. (2014). Macrophages

doi:10.6342/NTU202000204

modulate adult zebrafish tail fin regeneration. *Development, 141*(13), 2581-2591.

Pfannenstiel HD. (1974). Regeneration in the gonochoristic polychaete *Ophryotrocha notoglandulata*. *Mar Biol, 24*(3), 269-272.

Pirotte N, Stevens AS, Fraguas S, Plusquin M, Van Roten A, Van Belleghem F, . . . Smeets K. (2015). Reactive oxygen species in planarian regeneration: an upstream necessity for correct patterning and brain formation. *Oxid Med Cell Longev, 2015*, 392476.

Priyathilaka TT, Bathige S, Lee S & Lee J. (2018). Molecular identification and functional analysis of two variants of myeloid differentiation factor 88 (MyD88) from disk abalone (*Haliotis discus discus*). *Dev Comp Immunol, 79*, 113-127.

Prochazkova P, Roubalova R, Dvorak J, Navarro Pacheco NI & Bilej M. (2020). Pattern recognition receptors in annelids. *Dev Comp Immunol, 102*, 103493.

Pujol N, Link EM, Liu LX, Kurz CL, Alloing G, Tan MW, . . . Ewbank JJ. (2001). A reverse genetic analysis of components of the Toll signaling pathway in *Caenorhabditis elegans*. *Curr Biol, 11*(11), 809-821.

Qiu L, Song L, Yu Y, Xu W, Ni D & Zhang Q. (2007). Identification and characterization of a myeloid differentiation factor 88 (MyD88) cDNA from Zhikong scallop *Chlamys farreri*. *Fish Shellfish Immunol, 23*(3), 614-623.

doi:10.6342/NTU202000204

Radashevsky VI. (1996). Morphology, ecology and asexual reproduction of a new polydorella species (Polychaeta: Spionidae) from the South China Sea. *Bull Mar Sci, 58*(3), 684-693.

Reddien PW. (2018). The cellular and molecular basis for planarian regeneration. *Cell, 175*(2), 327-345.

Reddien PW & Sánchez Alvarado A. (2004). Fundamentals of planarian regeneration. *Annu Rev Cell Dev Biol, 20*, 725-757.

Ren Y, Xue J, Yang H, Pan B & Bu W. (2017). Comparative and evolutionary analysis of an adapter molecule MyD88 in invertebrate metazoans. *Dev Comp Immunol, 76*, 18-24.

Ribeiro RP, Ponz-Segrelles G, Bleidorn C & Aguado MT. (2019). Comparative transcriptomics in Syllidae (Annelida) indicates that posterior regeneration and regular growth are comparable, while anterior regeneration is a distinct process. *BMC Genomics, 20*(1), 855.

Roach JC, Glusman G, Rowen L, Kaur A, Purcell MK, Smith KD, . . . Aderem A. (2005). The evolution of vertebrate Toll-like receptors. *PNAS, 102*(27), 9577-9582.

Rodet F, Tasiemski A, Boidin-Wichlacz C, Van Camp C, Vuillaume C, Slomianny C & Salzet M. (2015). Hm-MyD88 and Hm-SARM: two key regulators of the

doi:10.6342/NTU202000204

neuroimmune system and neural repair in the medicinal leech. *Sci Rep, 5*, 9624.

Rosetto M, Engstrom Y, Baldari CT, Telford JL & Hultmark D. (1995). Signals from the IL-1 receptor homolog, Toll, can activate an immune response in a *Drosophila* hemocyte cell line. *Biochem Biophys Res Commun, 209*(1), 111-116.

Rossi L, Salvetti A, Lena A, Batistoni R, Deri P, Pugliesi C, . . . Gremigni V. (2006). *DjPiwi-1*, a member of the *PAZ-Piwi* gene family, defines a subpopulation of planarian stem cells. *Dev Genes Evol, 216*(6), 335-346.

Salic A & Mitchison TJ. (2008). A chemical method for fast and sensitive detection of DNA synthesis *in vivo*. *PNAS, 105*(7), 2415-2420.

Sanchez Alvarado A & Tsonis PA. (2006). Bridging the regeneration gap: genetic insights from diverse animal models. *Nat Rev Genet, 7*(11), 873-884.

Sasaki N, Ogasawara M, Sekiguchi T, Kusumoto S & Satake H. (2009). Toll-like receptors of the Ascidian *Ciona intestinalis*: prototypes with hybrid functionalities of vertebrate toll-like receptors. *J Biol Chem, 284*(40), 27336-27343.

Satake H & Sekiguchi T. (2012). Toll-like receptors of deuterostome invertebrates. *Front Immunol, 3*, 34.

Schikorski D, Cuvillier-Hot V, Boidin-Wichlacz C, Slomianny C, Salzet M & Tasiemski A. (2009). Deciphering the immune function and regulation by a TLR of the

doi:10.6342/NTU202000204

cytokine EMAPII in the lesioned central nervous system using a leech model. *J Immunol, 183*(11), 7119-7128.

Schnapp E, Kragl M, Rubin L & Tanaka EM. (2005). Hedgehog signaling controls dorsoventral patterning, blastema cell proliferation and cartilage induction during axolotl tail regeneration. *Development, 132*(14), 3243-3253.

Scimone ML, Kravarik KM, Lapan SW & Reddien PW. (2014). Neoblast specialization in regeneration of the planarian *Schmidtea mediterranea*. *Stem Cell Rep, 3*(2), 339-352.

Simkin J, Gawriluk TR, Gensel JC & Seifert AW. (2017). Macrophages are necessary for epimorphic regeneration in African spiny mice. *Elife, 6*.

Skanta F, Roubalova R, Dvorak J, Prochazkova P & Bilej M. (2013). Molecular cloning and expression of TLR in the *Eisenia andrei* earthworm. *Dev Comp Immunol, 41*(4), 694-702.

Skjaeveland I, Iliev DB, Strandskog G & Jorgensen JB. (2009). Identification and characterization of TLR8 and MyD88 homologs in Atlantic salmon (*Salmo salar*). *Dev Comp Immunol, 33*(9), 1011-1017.

Smith ME. (1985). Population and reproductive dynamics of *Nais communis* (Oligochaeta: Naididae) from a wisconsin limnocrene. *Am Midl Nat, 114*(1), 152-158.

doi:10.6342/NTU202000204

Sánchez Alvarado A. (2000). Regeneration in the metazoans: why does it happen? *Bioessays, 22*(6), 578-590.

Sánchez Alvarado A & Tsonis PA. (2006). Bridging the regeneration gap: genetic insights from diverse animal models. *Nat Rev Genet, 7*(11), 873-884.

Suga H, Sugaya M, Fujita H, Asano Y, Tada Y, Kadono T & Sato S. (2014). TLR4, rather than TLR2, regulates wound healing through TGF-beta and CCL5 expression. *J Dermatol Sci, 73*(2), 117-124.

Sun Y, Zhou Z, Wang L, Yang C, Jianga S & Song L. (2014). The immunomodulation of a novel tumor necrosis factor (CgTNF-1) in oyster *Crassostrea gigas*. *Dev Comp Immunol, 45*(2), 291-299.

Takeda K & Akira S. (2004). TLR signaling pathways. *Semin Immunol, 16*(1), 3-9.

Takeo M, Yoshida-Noro C & Tochinai S. (2010). Functional analysis of grimp, a novel gene required for mesodermal cell proliferation at an initial stage of regeneration in *Enchytraeus japonensis* (Enchytraeidae, Oligochaete). *Int J Dev Biol, 54*(1), 151-160.

Tauszig-Delamasure S, Bilak H, Capovilla M, Hoffmann JA & Imler JL. (2002). *Drosophila* MyD88 is required for the response to fungal and Gram-positive bacterial infections. *Nat Immunol, 3*(1), 91-97.

Toubiana M, Gerdol M, Rosani U, Pallavicini A, Venier P & Roch P. (2013). Toll-like

doi:10.6342/NTU202000204

receptors and MyD88 adaptors in *Mytilus*: complete cds and gene expression levels. *Dev Comp Immunol, 40*(2), 158-166.

Valanne S, Wang JH & Ramet M. (2011). The *Drosophila* Toll signaling pathway. *J Immunol, 186*(2), 649-656.

Venegas C & Heneka MT. (2017). Danger-associated molecular patterns in Alzheimer's disease. *J Leukoc Biol, 101*(1), 87-98.

Vickery MC, Vickery MS, Amsler CD & McClintock JB. (2001). Regeneration in echinoderm larvae. *Microsc Res Tech, 55*(6), 464-473.

Vizzini A. (2017). Gene expression and regulation of molecules involved in pharynx inflammatory response induced by LPS in *Ciona intestinalis*. *Invert Surviv J, 14*(1), 119-128.

Wang X & Lin Y. (2008). Tumor necrosis factor and cancer, buddies or foes? *Acta Pharmacol Sin, 29*(11), 1275-1288.

Wang Y, Cheng S, Chang Y, Li K, Chen Y & Wang Y. (2018). Identification and expression analysis of a TLR11 family gene in the sea urchin *Strongylocentrotus intermedius*. *Immunogenetics, 70*(5), 337-346.

Wenemoser D & Reddien PW. (2010). Planarian regeneration involves distinct stem cell responses to wounds and tissue absence. *Dev Biol, 344*(2), 979-991.

Wenger Y, Buzgariu W, Reiter S & Galliot B. (2014). Injury-induced immune responses

doi:10.6342/NTU202000204

in *Hydra*. *Semin Immunol, 26*(4), 277-294.

Wiens M, Korzhev M, Krasko A, Thakur NL, Perovic-Ottstadt S, Breter HJ, . . . Muller WE. (2005). Innate immune defense of the sponge *Suberites domuncula* against bacteria involves a MyD88-dependent signaling pathway. Induction of a perforin-like molecule. *J Biol Chem, 280*(30), 27949-27959.

Xin L, Wang M, Zhang H, Li M, Wang H, Wang L & Song L. (2016). The categorization and mutual modulation of expanded MyD88s in *Crassostrea gigas*. *Fish Shellfish Immunol, 54*, 118-127.

Xu M, Wu J, Ge D, Wu C, Changfeng C, Lv Z, . . . Liu H. (2018). A novel Toll-like receptor from *Mytilus coruscus* is induced in response to stress. *Fish Shellfish Immunol, 78*, 331-337.

Xu N, Wang SQ, Tan D, Gao Y, Lin G & Xi R. (2011). EGFR, Wingless and JAK/STAT signaling cooperatively maintain *Drosophila* intestinal stem cells. *Dev Biol, 354*(1), 31-43.

Yamamoto M, Sato S, Hemmi H, Hoshino K, Kaisho T, Sanjo H, . . . Akira S. (2003). Role of adaptor TRIF in the MyD88-independent toll-like receptor signaling pathway. *Science, 301*(5633), 640-643.

Yoneyama M & Fujita T. (2009). RNA recognition and signal transduction by RIG-I-like receptors. *Immunol Rev, 227*(1), 54-65.

doi:10.6342/NTU202000204

Zattara EE & Bely AE. (2011). Evolution of a novel developmental trajectory: fission is distinct from regeneration in the annelid *Pristina leidyi*. *Evol Dev, 13*(1), 80-95.

Zattara EE & Bely AE. (2013). Investment choices in post-embryonic development: quantifying interactions among growth, regeneration, and asexual reproduction in the annelid *Pristina leidyi*. *J Exp Zool B Mol Dev Evol, 320*(8), 471-488.

Zattara EE & Bely AE. (2016). Phylogenetic distribution of regeneration and asexual reproduction in Annelida: regeneration is ancestral and fission evolves in regenerative clades. *Invertebr Biol, 135*(4), 400-414.

Zhang L, Li L & Zhang G. (2011). A *Crassostrea gigas* Toll-like receptor and comparative analysis of TLR pathway in invertebrates. *Fish Shellfish Immunol, 30*(2), 653-660.

Zhang S, Li CZ, Yan H, Qiu W, Chen YG, Wang PH, . . . He JG. (2012). Identification and function of myeloid differentiation factor 88 (MyD88) in *Litopenaeus vannamei*. *PLoS One, 7*(10), e47038.

Zhang X, Luan W, Jin S & Xiang J. (2008). A novel tumor necrosis factor ligand superfamily member (CsTL) from *Ciona savigny*i: molecular identification and expression analysis. *Dev Comp Immunol, 32*(11), 1362-1373.

Zhang X, Zhang P, Li C, Li Y, Jin C & Zhang W. (2015). Characterization of two regulators of the TNF-alpha signaling pathway in *Apostichopus japonicus*: LPS-

doi:10.6342/NTU202000204

induced TNF-alpha factor and baculoviral inhibitor of apoptosis repeat-containing 2. *Dev Comp Immunol, 48*(1), 138-142.

Zhang Y, He X, Yu F, Xiang Z, Li J, Thorpe KL & Yu Z. (2013). Characteristic and functional analysis of Toll-like receptors (TLRs) in the lophotrocozoan, *Crassostrea gigas*, reveals ancient origin of TLR-mediated innate immunity. *PLoS One, 8*(10), e76464.

Zhang Z & Schluesener HJ. (2006). Mammalian toll-like receptors: from endogenous ligands to tissue regeneration. *Cell Mol Life Sci, 63*(24), 2901-2907.

Zheng L, Zhang L, Lin H, McIntosh MT & Malacrida AR. (2005). Toll-like receptors in invertebrate innate immunity. *Invert Surviv J, 2*(2), 105-113.

doi:10.6342/NTU202000204